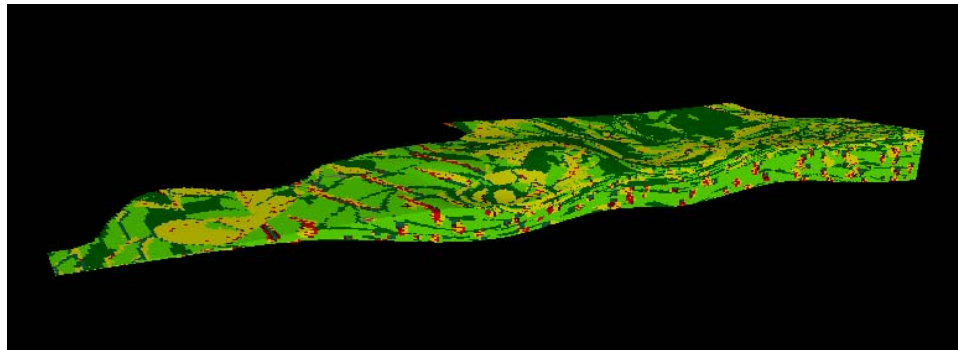


**AES/TG/10-26 Modeling Fluvial Reservoir Architecture
using Flumy Process**

September 2010 E.S.J. Deviese



Title : Modeling Fluvial Reservoir Architecture
using Flumy Process

Author(s) : E.S.J. Deviese

Date : September 2010
Professor(s) : Dr. A. Moscariello
Supervisor(s) : Dr. A. Moscariello
TA Report number : AES/TG/10-26

Postal Address : Section for Applied Geology
Department of Applied Earth Sciences
Delft University of Technology
P.O. Box 5028
The Netherlands

Telephone : (31) 15 2781328 (secretary)
Telefax : (31) 15 2781189

Copyright ©2010 Section for Applied Geology

*All rights reserved.
No parts of this publication may be reproduced,
Stored in a retrieval system, or transmitted,
In any form or by any means, electronic,
Mechanical, photocopying, recording, or otherwise,
Without the prior written permission of the
Section for Applied Geology*

Abstract

Modeling sedimentary heterogeneities of reservoir rocks is typically performed using geostatistical methods. Geostatistics reproduce the spatial distribution of heterogeneities based on available data. There are several geostatistical methods to build 3D reservoir model simulations, such as the object-based or variogram-based methods. MINES ParisTech has developed a new generation of models, both stochastic and process-based to reproduce the complex internal architecture of fluvial and turbidite reservoirs. The prototype software including this new approach is called Flumy. This process-based stochastic model simulates meandering channelized reservoirs at the reservoir scale.

The purpose of this study is to build a realistic 3D geological model of complex fluvial reservoir architectures using the latest version of the processing modeling software Flumy. The project consists of using the current stand alone version to model a fluvial facies architecture of a subsurface data set from a Carboniferous fluvial succession located in the Southern North Sea. A series of 3D facies models based on the sedimentological interpretation of logs and modeling parameters were thus realised. Facies models were then exported to Petrel for quantitative analysis (e.g. sensitivity analysis and volume calculations).

The process-based stochastic approach allows to obtain more realistic and reliable geological models. It respects the complexity of sedimentary processes and thus represents with more accuracy the lateral and vertical heterogeneities of fluvial reservoirs. The prototype software, Flumy, satisfies these requirements. However it is still under development and has limits and constraints which are described in this project.

Key words: geostatistics, stochastic, modeling, process-based, Flumy, fluvial, meandering, heterogeneity

Contents

I.	Introduction.....	6
II.	The challenge of 3D reservoir modeling	8
A.	Introduction.....	8
B.	Flumy model: a realistic process-based stochastic model	10
1.	Concepts.....	11
2.	Input parameters.....	12
III.	Characterisation of meandering and braided systems.....	14
A.	Fluvial environment.....	14
1.	Braided river system	16
2.	Meandering river system.....	16
B.	Fluvial sequence stratigraphy	18
IV.	Case study: The Schooner Field	20
A.	Regional geology	20
1.	Structure.....	20
2.	Stratigraphy.....	22
3.	Petroleum system.....	24
B.	The Schooner Field.....	24
1.	Structure.....	25
2.	Stratigraphy.....	26
V.	Data and workflow.....	35
A.	Workflow	35
B.	Data preparation.....	36
1.	Well data	36
2.	Topographic surface.....	37
3.	Sequence stratigraphy parameters.....	39
4.	Porosity analysis	43
5.	The Gas-Water contact	45
VI.	Results: Flumy & Petrel models	47
A.	Modeling	47
1.	Facies modeling (Flumy)	47
2.	3D static modeling (Petrel)	50
3.	The petrophysical model.....	53
B.	Quantitative analysis.....	56
1.	Volumetric analysis	56
2.	Uncertainty analysis.....	59
VII.	Interpretation/Discussion	60
VIII.	Conclusion & Recommendations	61

I. Introduction

Fluvial systems are presently the most studied environments, because of their accessibility and their direct economic impact on human development. They represent the transition between upstream continental deposits and marine environments and are characterised by a large variability ranging from large fluvial plains to marine marginal areas. Fluvial reservoirs form a large part of hydrocarbon reservoirs currently produced worldwide. The major difficulty presented by fluvial deposits is the degree and wide range of complexity of the overall architecture and facies heterogeneity (**Figure 1**). The architecture of these reservoirs reflects the complex sedimentary processes occurred during floodplain aggradation and incision by the river flowing downstream. The resulting facies association, sand bodies geometry, 3D architecture is therefore dependent on several geomorphic and dynamic parameters such as slope, avulsion rate, aggradation rate, base level evolution etc.

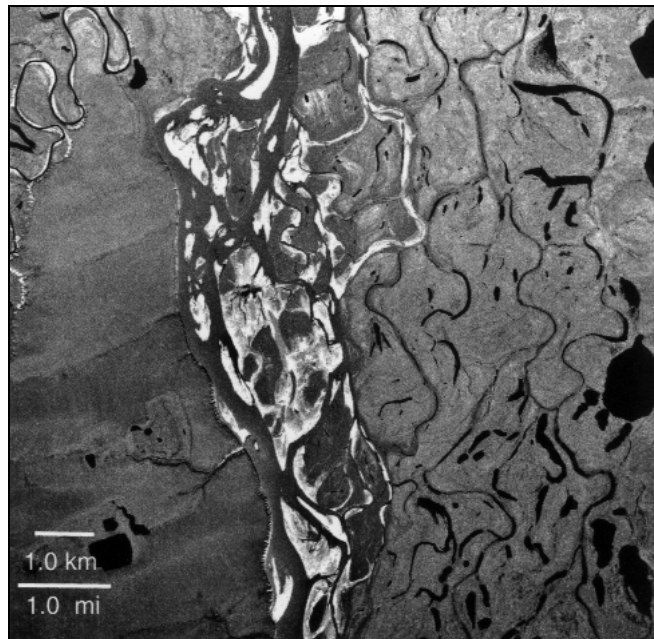


Figure 1: Three channel belts present in part of the Colville River flood plain, Alaska. Note the juxtaposition of the narrow channel belt of the Kogosukruk River (left) formed by a single, sinuous channel and the multiple, sinuous-to-braided channels in the much wider Colville River channel belt (center). Active and abandoned channels and bars are easily discernible. Photograph from July 1979 in the National Petroleum Reserve Alaska, approximately 40 km (25 mi) northeast of Umiat. (Bridge & Tye, 2000)

Over the last few years focused R&D activity made important step forwards to model such complex sedimentary systems providing modeling tools offering different degrees of modeling constraints (e.g. body modeling or stochastic) and predefined rules aimed to mimic the natural processes (e.g. process modeling).

Modeling sedimentary heterogeneities at reservoir scale is classically performed using geostatistical methods. Geostatistics reproduce the spatial distribution of heterogeneities based on from available data. They are several geostatistical methods to build 3D

reservoir model simulations, such as the object-based or variogram-based methods. None of these geostatistical methods is able to reproduce realistic and complex stratigraphic heterogeneity patterns.

Genetic models can reconstruct different and very realistic sedimentary architectures. These resulting images can be compared to field data which allows the identification of key parameters and the improvement of the conceptual models. Process-based sedimentology is beginning to provide inputs into geological model building. These methods have the advantage to generate realistic images of the geology, but they are difficult to constrain them to well data (Doligez *et al.*, 2007).

MINES ParisTech has developed a new generation of models, both stochastic and process-based. The prototype software including this new approach is called Flumy. This process-based stochastic model simulates meandering channelized reservoirs at the oil reservoir scale.

The following report presents a project done at the Delft University of Technology on the occasion of a Master thesis in Reservoir Geology. The purpose was to build a realistic 3D geological model of complex fluvial reservoir architectures using the latest version of the processing modeling software Flumy. The software license has been provided by Shell Exploration and Production, Rijswijk, The Netherlands.

The project consists of using of current stand alone version to model a fluvial facies architecture of a subsurface data set from a Carboniferous fluvial succession located in the Southern North Sea. During this project a series of 3D facies models were realised based on the sedimentological interpretation of logs and modeling parameters. Facies models will then be exported to Petrel for quantitative analysis (e.g. sensitivity analysis and volume calculations).

The subsurface data set has been provided by Andrea Moscariello and a 3D model in Petrel has been built by a MSc student during an internship, Mohammed Radam.

This report presents the geostatistics and geological settings of the project in the three first chapters. Then the workflow and the data provided are described in details in the fifth chapter. The following chapter presents the results of the modeling work made with Flumy and Petrel software. Finally a discussion and a conclusion with recommendations are given in the two last chapters.

II. The challenge of 3D reservoir modeling

Reservoir characterisation is an essential step in the oil industry. For the last fifteen years the need of models for heterogeneous reservoirs has stimulated the development of stochastic models, based either on the use of random functions or on the generation of random objects in space. As these approaches try only to reproduce a given heterogeneity of facies and do not take into account sedimentary processes, they often fail in producing realistic simulations (Cojan *et al.*, 2004). Another generation of models, both process-based and stochastic, is able to provide satisfactory modeling for heterogeneous reservoirs by reproducing the depositional processes.

A. Introduction

Reservoir modeling aims to provide one or more alternative numerical models in order to represent the relevant geometrical, geophysical and reservoir engineering aspect of the surface. A key problem faced in the development of a hydrocarbon reservoir is to construct a reservoir model that can generate reliable production forecasts under various development scenarios. After a few appraisal wells have been drilled, or after a few years of production, the reservoir geologist will provide a model of the inter-well geological architecture. A good deterministic model describing all of the main architectural characteristics of the interval could be built when a lot of input data are available. However the user must have good geological knowledge concerning the palaeogeographic setting of the interval (Davies *et al.*, 2009). Unfortunately, manual construction of 3D geological models (deterministically) is often very difficult as it requires a good knowledge of the reservoir based on large amount of data. This explains why geologists often limit their interpretation to 2D correlation panels, diagrams or maps. Geostatistic models provide interesting solutions to the main challenges of reservoir modeling, the construction of 3D geologically realistic representation of heterogeneity and the quantification of uncertainty through the generation of a variety of possible models.

Stochastic methods provide a set of facies models (i.e. realisations) with equiprobable facies distributions. In each model all the facies heterogeneity is represented aiming at reproducing the entire spatial structure and variability of facies distribution, even though the exact distribution of facies heterogeneities cannot be totally identified with the data provided. Representing all the facies heterogeneity is accomplished by the use of algorithms incorporating random numbers, which are sampled from probability distribution functions (Falivene *et al.*, 2007).

The most popular stochastic methods are pixel-based and object-based methods. **Pixel-based methods** are used for the stochastic modeling of discrete (e.g. rock types) and continuous variables (e.g. porosity, permeability, and fluid saturations) (**Figure 2**). Variograms are used to describe the geological continuity of “homogeneously heterogeneous” properties. This means that variograms are best suited for describing the

geological continuity of petrophysical properties within relatively homogeneous layers or major flow facies. This variogram quantifies the average square difference between measurements as a function of their separation distance. Variograms should not be used to describe facies geometry unless the facies distribution itself is fairly homogeneous (e.g. nearshore environment). Therefore, variograms are typically used to describe the continuity of porosity and permeability within layers or facies bodies (Caers, 2005).

Object-based methods are characterized by the introduction of objects replacing a background, which commonly represents the most laterally extensive facies (**Figure 2**). This approach is called also Boolean (Falivene *et al.*, 2007). Thus these models import geologically realistic shapes and facies associations directly into the reservoir model by means of objects. These objects are then moved around and locally transformed to match the local data (wells and seismic). Object-based methods provide realistic shapes but are harder to constrain to local reservoir data, such as dense well data, high-quality 3D/4D seismic, and production data (Caers, 2005). Therefore, object-based methods typically are applied with few wells and low-resolution seismic.

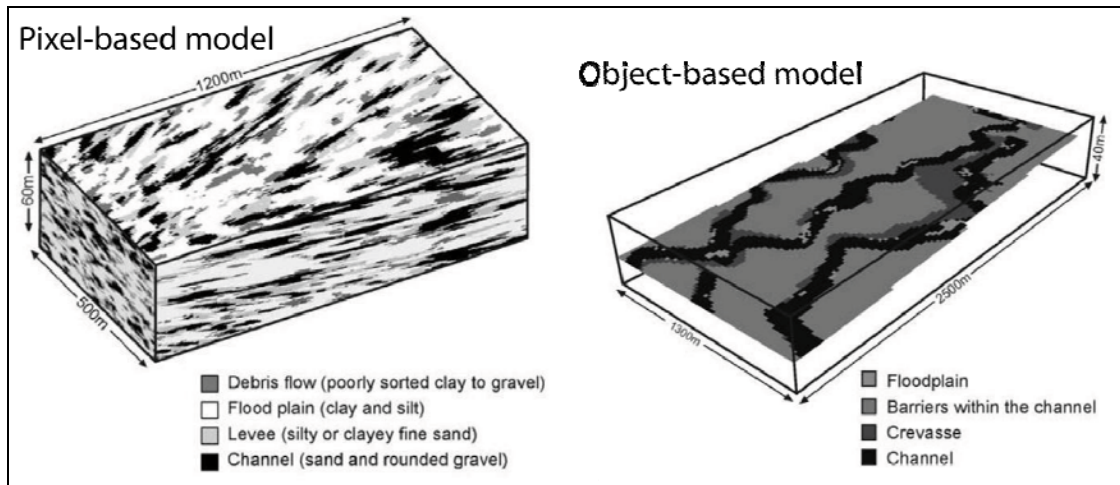


Figure 2: On the left: Three-dimensional facies simulation showing the architecture of alluvial fan deposits obtained by using a stochastic pixel-based modeling method. On the right: Horizontal section showing facies architecture from a three-dimensional model obtained by using a stochastic object-based modeling method designed to reproduce channelized depositional systems (Falivene *et al.*, 2007).

Another stochastic method which has been developed recently is the 3D training-image approach also called **Multi-point statistics (MPS)**. It is a tool for geologists to communicate their interpretations of geological heterogeneity style as a full 3D image. MPS are used to create simulations of spatial geological and reservoir property fields for subsurface reservoir modeling. MPS uses 1D, 2D or 3D “training images” as quantitative templates to model subsurface property fields (**Figure 3**). MPS modeling captures geological structures from training images and drops them to data locations. Then, the aim of geostatistics is to build reservoir models that mimic the geological heterogeneity of the 3D training image and, at the same time, constrain such models to actual location-specific reservoir data (Caers, 2005).

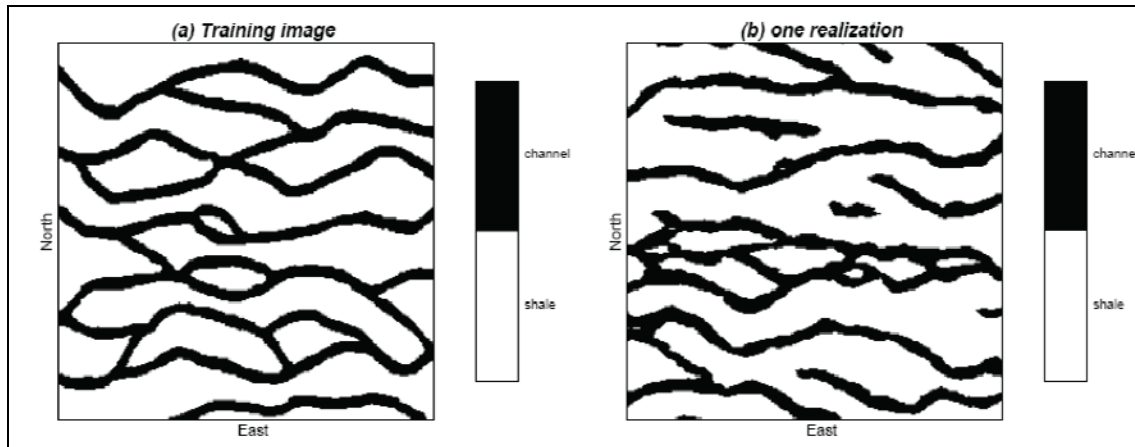


Figure 3: (a) Training image of fluvial type reservoir. The indicator statistics were calculated from this image. Two categories were represented. White represents shale deposits, and black represents black deposits. (b) Indicator-based image created using multiple-point statistics (Caers & Zhang, 2002).

A fourth stochastic method is the **process-based method**. Process-based models construct images of heterogeneity through mathematical models of the geologic processes governing sedimentary basin formation and filling (Figure 4). Process-based models using fundamental laws concerning hydraulic flow are used to model sediment transport and deposition in three dimensions. Most of these models are based on simplified versions of the Navier-Stokes equations describing flow in three dimensions for an isotropic Newtonian fluid (Labourdette, 2007). Sediment transport and deposition pose the greatest problems for hydraulic process models because it is particularly difficult to scale up the timing of processes and sediment transport. In any case, because of the attempt to reproduce more accurately sedimentary processes, this method allows a better identification and understanding of key physical parameters and providing possibly a better prediction of reservoir architecture.

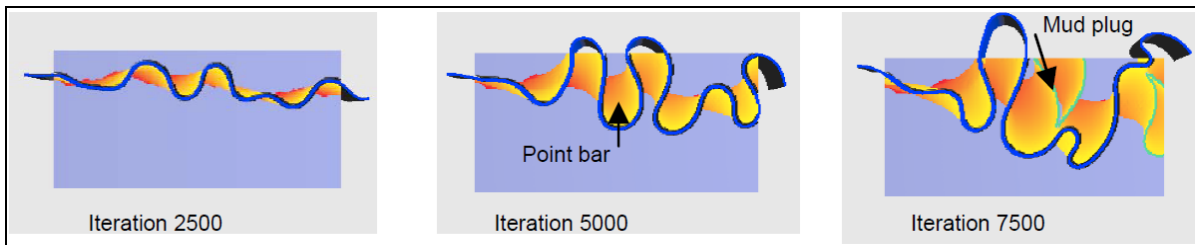


Figure 4: Top view of a channel meandering in time, depositing point bars (red to yellow) and mud plug (green) in abandoned loops obtained by using a stochastic process-based modeling method (Rivoirard *et al.*, 2008).

B. Flumy model: a realistic process-based stochastic model

MINES ParisTech developed a new generation of models, both stochastic and process-based. The prototype software including this new approach is called Flumy. This

process-based stochastic model simulates meandering channelized reservoirs at the oil reservoir scale.

Thanks to the combination of process-based and stochastic approaches, Flumy can simulate realistic sedimentary bodies and their arrangements. A limited number of key parameters generate various sedimentary architectures and can condition the model to seismic and well data (Mines ParisTech website, 2009).

The model is reproducing the depositional processes based on the evolution in time of the channel by migration, cut-off and avulsion, and on the deposition of point-bar sand, mudplug, crevasse splays, overbank alluvium and organic matter.

1. Concepts

The process-based stochastic model makes use of different sources of scientific knowledge including: physical processes, sedimentological processes, as well as a number of results and observations reported in the literature that are desirable to provide a realistic model. Practical consideration of the occurrence of levee breaches, and the shape and dimensions of crevasse splays, gives some insight into the number of parameters, whose values can be chosen to be constant or variable. The variability in the model is defined by randomizing parameters. For instance, the intensity of an overbank flood (i.e. the aggradation at levees) can be taken as fixed or be randomized with a given mean. Randomness is especially helpful to generate events whose occurrence is not exactly predictable: for example random selection of the location of a levee breach among a population of channel points with local maximum velocity, or the random generation of overbank floods with a given frequency. Then an explicit randomization of parameters allows multirealizations of the model (Cojan *et al.*, 2004).

In Flumy, the model is constructed with a truncated Gaussian simulation embedding the results of the genetic modeling of channels. The methodology is to use the numerical geological model generated with the genetic approach as a synthetic model on which is computed a 3D grid of proportions or probabilities of facies (Doligez *et al.*, 2007).

First a channel centerline spatial evolution model is built and integrates migration, avulsion, aggradation and incision processes. Then, several deposition models allow to construct progressively a comprehensive fluvial architecture along this centerline. The model produces channel bars, overbank flood deposits, crevasse splays, organic lowland deposits, etc.

Though the whole system is controlled by a very restricted number of parameters, it can reproduce various fluvial architectures. Then, combined with the stochastic approach, it generates quickly several distinct realizations of a 3D block with fluvial deposits. Some parameters can be inferred from global statistics and especially vertical proportion curves (Cojan, 2004). Then introducing a stochastic component on channel spatial evolution, the location of channelized deposits can be constrained and a certain type of well data can be honoured.

2. Input parameters

The Flumy model is based on the hydraulic model from Ikeda (Ikeda *et al.*, 1981). The channel is considered as its median line. This skeleton is associated with a facies model simulating the different deposits, according to the hydraulic conditions computed for the channel, the topography of the floodplain, and using a stochastic component in deposition (Doligez *et al.*, 2007). This allows the simulation of the sedimentation and erosion processes occurring during each lateral migration event of the channel. This process leads to the formation of meanders. The vertical aggradation ratio is computed as a function of the accommodation space, and is filling the space between the channel itself and a given equilibrium profile. The parameters are the spatial time-dependant characteristics of the accommodation space, the intensity and frequency of the flooding events, and the frequency of the regional avulsions.

From a practical point of view, the floodplain is described as a grid parallel to a slightly dipping reference plane. A channel to be initialized is flowing in a given direction. At each time step, migration is performed as a function of locally defined erodability. When overbank flooding occurs, alluvium is deposited on the floodplain, with thickness and granulometry decreasing exponentially from the channel. The rate of aggradation may be constrained by the distance between the elevation of the floodplain and an equilibrium profile parallel to the reference plane which can vary through time (Doligez *et al.*, 2007). Peat may be deposited in the lowlands. At some time a levee breach may occur within the domain producing either a chute cut-off, or a crevasse splay (**Figure 5**). Regional avulsions may also be caused by levee breaching upstream of the domain.

The main simulated deposits are:

- point bar, made of coarse sands on the convex banks of meanders,
- channel lags,
- overbanks deposits created during the flooding,
- mud plugs and sand plugs at the meanders cuts,
- wet land deposits such as peat located in the topographic lows.

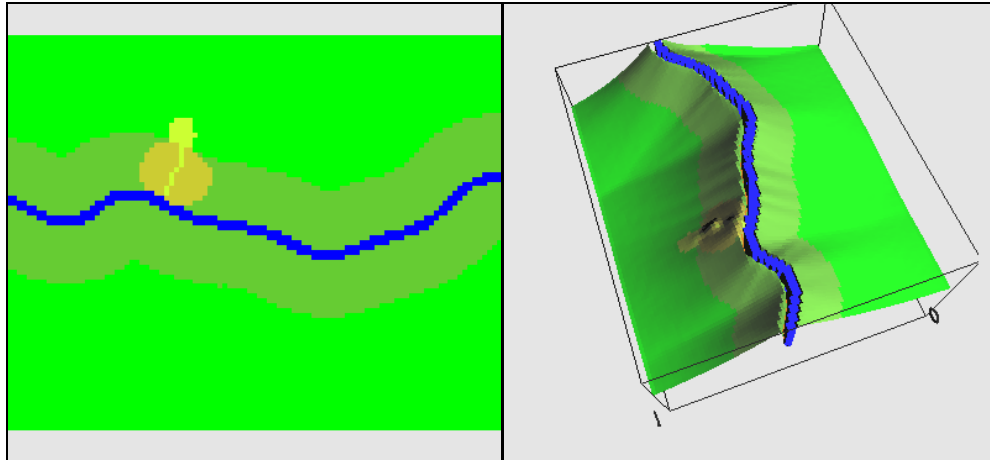


Figure 5: On the left: top view of a channel meandering (blue), its crevasse splay (orange to yellow), its levee (dark green) and its overbank deposits (light green); On the right: 3D view of a channel aggradating (Flumy tutorial, 2009).

The accommodation available for sediment accumulation is controlled by the elevation of the channel, its bankfull depth and the nature and intensity of overbank floods. The formation of floodplain is the product of the interaction of the accumulation of vertically accreted sediment and lateral reworking. Understanding the relationship between both processes is critical to explain how the architecture and composition of alluvial suites can change in response to allocyclic or autocyclic controls (Lopez *et al.*, 2002). For example, low intensity and frequency for overbank flood makes that the channel has the time to migrate all over its floodplain thus sandy point-bar deposits are preponderant. On the contrary, frequent overbank floods lead to quick vertical aggradation of the floodplain, thus leading to the deposition of a great proportion of clayey material.

III.Characterisation of meandering and braided systems

The major difficulty presented by fluvial deposits is the degree and wide range of complexity possible in overall architecture and internal heterogeneity. Fluvial hydrocarbon reservoirs are renowned for internal anisotropy and for possessing sporadic permeability barriers that can only be detected after many well have been drilled.

A. Fluvial environment

Fluvial processes involve streams and stream deposits. However, many important factors affecting streams (gravity, gradient, discharge, load, and channel geometry) affect any unidirectional flow, including run-off from melting glaciers or density flows along deepwater channels. From high mountain valleys to deepwater fans, moving fluid can build levees, meander, branch, shift courses, and adjust channel geometry to discharge, all in response to the same causes (Swanson, 1993).

When the channel migrates, it incises the outer side of the meanders, while depositing point bars in the inner side. The succession of these sigmoid deposits form complex shapes, the connectivity of which is important, as they are usually populated with sand having good reservoir properties. Where levee breaching occurs, crevasse splays are immediately deposited, and possibly followed by an avulsion. From time to time, an overbank flood occurs, resulting in the deposition of sediments over the floodplain and causing the aggradation of the system (increase of its level). The granulometry and the thickness of the deposit are decreasing away from the channel (as a negative exponential, in the model). This tends to increase the difference of height between the levees (borders) of the channel and the surrounding plain, until the phenomenon is compensated by an avulsion lowering the elevation of the channel on the plain (Cojan *et al.*, 2004). Finally lowland deposits such as organic matter, which constitutes good geological markers, may cumulate in the lowest parts of the floodplain in the interval between two overbank floods.

In any fluvial system, the deposit architecture will be a result of the interplay between aggradation rate, frequency of channel belt avulsions and the rate of channel migration (Figure 6).

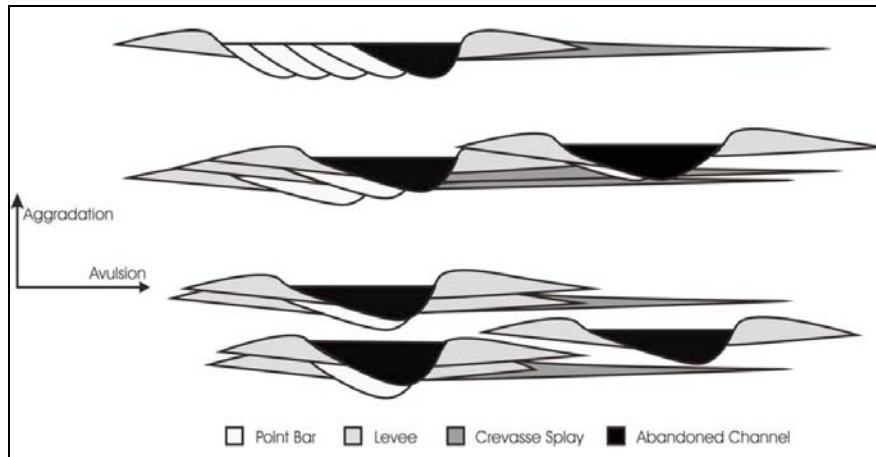


Figure 6: the effect of rate of avulsion and rate of aggradation on the evolution of architectural elements. Top part: low rate of aggradation and avulsion allow for the development of extensive later accretion elements; Middle part: higher rate of aggradation with increased avulsion; Bottom part: high rate of aggradation results in isolated sand bodies (Pyrzcz, 2003).

The classification recognizes three basic stream types based on channel morphology, nature of load, and character of associated deposits: straight streams, braided streams and meandering streams (**Figure 7**). Their distinctions relate to their coarse-grained components, stream-channel shape, nature of load, stream slope, discharge, nature of bank material, and geomorphic setting.

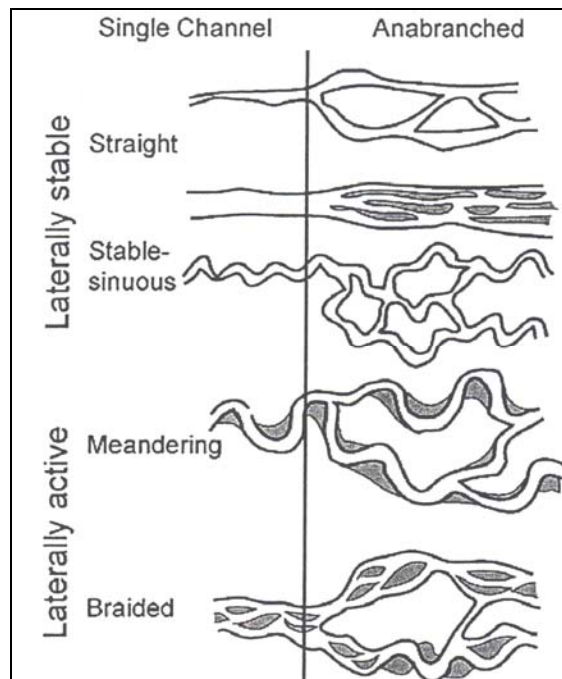


Figure 7: Channel pattern classification recognising four classes of channels (Labourdette, 2007).

1. Braided river system

Braiding occurs in streams with a relatively high discharge, large amounts of coarse bed load, relatively little suspended load, and a relatively high gradient. Braided streams generally have wide and relatively shallow channels with a high width/depth ratio and a rectangular shape (Swanson, 1993) (**Figure 8**). These channels accumulate sediment mainly by vertical accretion (**Figure 9**). Braided stream facies can be found alone or in composite reservoirs in major fields (Miall, 1977).

The sinuosity is the ratio of channel length to valley length. It is generally accepted that braided rivers have “low” sinuosity. In general braided rivers are observed in high-energy geomorphic environments and are associated with coarse-grained alluvial systems.

2. Meandering river system

Meandering streams result from natural phenomena that give flowing water in unconsolidated media the tendency to meander. These sinuous stream courses, with their point-bar reservoir deposits, occur when the slope is low and streams cut through fine-grained cohesive bank and bed material. Meandering streams usually carry more suspended-load than coarse bed-load material (Swanson, 1993) (**Figure 10**). Meandering river channels have a much lower width/depth ratio than do braided rivers, but their deposits have a similar broad, lenticular geometry because of the tendency of river meanders to migrate, producing channel-fill sequences by lateral accretion (Miall, 1977).

Coastal or deltaic plains far from the source of the clastic load are most favorable for development of meandering streams and their point-bar deposits (Swanson, 1993). Consequently, their reservoir facies usually are finer-grained than most braided-stream deposits.

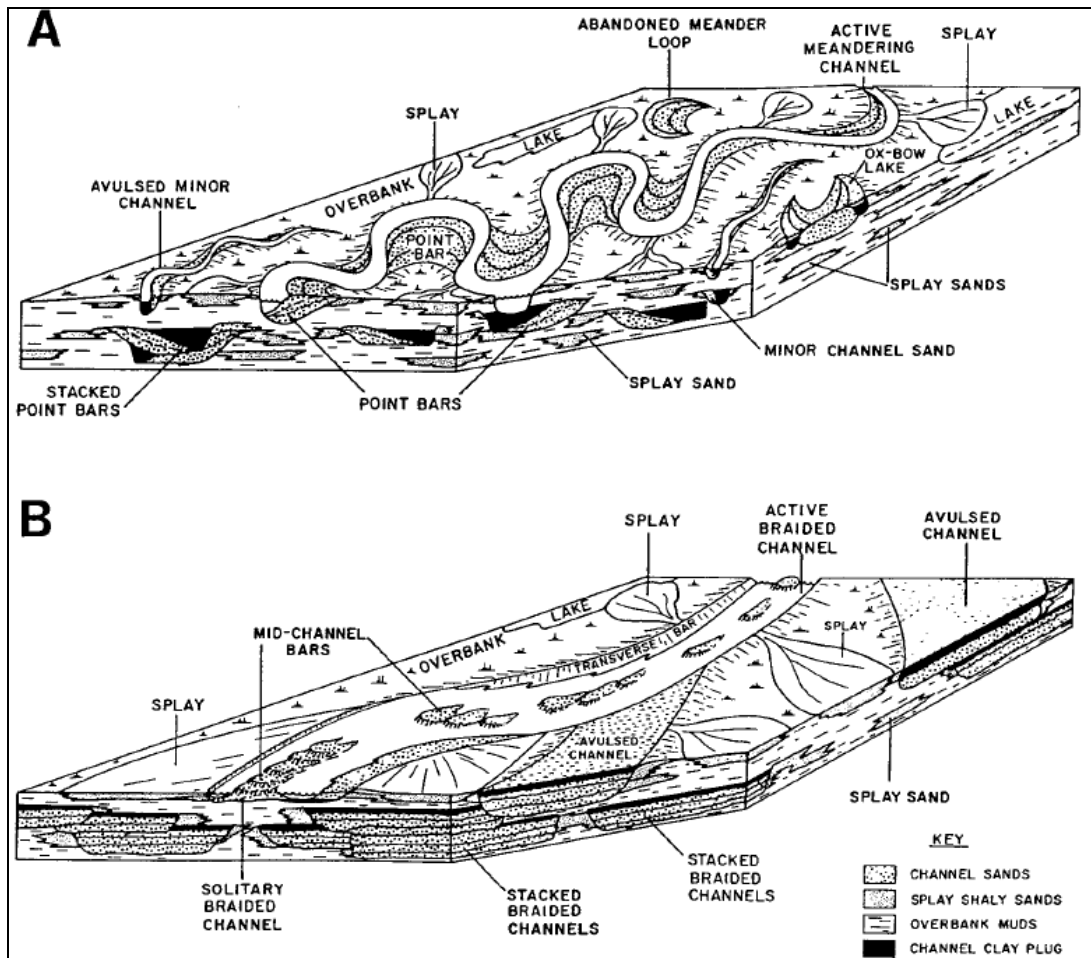


Figure 8: Schematic block model of A) meandering and B) braided channel systems illustrating lateral and vertical relationships among building blocks (no scale implied) (Davies *et al.*, 1992).

CHANNEL TYPE	COMPOSITION OF CHANNEL FILL	CHANNEL GEOMETRY			BEDDING CHARACTER	LATERAL RELATIONS
		CROSS SECTION	PLAN VIEW	SAND ISOPACH		
HIGH SINUOSITY (Mixed Bedload/Suspended Load) CHANNELS	HETEROLITHIC (CONGLOMERATE, SAND, SILT AND MUD)	MODERATE WIDTH/DEPTH RATIO (5 : 1)	SINUOUS	COMPLEX-BEADED TO DISCONTINUOUS PODS	LATERAL ACCRETION DOMINATES	OVERBANK DEPOSITS VOLUMETRICALLY EXCEED CHANNEL FILL
LOW SINUOSITY (Bedload) CHANNELS	HOMOLITHIC (DOMINANTLY SAND)	HIGH WIDTH/DEPTH RATIO (25 : 1)	STRAIGHT OR LOW SINUOSITY	BROAD, ELONGATE CONTINUOUS	VERTICAL ACCRETION DOMINATES	CHANNEL FILL VOLUMETRICALLY EXCEEDS OVERBANK DEPOSITS

Figure 9: Comparison of channel sand bodies in high sinuosity (meandering) and low sinuosity (braided) systems (Davies *et al.*, 1992).

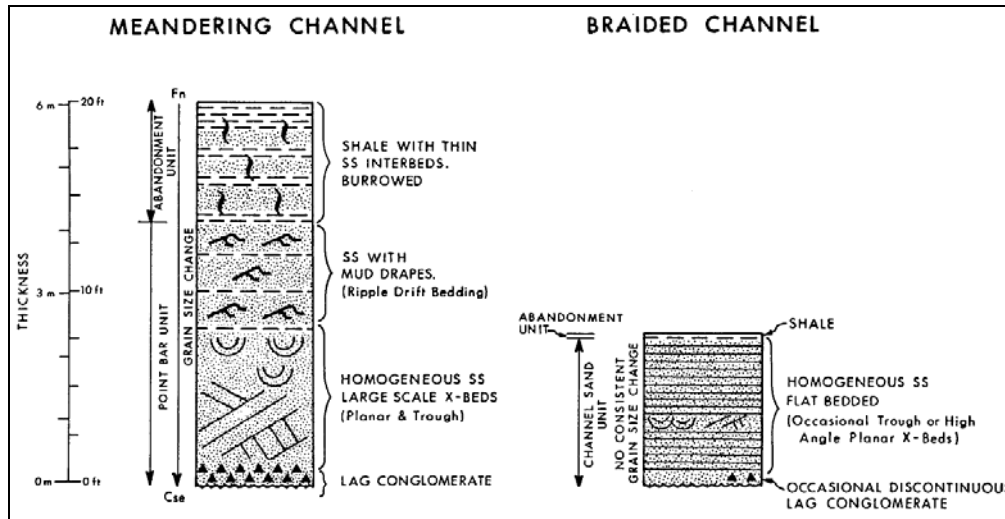


Figure 10: Vertical profiles illustrating the internal characteristics of Travis Peak meandering and braided channel deposits (Davies *et al.*, 1992).

B. Fluvial sequence stratigraphy

Sequence stratigraphy as a process-oriented stratigraphic analysis of the sedimentary record predicts stratal architecture and its origin within a time framework of unconformity surfaces (Rhee, 2006). This analysis is imperative to recognize sequential development pattern of systems tracts to predict facies relationships that are related to accommodation changes.

Fluvial sequence stratigraphic models can predict fluvial architecture and its geometry based on the change in the accommodation rate or base-level. The essential concept of the models is that during times of low accommodation rate, the channels will amalgamated, while during times of high accommodation rate, channels will become isolated and floodplain deposits will be more widespread (Figure 11). According to the model, stratigraphic variations of the proportion and interconnectedness of channel sandbodies encased by floodplain deposits reflect the changes in the ratio of accommodation to sediment supply rate (A/S) with time.

Accommodation in inland fluvial settings is commonly defined by (stratigraphic) base level which is an undulating, lithosphere surface representing equilibrium between aggradation and degradation (Rhee, 2006).

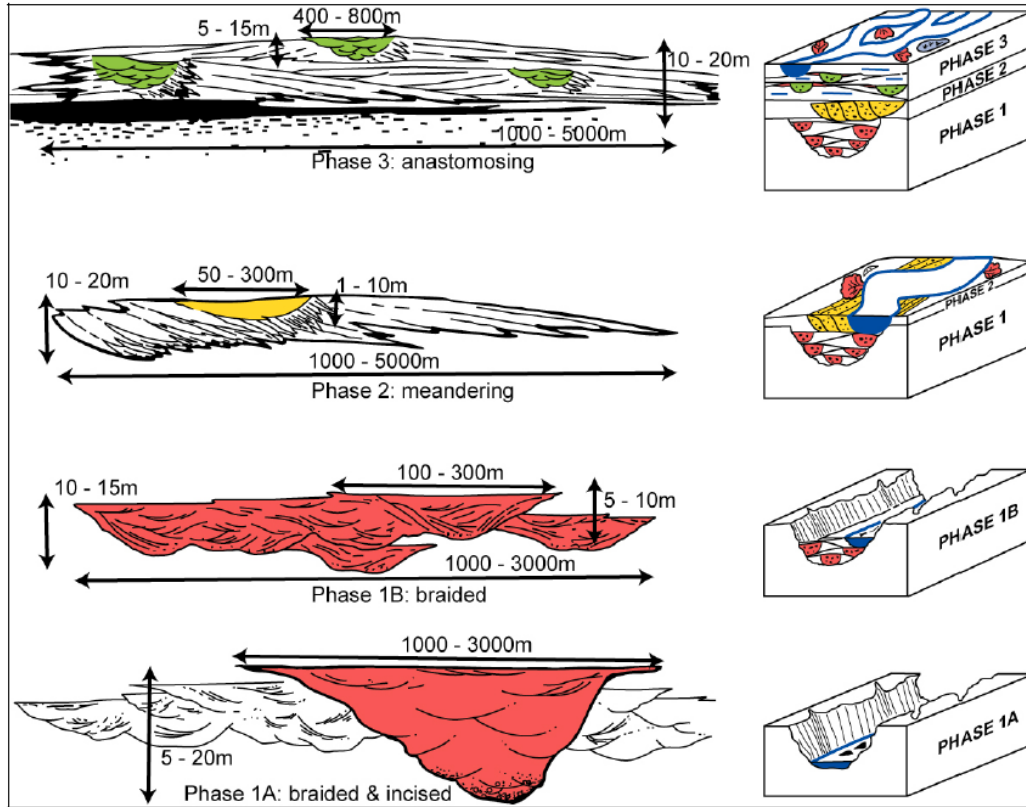


Figure 11: evolution of the fluvial style in a relative sea-level cycle (Doligez *et al.*, 2007).

Existing models of fluvial sequence stratigraphy are based on the importance of avulsion frequency, sedimentation rate and the ratio of channel belt and floodplain width in stacking of channel bodies. It is assumed that channels avulse more frequently with increases in sedimentation rate, promoting the formation of isolated meandering channel fills. However the relation among the avulsion frequency, the sedimentation rate and resultant channel fill architecture isn't so simple. These control parameters influence mobile channel belts, but for fixed-channel systems they are less effective than the local geomorphic factors such as bank erodibility and channel aggradation. On the other hand, variation in channel pattern or architecture of systems tracts of the models cannot be readily and securely related to the change in accommodation or vice versa because different channel types of various dimensions coexist simultaneously or within a limited stratigraphic range (Rhee, 2006).

IV. Case study: The Schooner Field

The fluvial Barren Red Measures (BRM) form the main reservoir interval in several gas fields within the Silverpit Basin of the Southern North Sea. The reservoir is characterized by a low to moderate net to gross sand ratio and a high degree of internal, lateral and vertical reservoir variability. The braidplain deposited sandstone bodies are the main contributing facies within the BRM and the understanding of their spatial distribution and interconnectivity is an essential pre-requisite for effective development of the reservoir. Due to a combination of poor seismic quality (resulting from complex Zechstein salt diapirism in the overburden) and channel body size generally being below the resolution of seismic, the sand bodies can only rarely be imaged using seismic techniques (Stone & Moscariello, 1999). As a result it is necessary to model the channel body distribution stochastically.

A. Regional geology

The Schooner Field lies in Blocks 44/26a and 43/30 of the UK sector of the southern North Sea (**Figure 12**). This field was previously owned by Shell and now by Tullow oil. It is Shell UK's first Carboniferous gas development in the North Sea. It is located in the Silver Pit Basin approximately 150km off the South Yorkshire coast (Moscariello, 2003).

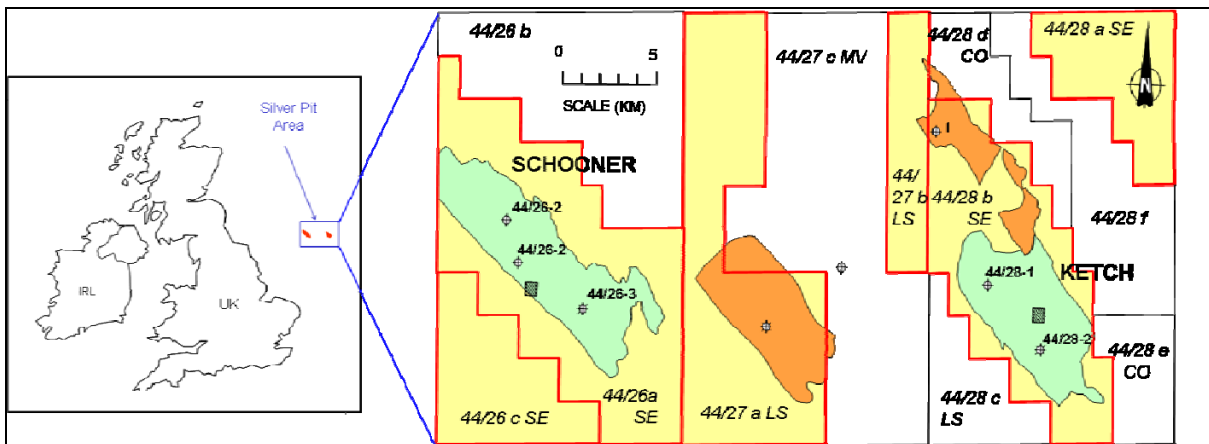


Figure 12: Schooner Field location in the North Sea (Stone & Moscariello, 1999)

1. Structure

The Silver Pit Basin is a loosely defined area situated to the north of the main Rotliegend Group (Permian) gas fields of the late Cimmerian Intra Shelf and the late Cretaceous to Tertiary Sole Pit Inversion Zone (**Figure 13**) (Moscariello, 2003).

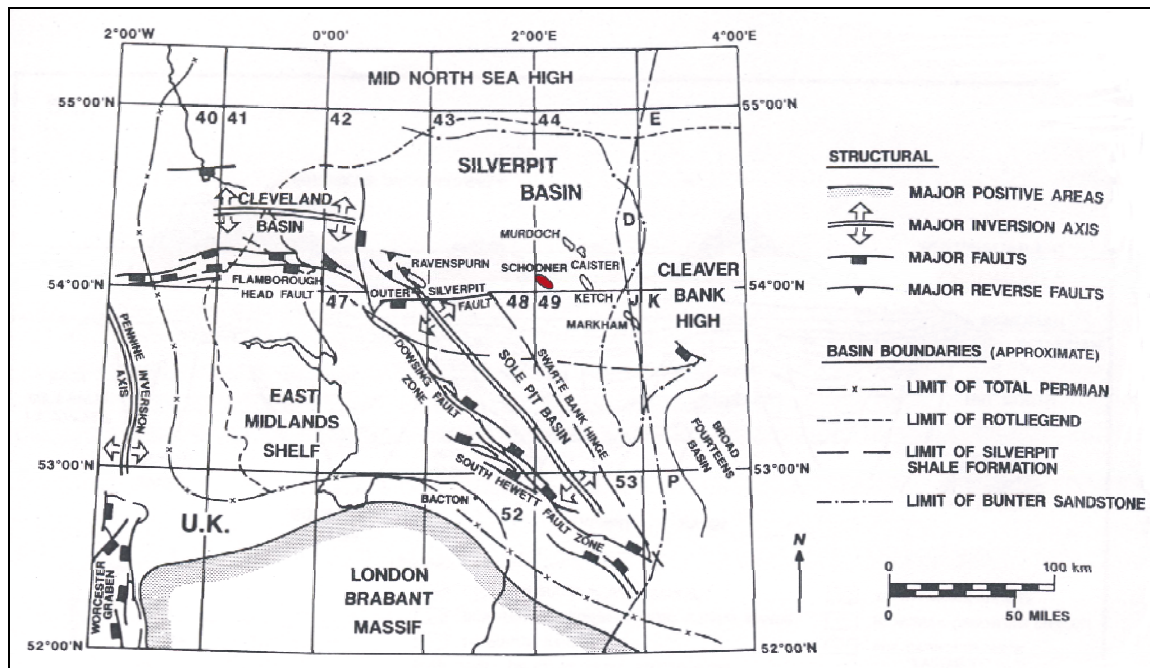


Figure 13: Regional features map of the Southern North Sea with pointed in red the Schooner Field (Bailey *et al.*, 1993).

The Silver Pit Basin developed in an equatorial to subequatorial position north of the then active Devonian to Carboniferous Hercynian orogenic belt. This basin was strongly influenced by this orogen and its northward migration. The area suffered lithospheric extension in late Devonian to mid-Carboniferous times. Thermal subsidence of the Southern North Sea continued into the Westphalian with the deposition of typical cyclical Coal Measures sediments of Westphalian A/B age (Bailey *et al.*, 1993).

Active fault-bounded half-grabens and tilted fault blocks developed along a dominant NW-SE grain, succeeded in the Upper Carboniferous by a post-rift phase of regional sag caused by thermal re-equilibration. This resulted in the creation of two lowland areas separated by the NW-SE trending Murdoch fault system. The Schooner Field lies immediately south of this high Variscan tectonism deformed the Upper Carboniferous strata by both folding and faulting along a dominant NW-SE fault trend. The early-formed basement faults at least intermittently controlled the location of channel belts during the deposition of the Upper Carboniferous.

Late Cimmerian reactivation of the Variscan faults, together with Tertiary Alpine wrench movements along NW-SE trending basement fault zones, resulted in the formation of tilted fault blocks at Saalian Unconformity level. These are usually bounded by complex reverse faults and form the principal proven gas-bearing structures in the Silver Pit Basin (Moscardiello, 2003).

2. Stratigraphy

The stratigraphical succession in the Schooner Field area consists of the Carboniferous (our zone of study), the Permian, the Triassic, the Jurassic, the Cretaceous and the Tertiary-Quaternary (Figure 14).

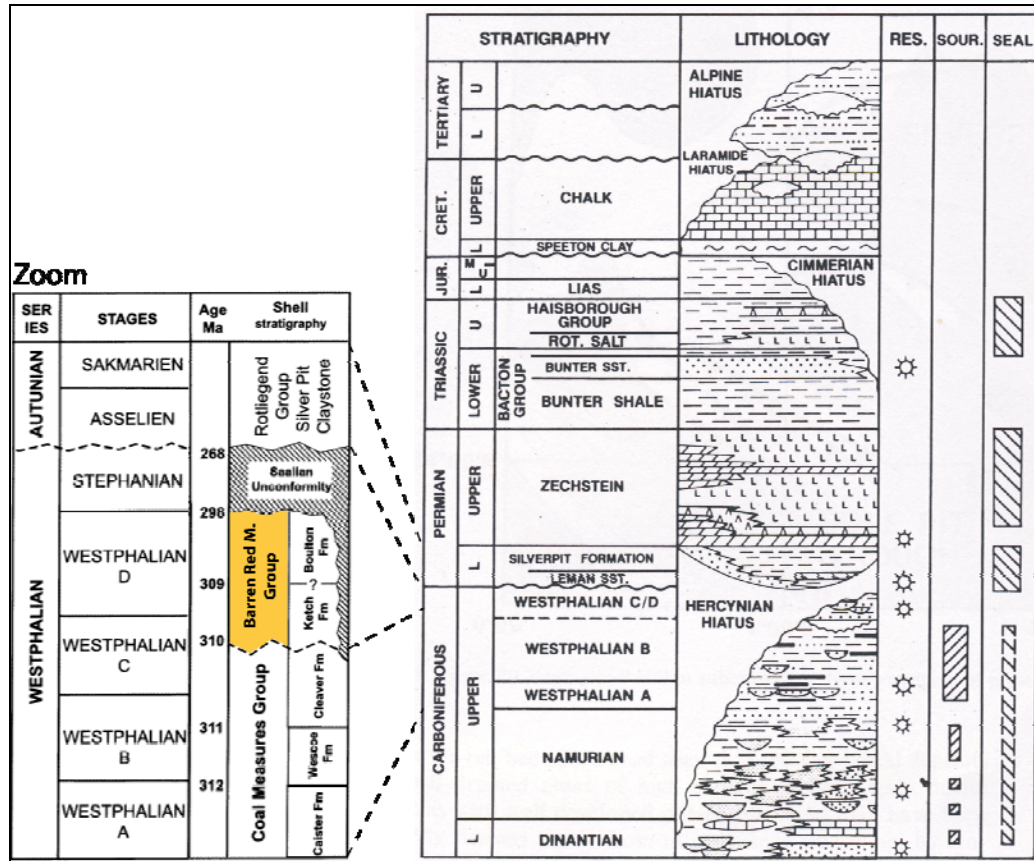


Figure 14: On right: Silver Pit Basin stratigraphic column highlighting reservoir, source and seal development (Bailey *et al.*, 1993); on left: details of the chronostratigraphic setting of the Westphalian Barren Red Measures and Coal Measures (Moscariello, 2003)

a) Carboniferous

The fluvio-deltaic Millstone Grit Group of Namurian age is overlain by a thick fluvio-deltaic and fluvial Westphalian succession that can be subdivided into the Coal Measures (CM, Westphalian A, B and early C) and Barren Red Measures (BRM, Westphalian late C and D).

The Coal Measures Group is subdivided in three formations. These are, from bottom upwards: the Caister Formation (Westphalian A), the Westoe Formation (Westphalian B) and the Cleaver Formation (late Westphalian B-early and middle Westphalian C).

The transition from Westphalian A to late Westphalian B interval shows a gradual decrease in channel size and sand content (down to 5-10% net-to-gross) with a corresponding decline in reservoir potential (Moscariello, 2003).

During the late Westphalian the climate began to dry. This was partially in response to the drift of the area into a higher latitude but also because the basin now lay in the rain shadow of the Hercynian mountains. The change in climate and tectonic setting is reflected in the shift of deposition from coal-bearing deltaic swamp to arid fluvial plain. This change, which took place around the Westphalian B/C boundary, is gradational and probably diachronous. No major regional unconformity occurs between the two lithofacies associations, deposition was continuous, with interfingering of red and grey facies (Bailey *et al.*, 1993). Thus from the late Westphalian B onwards, a gradual increase in sand content is recorded into the Westphalian C which is represented here by Upper Coal Measures (21% net-to-gross) and lower Barren Red Measures Group (28-38% net-to-gross) (Moscariello, 2003). Therefore the main reservoir belongs to the Westphalian C intervals.

The variable thickness of the Westphalian succession is primarily controlled by the Saalian Unconformity, which progressively erodes the Carboniferous succession towards the NE. In the Schooner Field, only the sand-rich Lower Ketch Formation (early Westphalian D) is present. The measured BRM thickness ranges between 0 and 280m depending on the depth reached by the erosional Saalian Unconformity (Moscariello, 2003).

b) From Permian to Quaternary

The lower Permian is represented by the Silverpit Formation (Rotliegend Group), which developed in a desert lake as interbedded evaporites and claystones. This is overlain by the Zechstein Group, which in this area displays a variable thickness ranging between 1035 and 1700m forming a major elongate salt swell overlying the field. Extensive movement of the salt, coupled with faulting has contributed to the deformation and displacement within the salt of mid-Zechstein couplets of anhydrite and carbonates (Moscariello, 2003).

At the base of the Triassic is the Bacton Group which consists of about 455m thick succession of reddish-brown floodplain and lacustrine mudstones and fluvial sandstone. The Bacton Group is overlain by the Haisborough Group, represented by marine and subordinate lacustrine evaporites, mudstones and limestones. The Upper Triassic and the entire Jurassic succession are absent having been eroded during the Lower Cretaceous uplift (Cimmerian Unconformity).

The uppermost Lower Cretaceous is represented by the argillaceous Cromer Knoll Group, which is overlain by the Chalk Group (Upper Cretaceous) consisting of a thick sequence of recrystallized and chert-rich limestones, chalks and marls. This is locally affected by the Oligocene Unconformity.

The Tertiary is represented by the 68m thick North Sea Group, which consists of marine and glacio-marine unconsolidated argillaceous sand, clay and silt (Moscariello, 2003).

3. Petroleum system

In the Silver Pit Basin and its immediate margins, hydrocarbons have been discovered in Paleozoic reservoirs ranging from Dinantian sandstones to Zechstein carbonates. Within the Carboniferous the most significant reservoirs are fluvio-deltaic sandstones within the Westphalian and Upper Namurian (Bailey *et al.*, 1993).

The Schooner Field is a complex elongate NW-SE-trending anticlinal closure, formed by a succession of movements along Hercynian trends. Top seal at the Saalian Unconformity level is provided by the thick Silverpit Formation (Rotliegend Group) consisting of desert-lake shales and evaporates (Moscariello, 2003).

The Coal Measures Group represents 30% of bulk rock volume of the reservoir (2% of reserves), as only a short sequence of the Middle and Upper Coal Measures (Westphalian B-C) is present above the free water level (FWL). The penetrated Coal Measures are characterized by a laterally variable low net/gross ratio distribution ranging between 19 and 22%.

Most of the Schooner gas reserves (98%) are contained in the BRM (Lower Ketch Formation), which forms 70% of the gross rock reservoir volume. The BRM part of the Schooner reservoir is characterized by a low to moderate net/gross reservoir ratio (30% mode) and a high degree of internal, lateral and vertical reservoir variability. Reservoir quality in the sandstones of the Barren Red Measures Group is generally good to excellent, with an average porosity of 12% and permeabilities that range from 10 to 1000mD (Mijnssen, 1997).

The source-rock of the gas in the Schooner Field is the underlying Coal Measures formation (Namurian and Westphalian coals).

Over much of the area, the presence of the Silverpit Formation and a thick Zechstein salt succession precludes hydrocarbon migration from the Coal Measures into the upper reservoirs such as the Triassic Bunter Sandstone. Migration paths are supplied by the sandstones within the Westphalian BRM and CM, which have extensive areas of contact with both the coals and carbonaceous shale. Source and reservoir sandstone thus lie at the same stratigraphical level (Moscariello, 2003).

B. The Schooner Field

Sand body connectivity has been identified as the most important attribute to model in order to optimize development of the Schooner Field. The main uncertainties associated with sand body connectivity are the presence or absence of minor faults, channel width, and channel orientation.

1. Structure

The Schooner Field is an elongate NW-SE trending anticlinal closure bounded to the SW by major NNW-SSE high-angle transpressional oblique-slip faults (**Figure 15**). The structure is believed to be the result of tectonic inversion of Cimmerian and/or Tertiary age and formed by uplift along a major reserve fault trend that is probably of Hercynian origin. The closure is 16km long by 4km wide with the crest slightly offset to the SW (Mijnssen, 1997).

Within the structural closure, the Carboniferous strata have been deformed into a broad southeast plunging anticlinal swell. The main reservoir, the alluvial BRM (Barren Red Measures), forms a southeasterly thickening wedge that is progressively truncated by erosion at the Saalian Unconformity towards the NE over the crest of the structure (Moscariello, 2003).

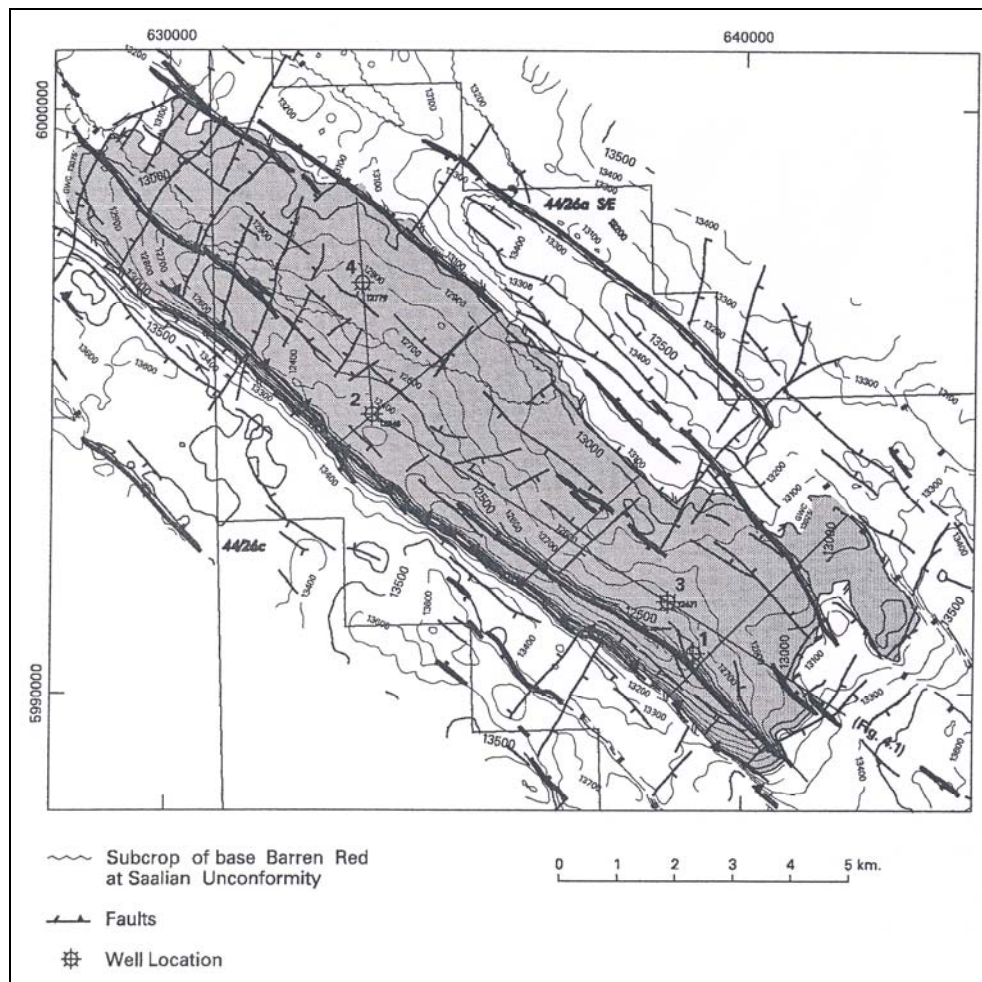


Figure 15: Structure map of the Top Carboniferous in the Schooner Area showing location of the discovery and appraisal wells (Mijnssen, 1997).

2. Stratigraphy

a) Barren Red Measures subdivision

An initial stratigraphic subdivision of the reservoir was based on the identification of potential ‘flooding surfaces’ derived from the correlation of Gamma Ray peaks within the well database. This litho-stratigraphic subdivision divided the reservoir into three units (**Figure 16**). This subdivision was used as the framework to build static and dynamic reservoir models (Stone & Moscariello, 1999).

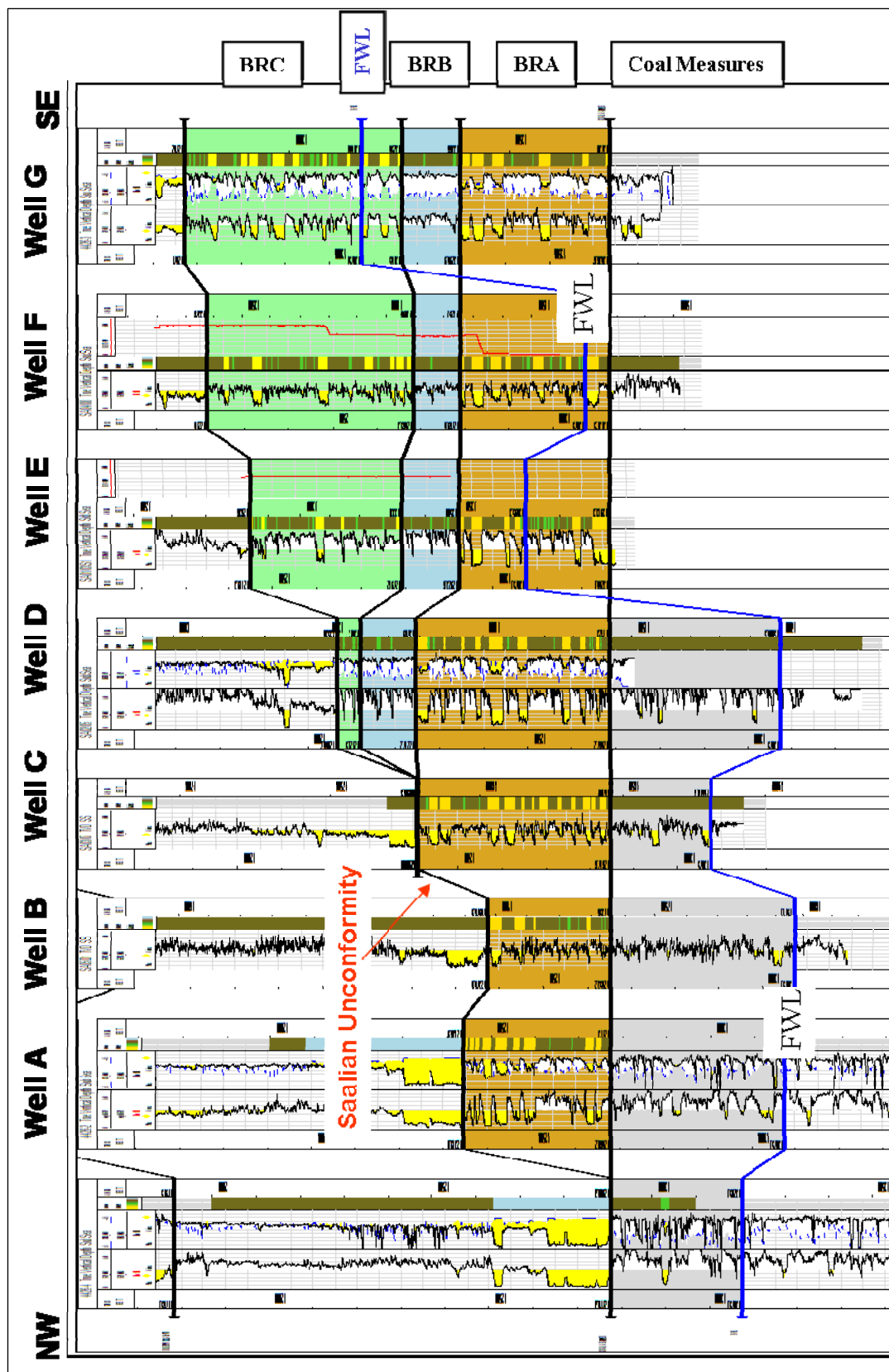


Figure 16: Lithostratigraphic correlation across Schooner Field (hung from Base of BRM) (Moscariello, 2009).

After the initial production from this reservoir the total connected reserves to wells weren't matched model forecasts. This indicated that the connectivity of modelled discrete sand bodies was not adequately represented by the model. To re-evaluate the internal stratigraphic zonation of the Barren Red Measures a chemostratigraphic correlation technique was chosen to generate a robust stratigraphic framework.

Geochemical analysis has enabled the generation of a robust, 5-zone chemostratigraphic correlation framework based on correlatable geochemical signatures in eight wells (**Figure 18**). Each zone defined broadly equivalent packages of strata, recording changes in the basin wide hydrology of the depositional system, and as a result provided a reliable, stratigraphic subdivision (Stone & Moscariello, 1999) (**Figure 19**).

Lateral distribution and vertical patterns of pedofacies types is used as an indicator of different styles of lateral and vertical aggradation rates. Thus the vertical distribution of pedofacies which is consistent with the chemostratigraphical zonation, supports the new reservoir subdivision (**Figure 17**).

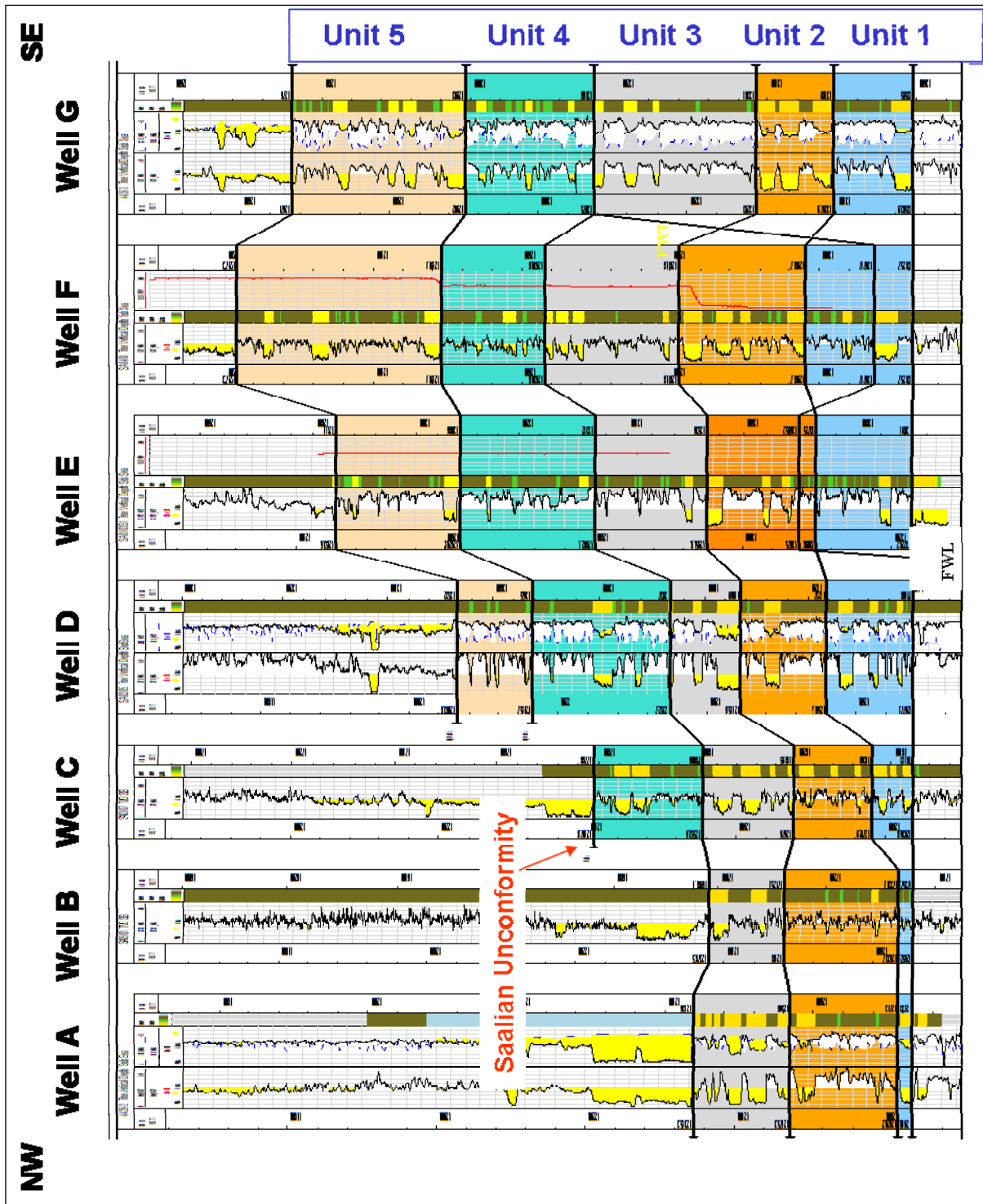


Figure 17: Chemostratigraphic correlation across Schooner Field (hung from base of BRM). Note that Units 4 and 5 are eroded towards the NW of the region (Moscariello, 2009).

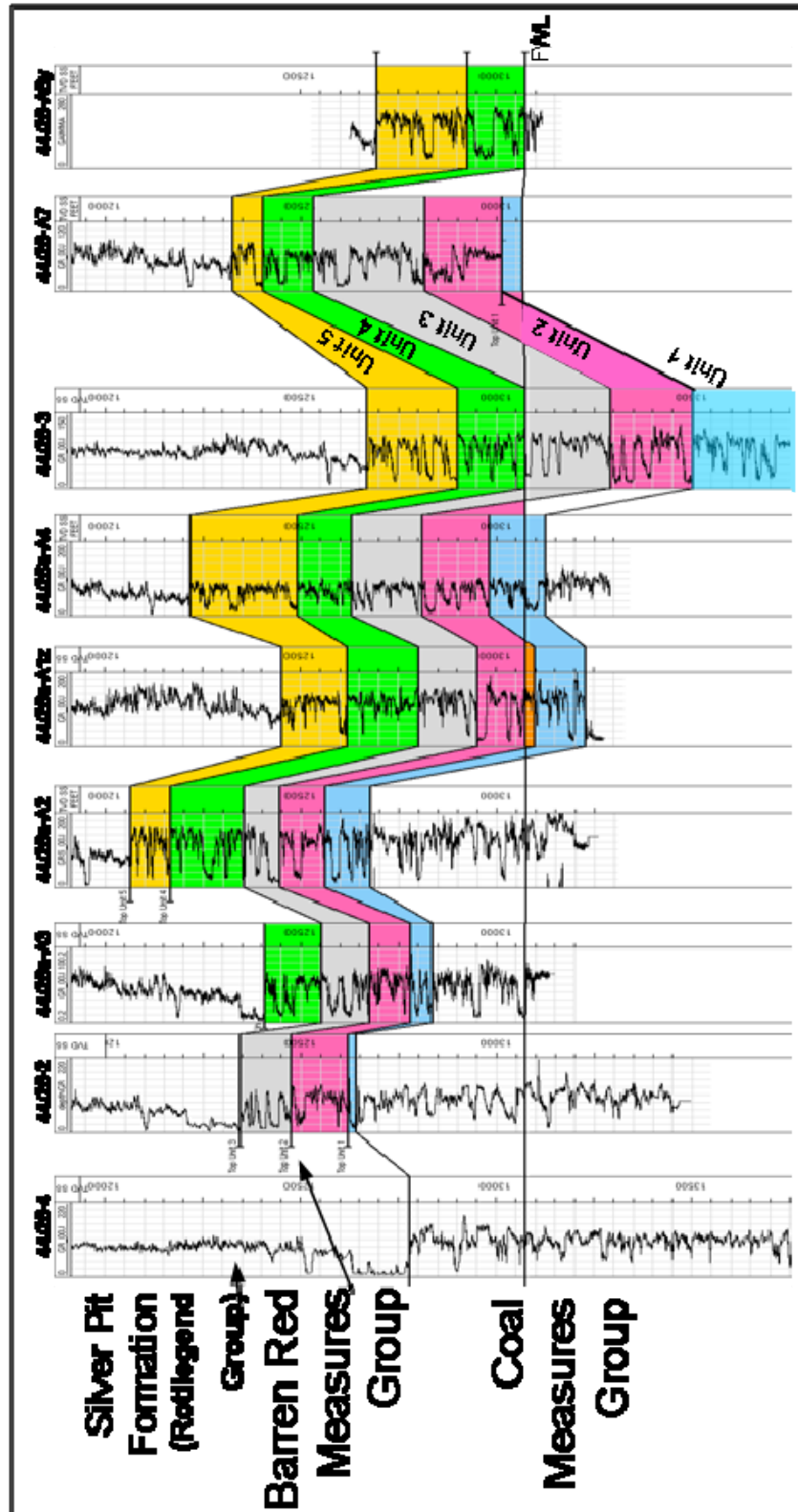


Figure 18: Chemostratigraphic correlation of the Schooner Field (Moscariello, 2009).

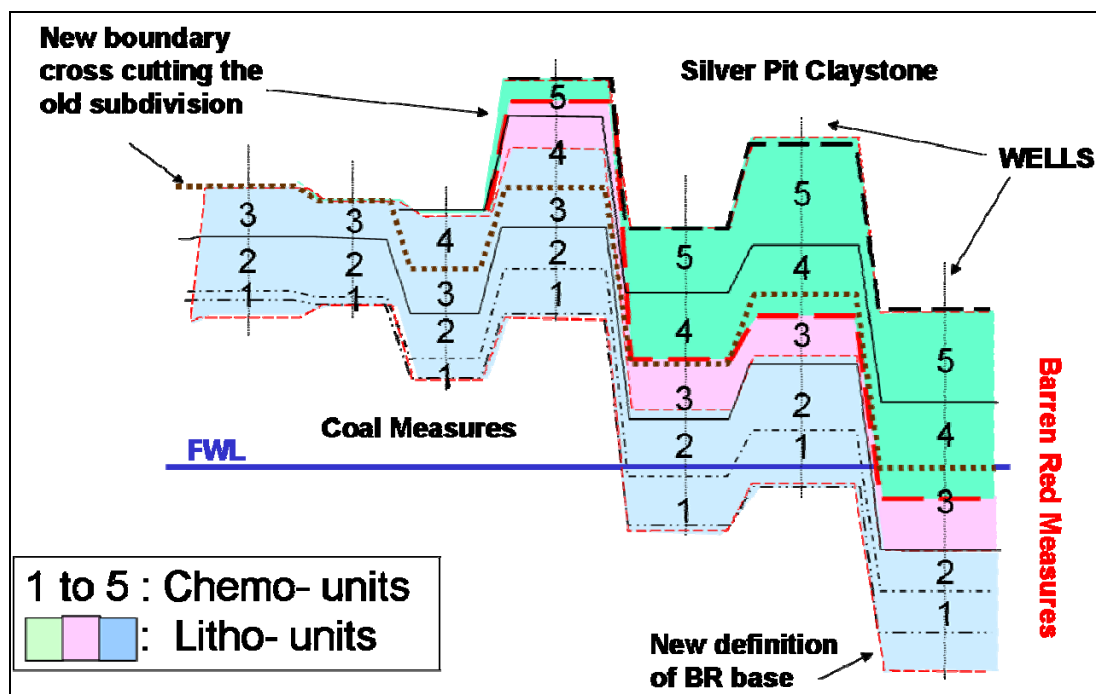


Figure 19: Lithostratigraphic and Chemostratigraphic correlation – comparison between the old and new model (Moscariello, 2009).

b) Sedimentary facies

(1) Composite low-sinuosity channel fill

This facies consists of 4.5-9m thick vertical stacks of 0.6-2.5m thick sand bodies characterized by several lithologies: poorly stratified, clast-supported, conglomerates consisting of poorly sorted, sub-angular, fine to medium pebbles and granules; trough cross-bedded sandstones and ripple-laminated medium to coarse sandstones. The sediment composition and sedimentary features of these channel fills suggest deposition in a fluvial environment dominated by competent flows associated with high energy flood events. Massive conglomerate and coarse sand with trough cross-bedding at the base of the channel fill are interpreted as the result of migration of large scale bedforms developed in braided stream channel. A blocky GR response and a clear FDC/CNL positive separation characterize this facies (Moscariello, 2003).

(2) Single low-sinuosity channel fill

Another channel facies has been identified and consists of 2.5-5m thick medium to coarse sandstone packages characterized by trough cross-bedding and ripple-lamination. In general this facies shows a fining-upwards sequence resulting in a bell shaped GR response and clear FDC/CNL positive separation (Moscariello, 2003).

(3) Proximal overbank deposits crevasse splay deposits

They are formed by 1.2-2.5m thick medium to fine-grained sandstone. They are characterized by 30-90cm thick fining upward sequences formed by homogenous, structureless, medium sand at the base passing upwards to ripple lamination and shale drapes at the top. These sequences indicate successive events of rapid deposition followed by settling processes in a temporary flooded interfluvial plain. Bioturbation and root mottling characterize this unit. A spiky GR response and a vague FDC/CNL positive separation characterize these units (Moscariello, 2003).

(4) Floodplain deposits and paleosols

These consist of laminated or massive fine-grained sandstones and horizontally laminated mudstones accumulated on a distal floodplain where temporary shallow lacustrine environments could develop. The thickest continuous succession of these sediments reaches 20m. Pedogenetic features (rootlets, bioturbation, mottling, nodules) are very common indicating the presence of vegetation occupying the floodplain. Four types of pedofacies have been distinguished according to the degree of paleosol maturity. The vertical repetition of specific trends indicates a dynamic fluvial system characterized by periodic channel avulsion over the floodplain where intense pedogenetic processes could take place. High and spiky GR response characterizes this genetic unit (Moscariello, 2003).

c) Depositional setting

The overall depositional setting of the BRM is interpreted to be fluvial, characterized by braided channels draining a low gradient alluvial plain probably developed in an endorheic basin. Within this system, major low-sinuosity channels developed. Minor single channels formed small subsidiaries flowing between the large channels. Proximal overbank deposits formed adjacent to the main channel areas during flooding events while in the large interfluves only fine-grained deposits were accumulated allowing the development of vegetated soils (**Figure 20**). Log correlation and isopach mapping indicate that the channels are predominately oriented NE to SW (Moscariello, 2003).

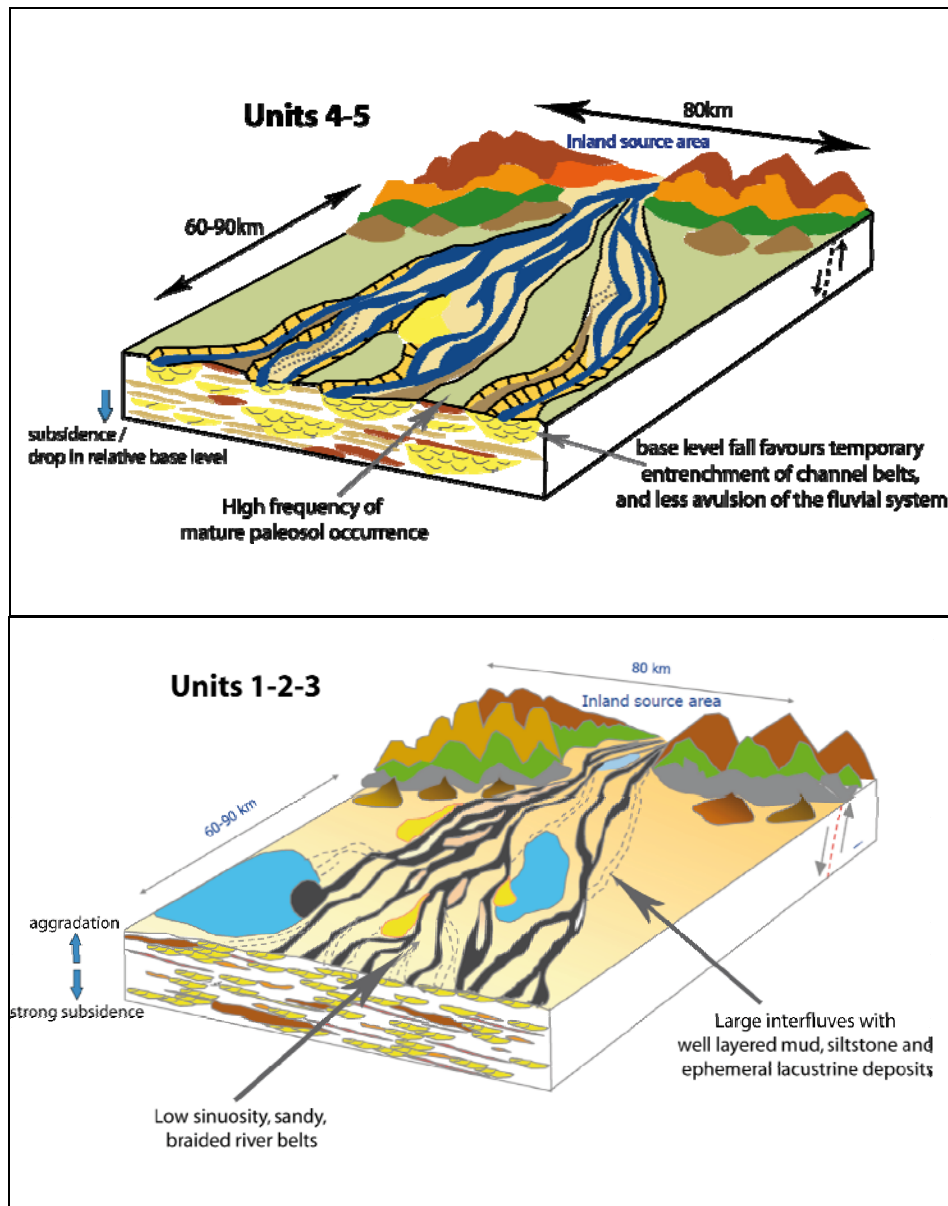


Figure 20: Schematic block diagram showing the paleogeographical setting proposed for the deposition of Units 1-2-3 (bottom part) and Units 4-5 (top part) (Stone and Moscariello, 1999).

Two main chemostratigraphical unit assemblages have been identified and are due to different sedimentary basinal settings. The lower three chemostratigraphical units (1 to 3) can be distinguished from the upper two units (4 and 5) by different internal geometry. This geometry is believed to be directly controlled by the variation of several factors over time. These are: 1) climatically driven sediment supply to the alluvial plain; 2) climatically controlled frequency of catastrophic flood events, and in turn channel avulsion; and 3) the modifications in tectonic regime, which induced changes on alluvial plain evolution and channel distribution (Moscariello, 2003).

(1) Units 1, 2 & 3

During deposition of Units 1, 2 and 3 a strong and prolonged subsidence during the Late Carboniferous resulted in large amounts of accommodation space occupied by the fluvial plain aggradation. Fluctuation in base level resulted in an alternation of braided river systems formed during relative base level (lacustrine) low stands and meandering river systems, formed during high stands. During this period, the braided river system constantly avulsed and bifurcated, resulting in a wide range of channel sizes and distribution, the latter being controlled by autocyclic processes related to climate-driven discharge into the basin (Moscariello, 2003).

(2) Units 4 & 5

During depositions of Units 4 and 5 however, the fluvial channels are temporarily confined in specific areas, forming stacked channel belts up to 6-10m thick. This is likely to be associated with longer time scale, local relative base level falls which induced minor, short lived incisions, which in turn favoured the formation of composite stacked channels. The changes in the fan topography and overall evolution of the sedimentary basin most likely resulted from a combination of climatic factors (progressive increase in aridity at the end of the Westphalian D) and increase in tectonic activity (subsidence rate, tilting) related to the early Variscan orogenesis (Moscariello, 2003).

V. Data and workflow

Based on subsurface data provided by Andrea Moscariello and on a 3D model built by a MSc student, Mohammed Radam, the input parameters needed for modeling have been collected and synthesized. A bibliographical research allows to complete the necessary information.

A. Workflow

Three-dimensional reservoir modeling comprises a broad field of expertise in which geostatistics is one of several key components. Many sources of data are available for reservoir modeling.

Concerning the Schooner Field, different kind of data have been provided: well logs, structural model, sequence stratigraphy and depositional model. These data have been used through the different steps of the project (**Figure 21**).

The following steps have been followed to reach the objectives of the project:

- Review of fluvial sedimentary processes (bibliographical research)
- Familiarisation with the Flumy software
- Determination of the input parameters corresponding to the case study
- Data preparation: well logs, topography surface, porosity data
- Facies modeling with Flumy: pessimistic, medium and optimistic cases
- 3D static modeling in Petrel
- Quantitative analysis in Petrel: volumetric, uncertainties

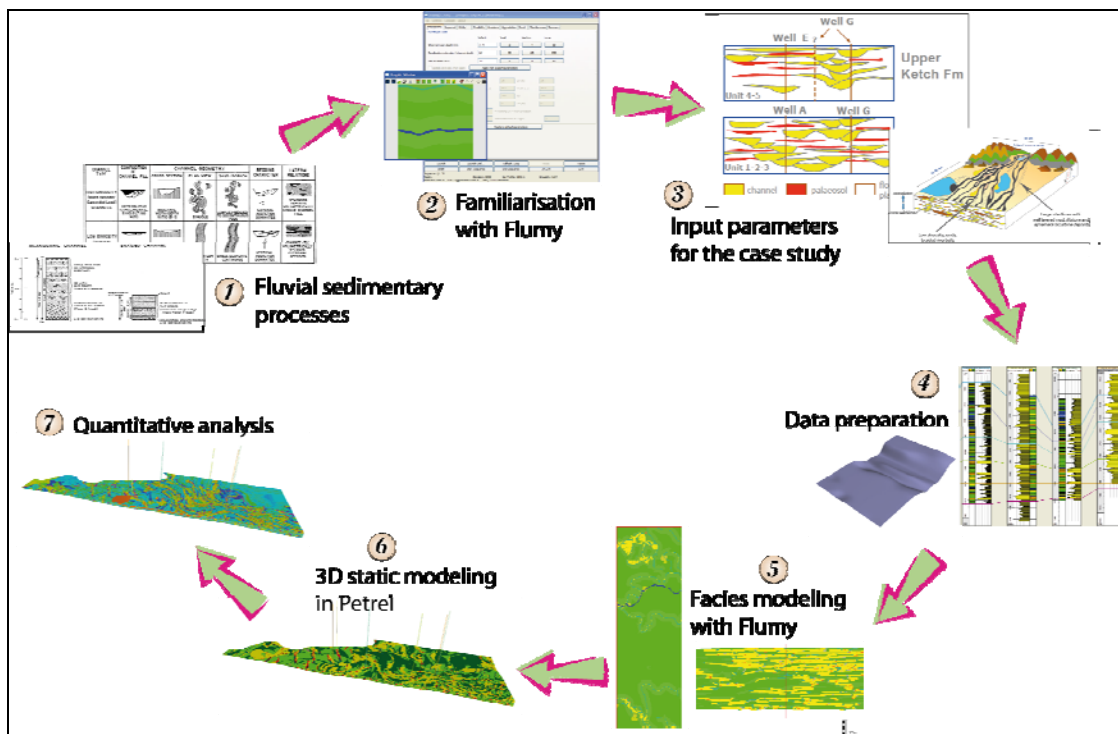


Figure 21: Workflow diagram of the project.

B. Data preparation

Thanks to a work done previously by the MSc student Mohammed Radam, a 3D model including faults, horizons, well logs etc was already available in Petrel. However few data preparations had to be done to fit the requirements of the project. The following chapter presents the different data available at the beginning of the thesis.

1. Well data

The Gamma Ray logs were already integrated into the Petrel model. This work has been done by a student, M. Radam, during an internship at TU Delft. The facies interpretation has been done for four well logs and four other well logs were interpreted during the project (Figure 22).

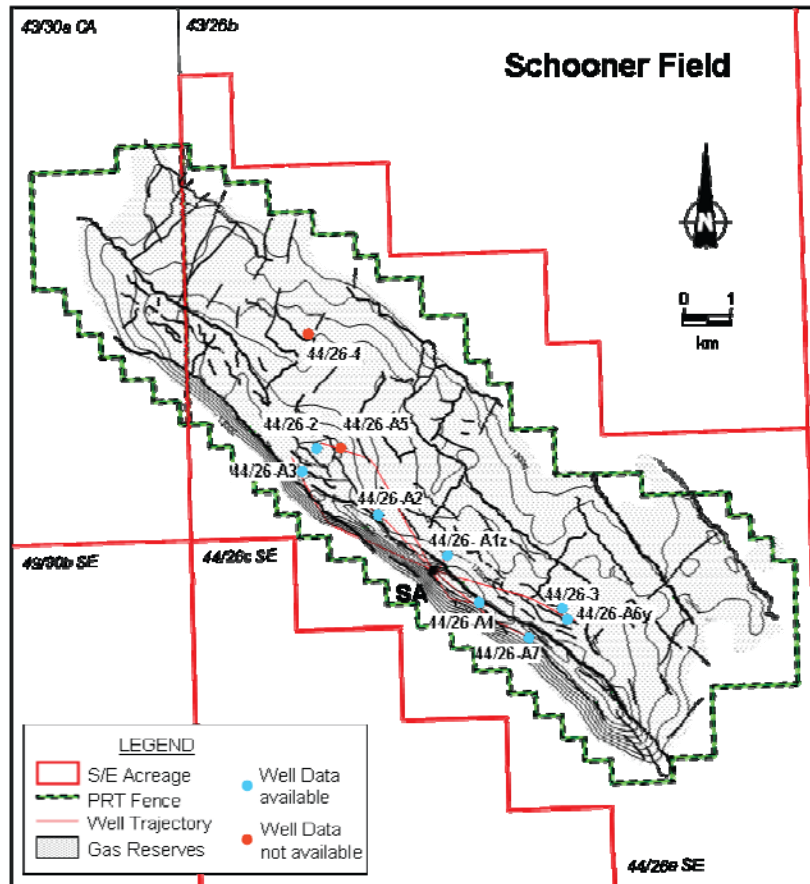


Figure 22: Wells location and structure map of the BRM Group.

First the interpretation of the logs has been checked or done depending on the wells. The channel deposits present a blocky GR response for composite channel fill or a bell shaped GR response for single channel fill resulting from a fining-upwards sequence. A spiky GR response characterizes crevasse splay units while floodplain layers have a high and spiky GR response.

In Petrel, the facies code has been distinguished between four categories: Floodplain, Crevasse Splay, Composite Channel Fills and Single Channel Fills; whereas in Flumy there are nine facies codes: Undefined, Channel Lag, Sand Plug, Point Bar, Crevasse Splay (three different types), Mud Plug, Overbank and Levee.

Then these eight well logs have been exported from Petrel with the aim of importing them into Flumy. However the Petrel files (LAS format) have been modified to suit the Flumy format (MCRC format) and its different facies code. Channel deposits have been defined as Point Bar, Sand plug and Channel lag facies code, floodplain as overbank and crevasse splay didn't change of code.

2. Topographic surface

Flumy allows surface conditioning. There are four different options:

- Replace by imported surface
- Aggrade up to imported surface
- Erode down to imported surface
- Stop when exceeded imported surface

We chose to test the “replace by imported surface” option to obtain a model based on a more realist topographic surface. The purpose is to include the variations of the topographic surface which influences the sedimentary process and channels distribution. Assuming that the deposition process took place in an area without faults activity (e.g. only subsidence), the topographic surface has been obtained from Petrel by flattening the model at the horizon corresponding to the top of the Unit 1 (**Figure 23**).

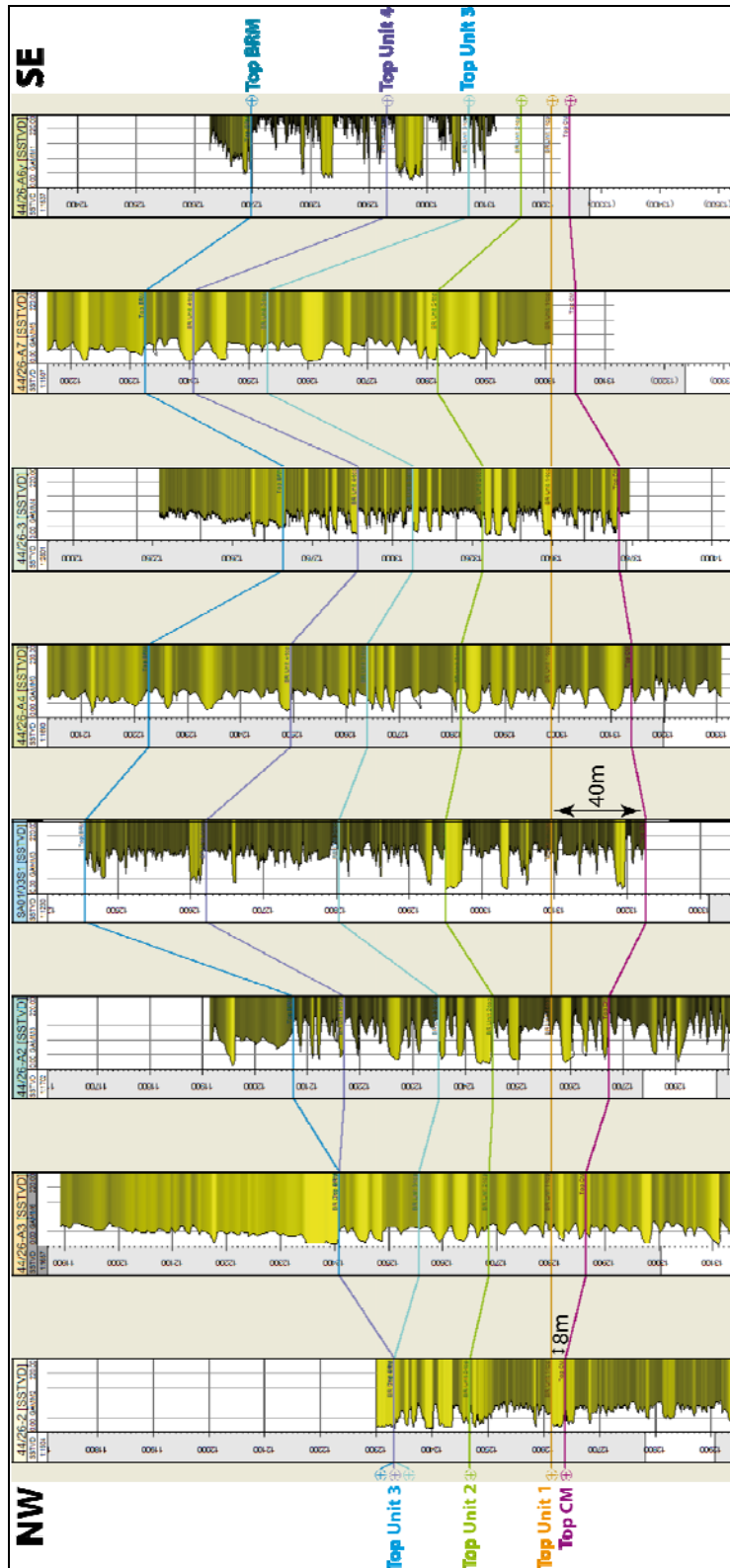


Figure 23: Wells correlation panel presenting the GR logs of the BRM Group and the units subdivision; few wells are incomplete: Units 1-2-3 are not logged at the SE part of the field and Units 4-5 are missing at the NW area of the field.

It appeared that there was a slight paleovalley at the SE part of the field (**Figure 24**). This topographic surface has been constrained by only eight wells and extrapolated on a 92 km² area. Therefore this surface is a hypothetical surface with a high degree of uncertainty. The obtained surface has been exported from Petrel under the CPS-3 ASCII grid file format and then imported into Flumy successfully.

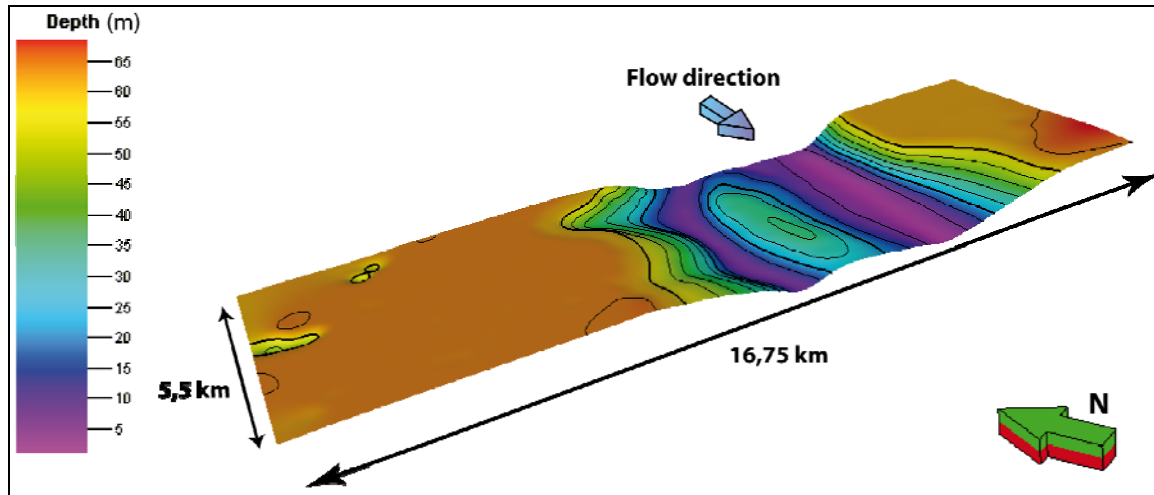


Figure 24: Topographic surface modelled in Petrel and then imported in Flumy.

3. Sequence stratigraphy parameters

The definition of the modeling parameters is based on the sequence stratigraphy analysis, using a chemostratigraphic correlation method, which has been done by Andrea Moscariello (Moscariello, 2003).

This interpretation defines the different sequences as already explained in the chapter IV “Case Study: the Schooner Field” (paragraph B. 2. a) p.28). The type of fluvial system and the cores description will define the channel shape: depth, width and sinuosity (**Figure 25**). The stacking pattern is defined by the regional avulsion frequency. The aggradation rate depends mainly on the oberbank flood frequency and the erodibility coefficient.

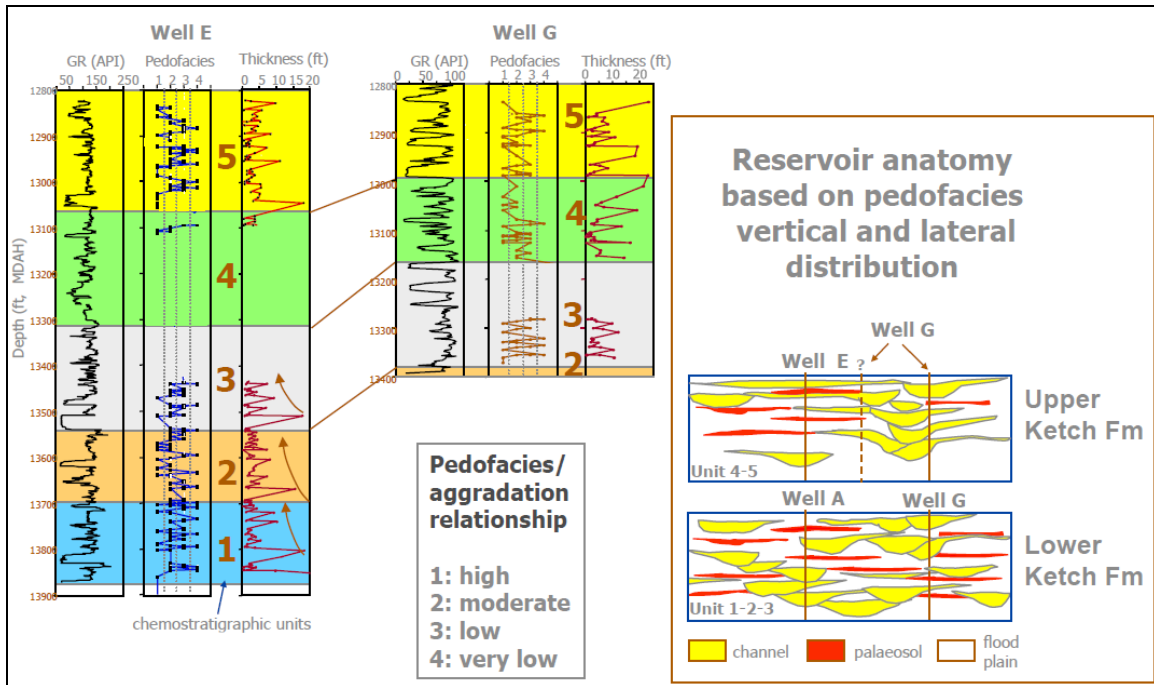


Figure 25: Example of lateral correlation and pedofacies distribution for two wells in the Schooner Field (Upper Ketch Formation, Westphalian C/D). Occurrence and thickness of four types of pedofacies recognized in core are plotted against gamma ray log (Moscariello, 2003).

The BRM part of the Schooner reservoir is characterized by a low to moderate net to gross (N/G) reservoir ratio (30% mode) and a high degree of internal, lateral and vertical reservoir variability (Table 1 & Figure 26). The net to gross range is 20-38% (Moscariello, 2003). The pattern of net to gross distribution in space and time suggests a constantly avulsing channel system, with multiple preferential channel belt locations in Units 1, 2 and 3, but a more stable system with less avulsion in Units 4-5.

Reservoir unit	Mean porosity (%)	Mean permeability (mD)	Mean net-to-gross
BRM 5	10.8	116	0.30
BRM 4	9.3	70.8	0.28
BRM 3	12.6	172.1	0.35
BRM 2	8.27	90.1	0.33
BRM 1	11.6	193.4	0.38
CM	6.2	33.4	0.21

Table 1: Reservoir property distribution for each BRM (Barren Red Measures) chemostratigraphic unit and CM (Coal Measures) (Moscariello, 2003).

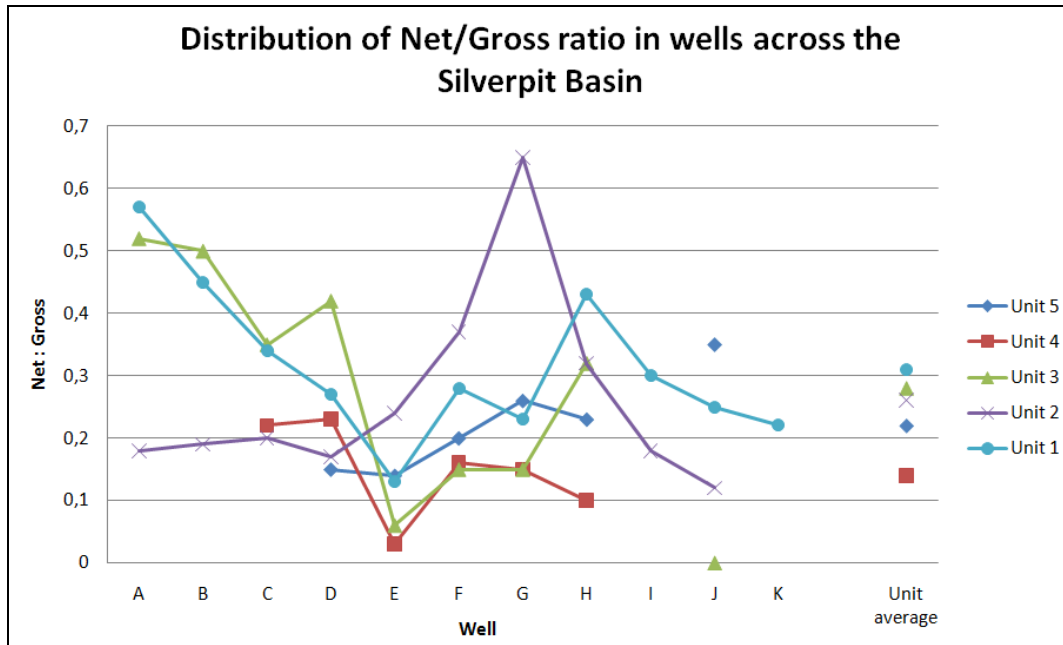


Figure 26: Distribution of the N/G ratio in wells across the Silverpit Basin, shown by chemostratigraphic Unit (Stone & Moscariello, 1999).

To model the fluvial deposits into Flumy, the thickness of each unit has to be known. The well tops provided allowed to model the horizons in Petrel. Knowing that the Saalian Unconformity truncated the BRM reservoir towards the NE, the lack of deposit has to be taken into account. Furthermore the last two wells located in the SE part of the field haven't been completely logged: Units 1, 2 and 3 are missing (**Figure 27**).

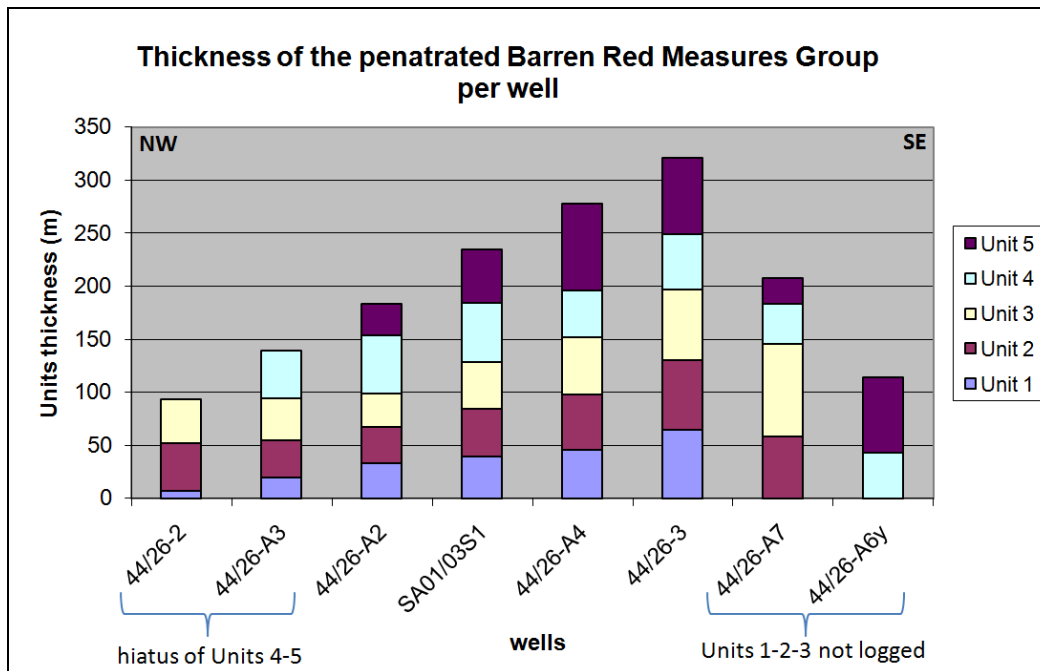
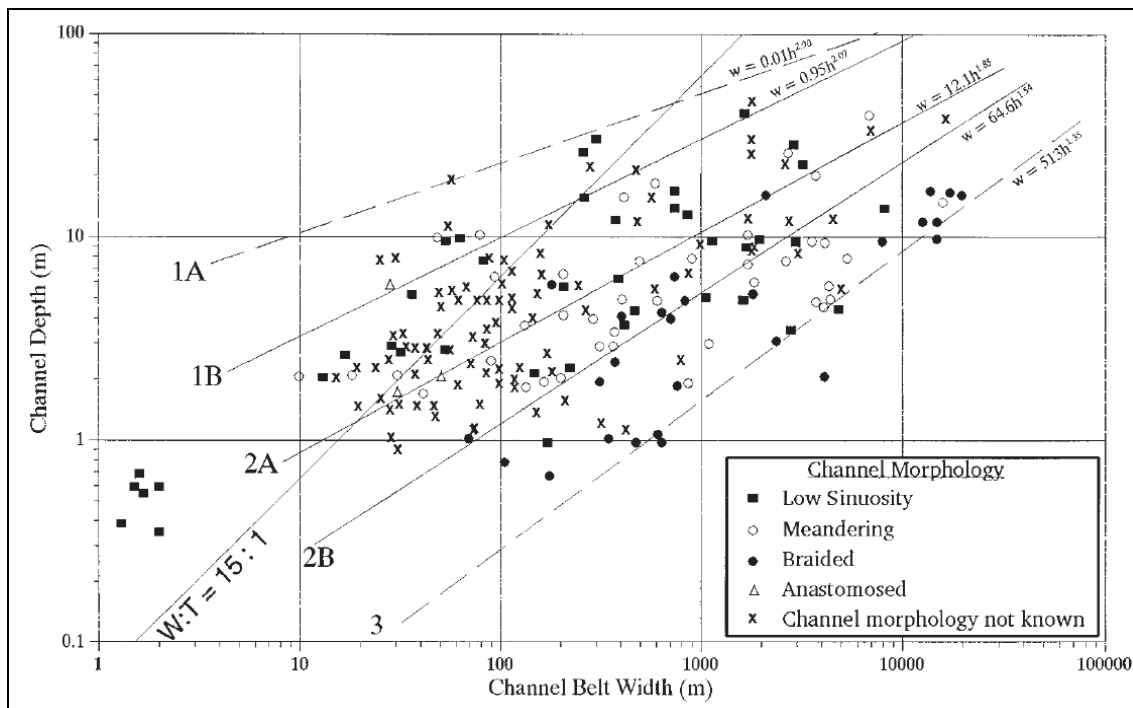


Figure 27: Thickness of the five units in the BRM Group at well logs.

The channel orientation is known from the literature. Regional well log correlations and isopach mapping suggest that channels in the Barren Red Measures Group and Coal Measures Group are predominantly oriented NE-SW. However, there are no indications that local trends could not be different. For example channel orientations could have been controlled by pre-existing fault trends, in which case they might be oriented SE-NW. There is no dipmeter or other dip information that uniquely defines a particular channel orientation in the Schooner Field area (Mijnssen, 1997). In the project the NE-SW orientation has been favoured.

On cores, it is difficult to interpret the width of channels, only a part of their depth is visible. Thus geologists developed relationship equation based on the observation of fluvial reservoir, outcrops and actual fluvial environment (Figure 28).



1A: Upper limit of all data; describes incised, straight, nonmigrating channels; an extreme case

1B: Upper limit of meandering channel deposits

2A: Best fit line for all data; geometric mean of all data types

2B: Empirical relationship for modern, fully-developed meandering streams

3: Lower limit of all data; describes laterally unrestricted (braided?) fluvial systems

Figure 28: Log/log cross plot of channel depth vs. channel belt width for various types of modern and ancient channel deposits (Robinson & McCabe, 1997)

According to the fluvial systems, reservoir analogues and cores description (average channel depth), we could find an equivalent for the width of fluvial channels (Table 2). Thus the units 1-2-3 which are mainly constituted by braided channels, have wide and relatively shallow channels with a high width/depth ratio and a rectangular shape. The meandering system represented by the units 4-5 have a much lower width/depth ratio than braided rivers, but their deposits have a similar broad, lenticular geometry.

Floodplain and channel parameter		
Floodplain slope	Observed values in natural and experimental systems	
	Min	Max
	0.001	0.016
Channel geometry From Bridge, 2003, table 5.5 width $\approx 21.3 d_m^{1.45}$ d_m channel mean depth	Compiled from natural and experimental observations	
	Width	Mean depth
	50 m	1.8 m
	100 m	2.9 m
	150 m	3.8 m
	200 m	4.7 m
	300 m	6.2 m
	400 m	7.5 m
	500 m	8.8 m
Overbank parameters From Bridge, 2003, p. 268 Floodplain aggradation rate per year $r \approx 10 t^{-0.33}$ t time interval between event recurrence In the model Overbank intensity $\approx r * \text{time interval} * 2$ $I \approx 20 t^{0.67}$	Deposited thickness varies with the average time interval between event recurrence	
	OB every 10 years	Intensity: 0.10 m
	OB every 20 years	Intensity: 0.15 m
	OB every 30 years	Intensity: 0.20 m
	OB every 40 years	Intensity: 0.24 m
	OB every 50 years	Intensity: 0.28 m
	OB every 75 years	Intensity: 0.36 m
	OB every 100 years	Intensity: 0.43 m
Relationship between channel data and floodplain grid		
Channel width/ lag	If channel width < lag(x or/and y) Channel discretization will give a dotted line	
	Channel width ≥ 2 lag (max of x or y)	
Channel geometry/ floodplain width	If floodplain is too narrow then meander loops will not be fully displayed on screen.	
	Floodplain width ≥ 40 channel width	
Channel geometry/floodplain length	If floodplain is too short then meander loops will not be fully displayed on screen.	
	Floodplain length ≥ 40 channel width	

Table 2: Table presenting the guidelines for the Flumy key parameters (Flumy userguide, 2009)

4. Porosity analysis

The porosity values have been derived from reverse Gamma Ray logs thanks to the following equation:

$$\text{Porosity} = (\text{X Gr reverse} - \text{Min GR reverse}) * ((\text{Max Porosity} - \text{Min Porosity}) / (\text{Max GR Reverse} - \text{Min GR Reverse}))$$

After computing porosity logs, they have been imported into Petrel and upscaled in order to do the petrophysical modeling (**Figure 29**). When modeling the properties, each grid cell has a single value attributed for each property. As the grid cells are larger than

the sample density for well logs, well log data must be scaled up before assigning a porosity value to each grid cell. The purpose of upscaling is to reduce the number of grid blocks in a geological model to produce simulation later.

As soon as log data were upscaled it was possible to perform continuous property modeling over the entire reservoir. The objective of property modeling is to distribute properties between the available wells so it realistically preserves the reservoir heterogeneity and matches the well data.

The arithmetic method has been used to average the porosity well logs. Typically used for additive properties such as porosity, saturation and net to gross, the arithmetic averaging method allow to average continuous values. Volume weighting will produce a more appropriate arithmetic mean when input values have variable presence within the resulting cell.

Formula used of the arithmetic method:

$$X_{arith} = \frac{\sum_{j=1}^n X_j h_j}{\sum_{j=1}^n h_j}$$

The upscaled porosity logs are used to distribute the porosity property over the entire reservoir. The porosity property model computed by M. Radam in Petrel has been used to model the new porosity model using the new facies model built with Flumy. The porosity is conditioned by the facies property. The porosity distribution slightly changes through units (Table 3).

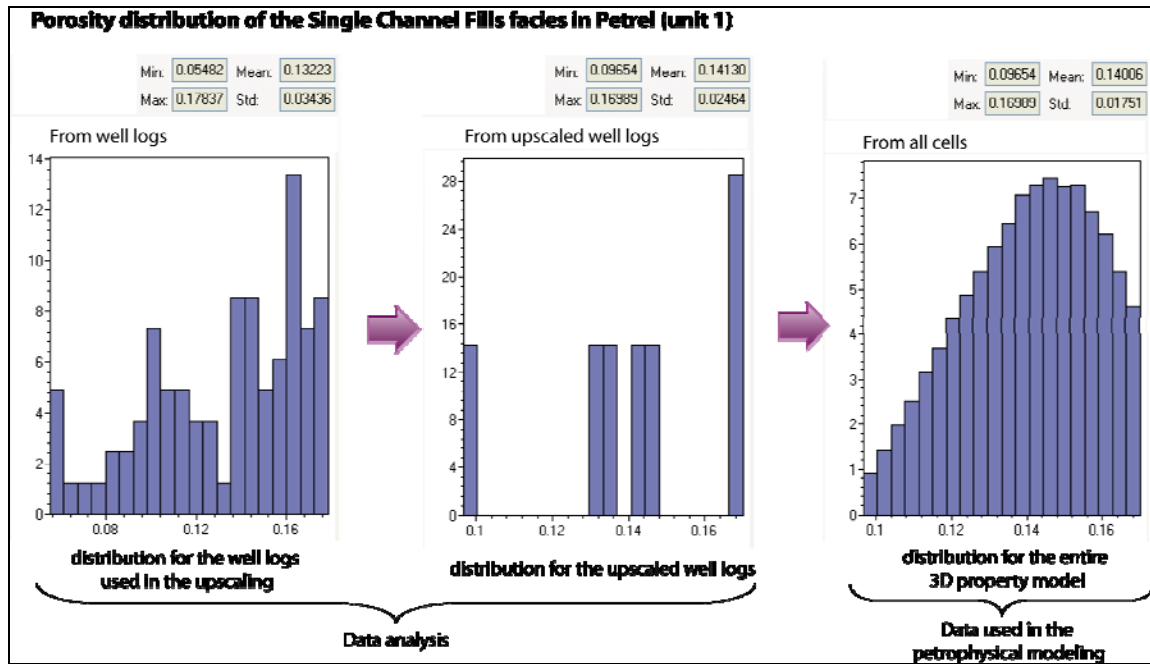


Figure 29: Example of porosity distribution used to do the new petrophysical model in Petrel.

Data, such as porosity and permeability, are distributed between the wells in Petrophysical modeling. The inputs are the well data and the modeler's conceptual model of the geology. The well data must be considered together with the conceptual model, analysed and possibly manipulated, in order to generate a 3D model that fits both the data and the conceptual model.

A transformation process has been applied into Petrel and corresponds with the preparation of a real data set into an internal data set that meets the statistical requirements given by a chosen algorithm. Data transformation will make the data stationary and standard normally distributed before the actual modeling process. A stationary distribution is a basic requirement for input data to most geostatistical algorithms. Standard normal distribution is a requirement of the Sequential Gaussian Simulation algorithm used for stochastic petrophysical simulation. The data must be transformed so that it fits this criteria. That's why the porosity distribution of the 3D property model is different of the porosity distribution of well data (**Figure 29**).

Reservoir unit	Maximum porosity (%)	Mean porosity (%)	Maximum permeability (mD)	Mean permeability (mD)
BRM 5	17.8	10.8	1990	116
BRM 4	16.4	9.3	954	70.8
BRM 3	18.4	12.6	2100	172.1
BRM 2	17.9	8.27	520	90.1
BRM 1	18.9	11.6	1895	193.4
CM	20.1	6.2	1000	33.4

Table 3: Reservoir property distribution for each BRM (Barren Red Measures) chemostratigraphic unit and CM (Coal Measures) (Moscariello, 2003)

5. The Gas-Water contact

An important information to obtain from the petrophysical data is the oil and/or gas water contact.

In the Schooner Field, there is only gas with a GWC located at 13 075 ft depth (~3 985m depth) (**Figure 30**). The maximum gas column is 1 275 ft (~388m) with the crest at 11 800 ft depth (~3 596m depth). The BRM contains 88% of the gas-in-place, with the remaining 12% being located in the CM (Moscariello, 2003).

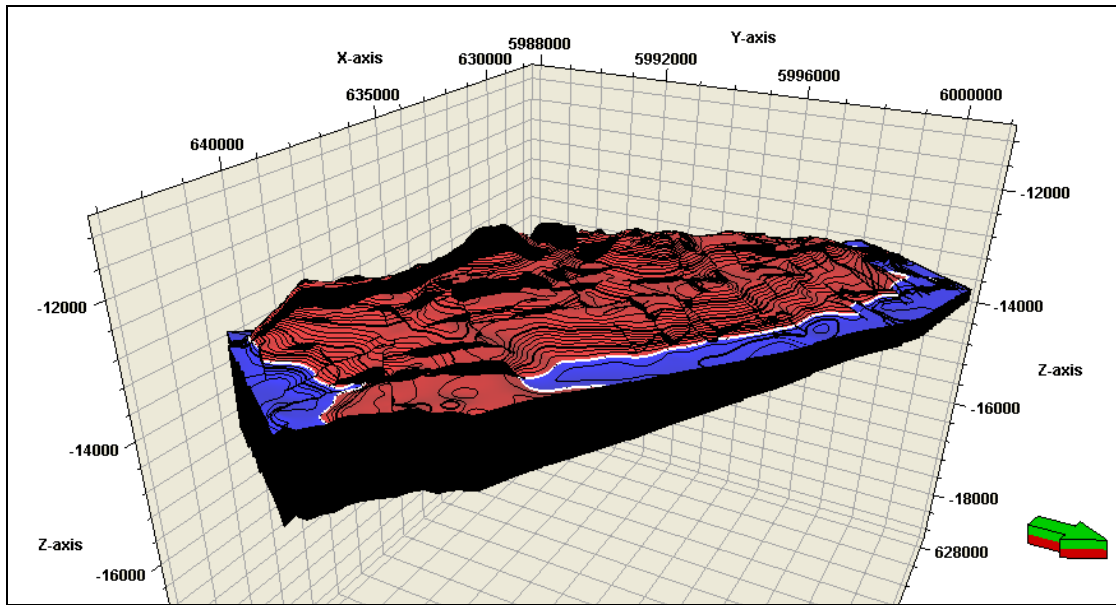


Figure 30: Gas-Water contact of the BRM Group, 13 075 ft depth.

VI. Results: Flumy & Petrel models

Because net to gross is low in the Schooner Reservoir, sand body connectivity is the key geological factor influencing reservoir behaviour. The main uncertainties that effect connectivity are the presence of minor faults in the Barren Red Measures Group, channel orientation, and channel width.

After the synthesis of data and the study of the literature concerning the Schooner Field and fluvial deposits, the modeling work has been performed in two steps. At first a new facies model has been built with Flumy, then exported. Secondly a new 3D grid in Petrel has been computed to receive the new facies property and a new petrophysical model has been created. Finally a quantitative analysis has been done in Petrel.

A. Modeling

1. Facies modeling (Flumy)

Due to numerical limitations, the sequences 1 (Units 1-2-3) and 2 (Units 4-5) have been built separately in Flumy (Figure 31). The net to gross distribution has been respected as well as the sequence stratigraphy features.

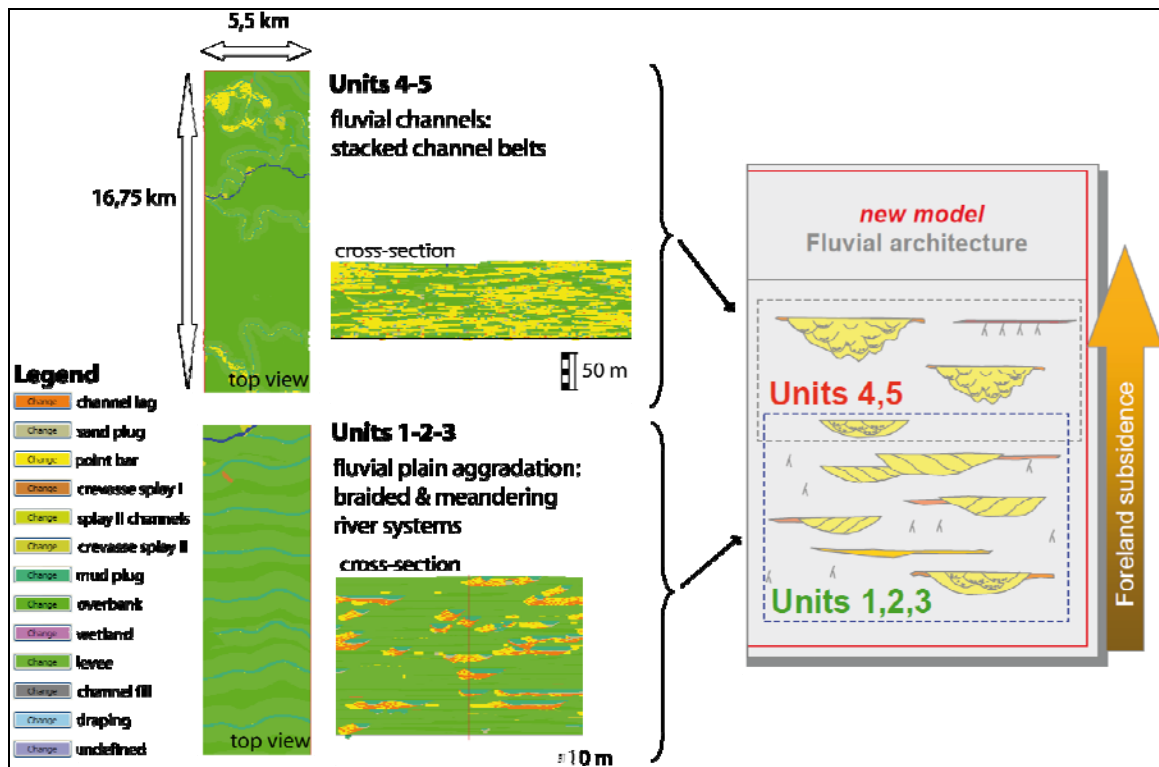


Figure 31: Sequence stratigraphy of the BRM Group versus the facies model built in Flumy.

A long period of test was necessary to find the good adjustments and to understand what is the impact of each parameter on the model construction (Table 4).

sequences	units	thickness (m)	N/G	mean channel depth (m)	mean channel width (m)	erodibility coeff.	regional avulsion freq.	overbank flood freq.
Sequence 2	Unit 5	55	0,30	2	58	7,00E-08	50000	19
	Unit 4	55	0,28			7,00E-08	40000	17
Sequence 1	Unit 3	60	0,35	3,75	145	3,40E-08	300	8
	Unit 2	55	0,33			3,00E-08		
	Unit 1	45	0,38			4,00E-08		

Table 4: Table presenting the main parameters used during the facies modeling in Flumy.

The grid size defined in Flumy respects the grid size of the Petrel model and thus the field size (Figure 32). The compatibility between the two softwares depends on the grid size but also on its orientation. In Flumy an orientation of 231.5° has been defined to fit exactly the grid in Petrel.

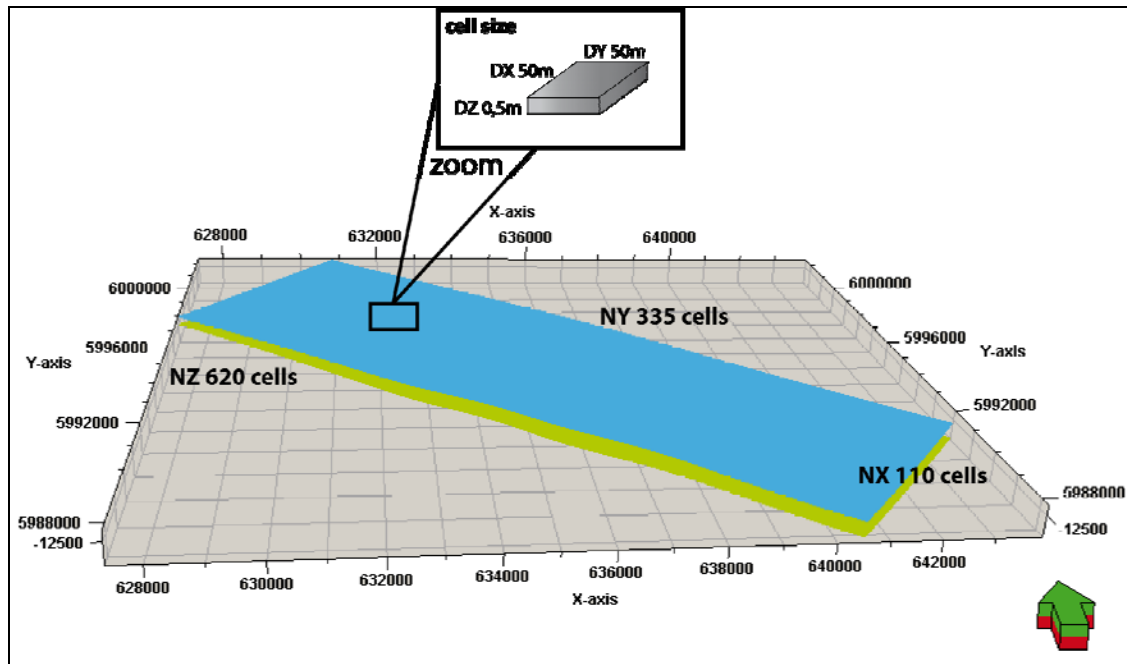


Figure 32: Grid used in Flumy and in Petrel; there are 22 847 000 cells in total.

Three different models have been computed: a pessimistic model, a medium model and an optimistic model. They illustrate the net to gross range which varies between 20% and 38% (Table 5).

sequences	units	Net to Gross ratio		
		Pessimistic case	Medium case	Optimistic case
Sequence 2	Unit 5	0,20	0,30	0,38
	Unit 4	0,18	0,28	0,36
Sequence 1	Unit 3	0,25	0,35	0,43
	Unit 2	0,23	0,33	0,41
	Unit 1	0,28	0,38	0,46
Mean		0,20	0,32	0,38

Table 5: Table presenting the N/G ratio values used for the three models built in Flumy.

Moreover another type of case concerning only the sequence 1 has been computed. Three models have been built with a topographic surface by using the option “replace by imported surface” in Flumy. The purpose is to obtain a model more realistic with a better channels distribution.

This topographic surface characterises a slight paleovalley located at the SE part of the field up to 50-60m depth. To have a better insight of the model including the topographic surface, the facies model built with Flumy has been applied on a 3D regular grid in Petrel (Figure 33). One iteration is corresponding to one year according to the Flumy userguide.

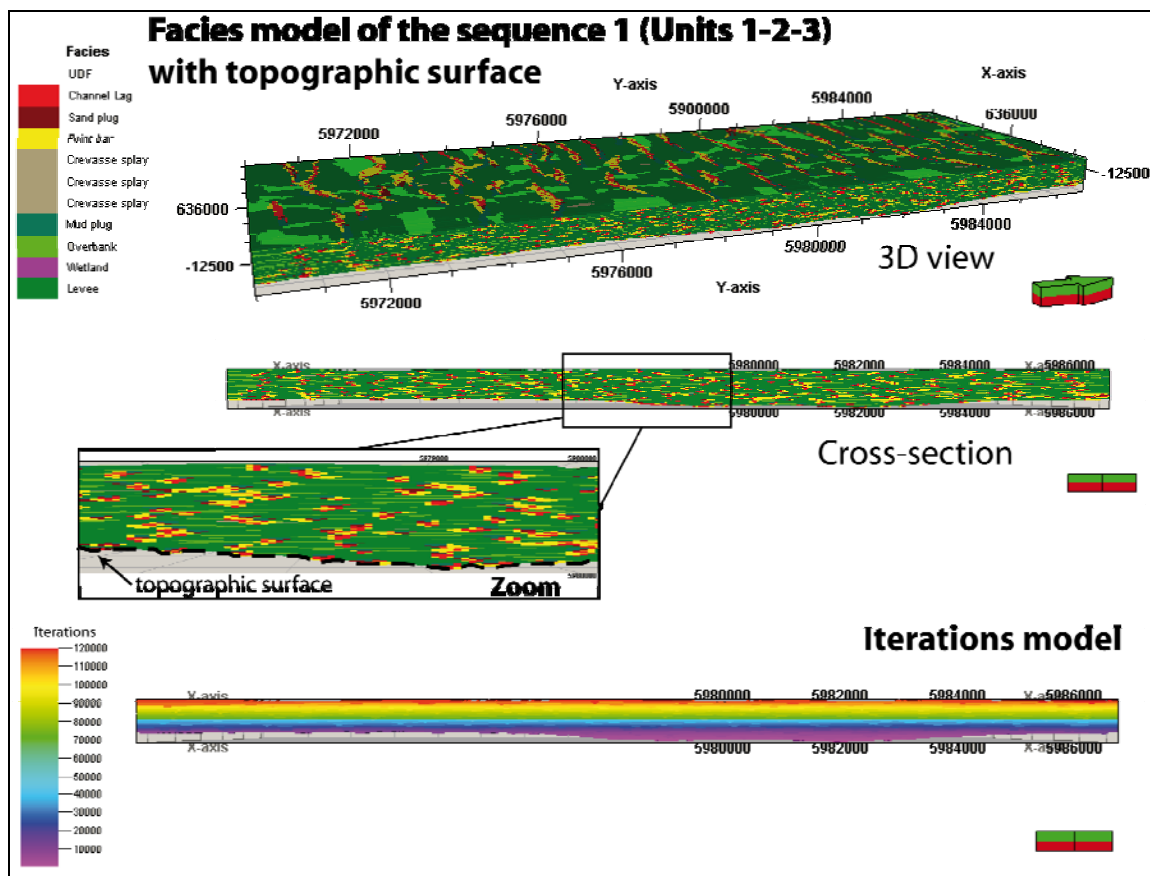


Figure 33: example of facies model of sequence 1 integrating a topographic surface.

A well conditioning option is also available in Flumy. The well logs have been prepared to test it. Unfortunately, due to numerical problems, it wasn't possible to build a full sequence with well conditioning.

2. 3D static modeling (Petrel)

Petrel offers several algorithms for modeling the distribution of petrophysical properties in a reservoir model. Well data, facies realization, variograms, a secondary variable and/or trend data can be used as input and various user settings are available.

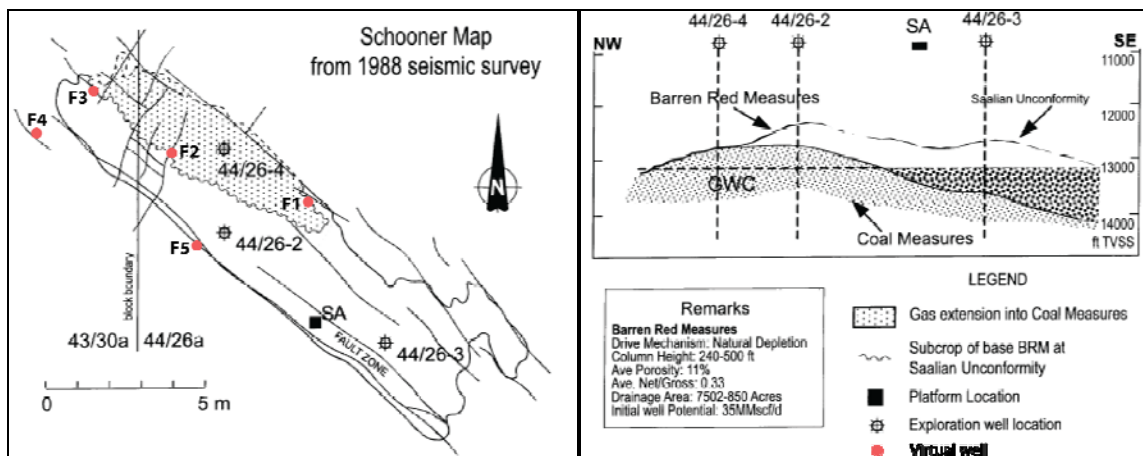
Different options provided by Petrel for the facies modeling:

- Object-based method
- Truncated Gaussian Simulation
- Sequential Indicator Simulation
- Indicator Kriging
- Multi-point Facies Simulation

For this project, we imported the facies model built in Flumy using a GSLIB format to fill the facies property. Thus the classic facies modeling process used in Petrel has been skipped.

The grid in Petrel has to have the same size than the one defining by the GSLIB file, in x, y and z directions. That's why it is important to check the layering of the Petrel grid and change it if necessary before to import the facies property.

As previously explained in the chapter IV, the BRM forms a southeasterly thickening wedge that is progressively truncated by erosion at the Saalian Unconformity towards the NE over the crest of the structure (**Figure 34**) (Moscariello, 2003). Therefore few virtual wells have been added to the Petrel model to constrain the erosion surface.



Nine facies code are represented in the new facies property built by Flumy: Channel Lag, Sand Plug, Point Bar, Crevasse Splay (three different types), Mud Plug, Overbank and Levee (**Figure 35**, **Figure 36** & **Figure 37**).

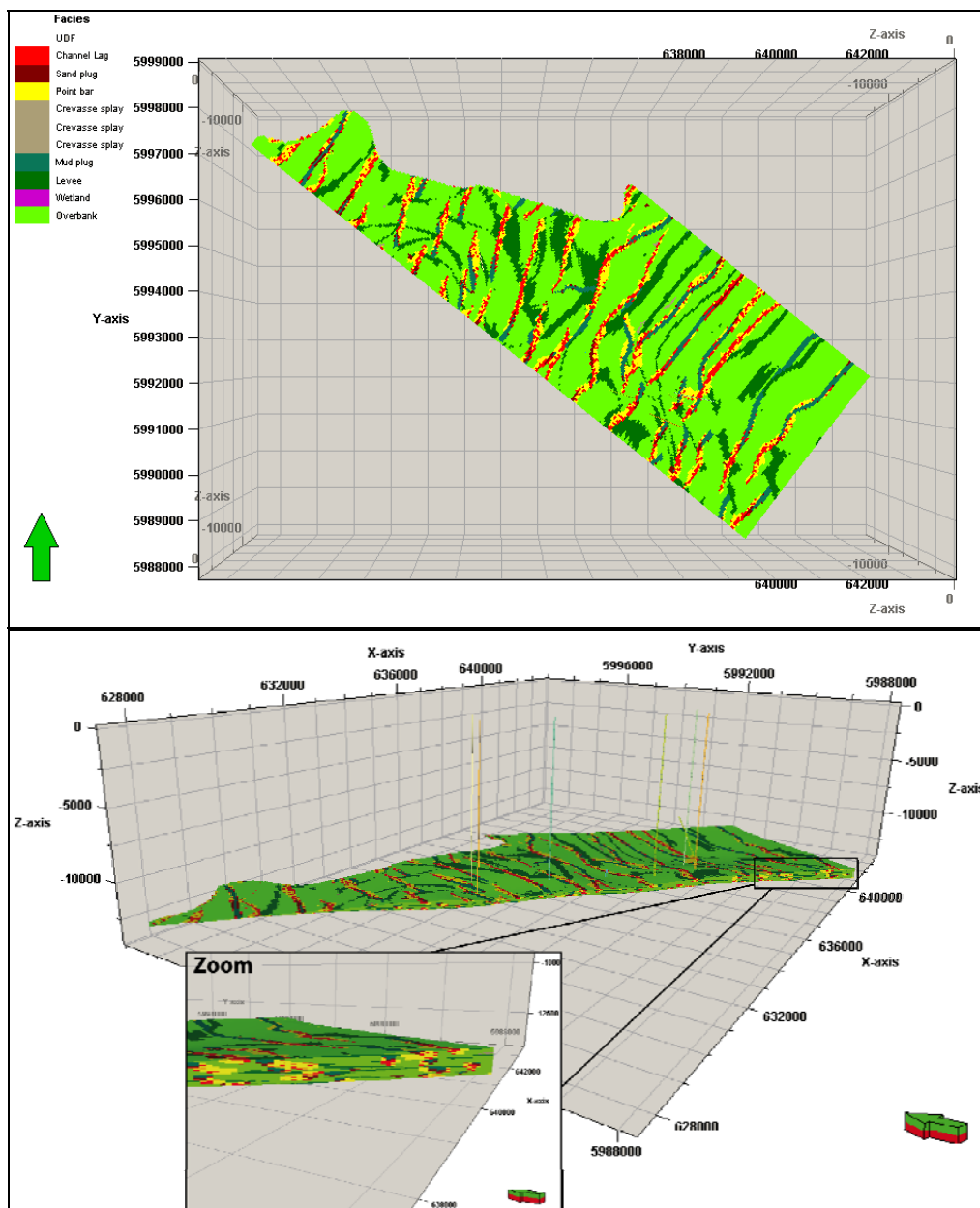


Figure 35: Facies model of the sequence 1 (units 1-2-3) built with Flumy and imported in Petrel - medium case, top view and 3D view in Petrel

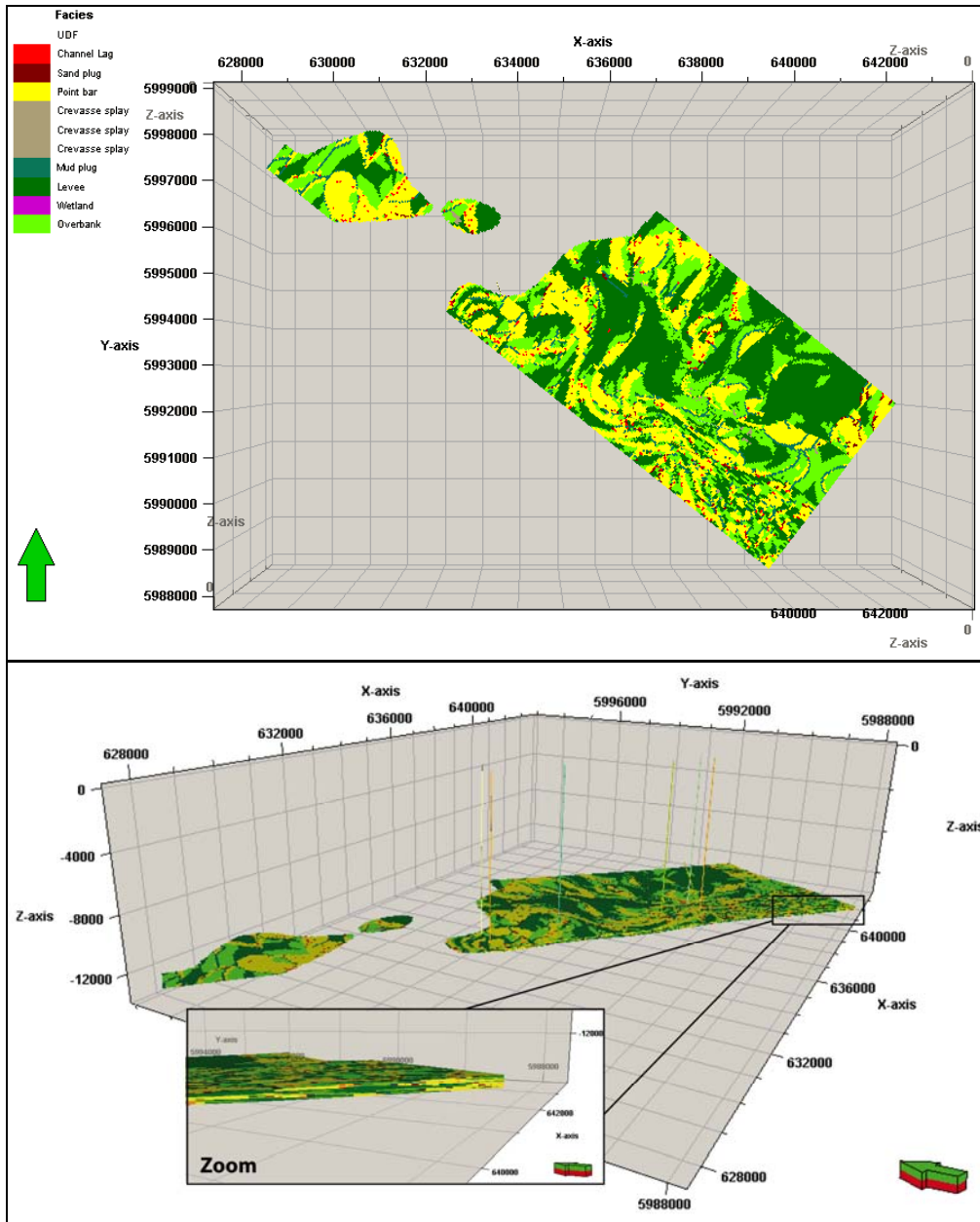


Figure 36: Facies model of the sequence 2 (units 4-5) built with Flumy and imported in Petrel - medium case, top view and 3D view in Petrel

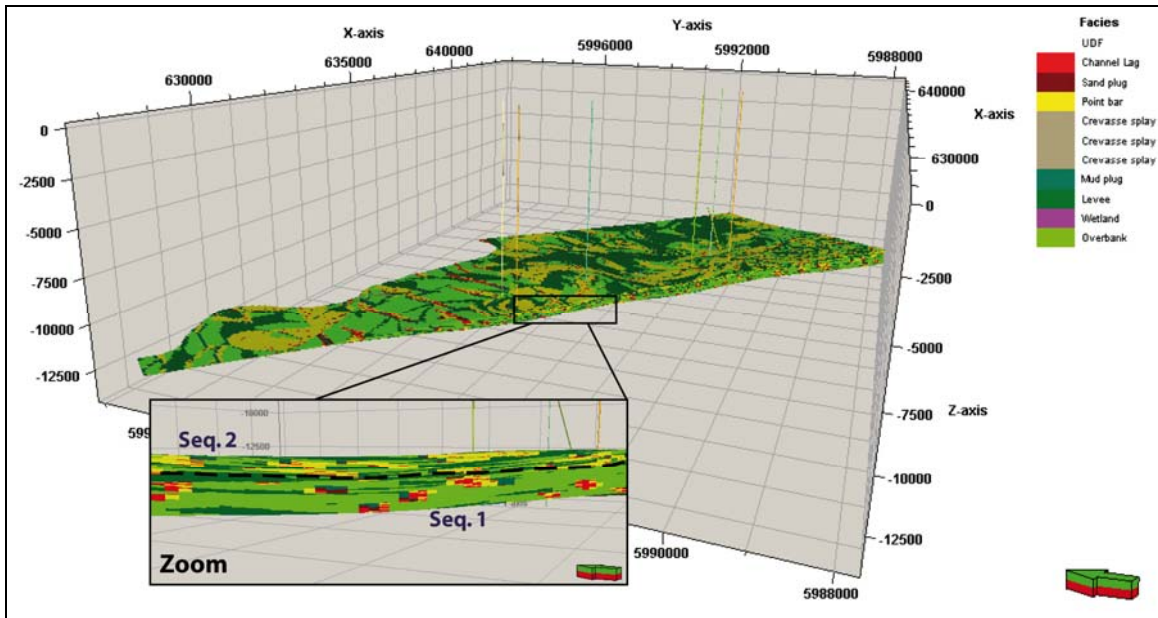


Figure 37: Facies model of the BRM Group built with Flumy and imported in Petrel - medium case, 3D view in Petrel

3. The petrophysical model

It is possible to condition the petrophysical modeling to any 3D discrete property, such as a 3D facies model. Settings such as the algorithm to use, the variogram, etc. are then set individually for each facies. For porosity modeling we used 3D facies model for conditioning the realization. This approach allowed us to model porosity in Petrel by using facies trend, and to link these two properties. It also allowed to populate porosity values over entire zones according to facies model.

Usually the upscaled porosity logs are used to distribute the porosity property over the entire reservoir. In our project, we used the porosity property model computed by M. Radam in Petrel to model the new porosity model (Figure 39 & Figure 40). Therefore the porosity values correspond to well logs and fit the new facies distribution.

The porosity distribution of the four facies code initially present in the Petrel model has been applied to the Flumy facies code. Channel deposits (Point Bar, Sand plug and Channel lag Flumy code) correspond to the initial composite and single channel fills facies code in Petrel, crevasse splay deposits (Crevasse splay and Levee Flumy code) to the initial crevasse splay code and floodplain deposits (Overbank Flumy code) to the initial floodplain code. A constant porosity value of 0 has been assigned to the Mud plug Flumy code (Figure 38).

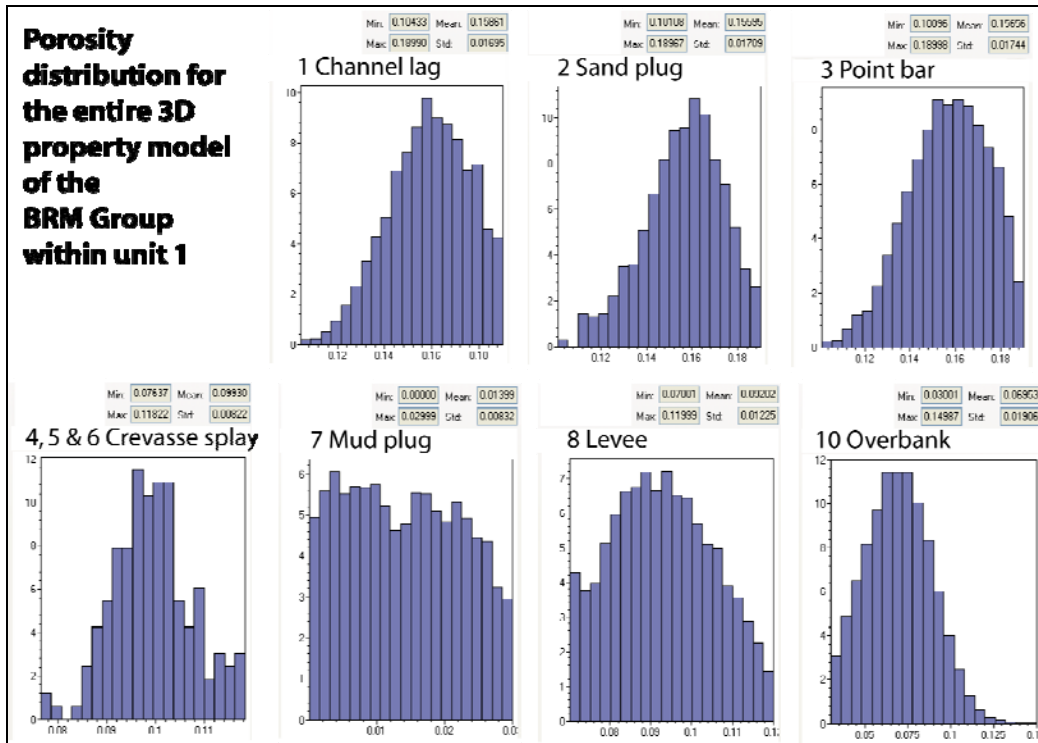


Figure 38: Example of porosity distribution used to populate the new petrophysical model.

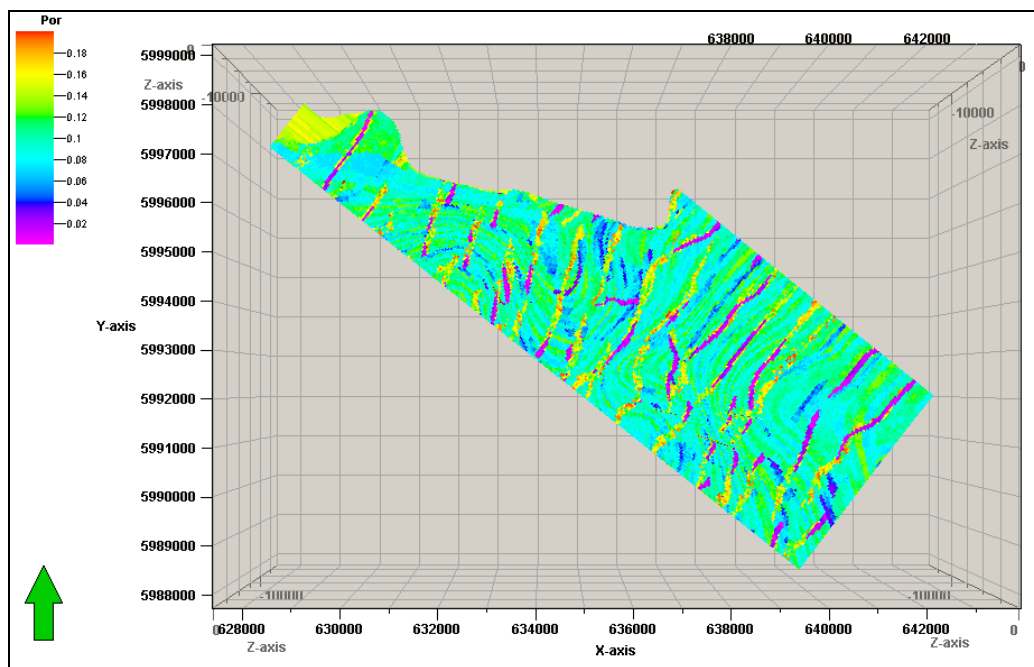


Figure 39: Porosity distribution within sequence 1 (units 1-2-3) of the BRM Group

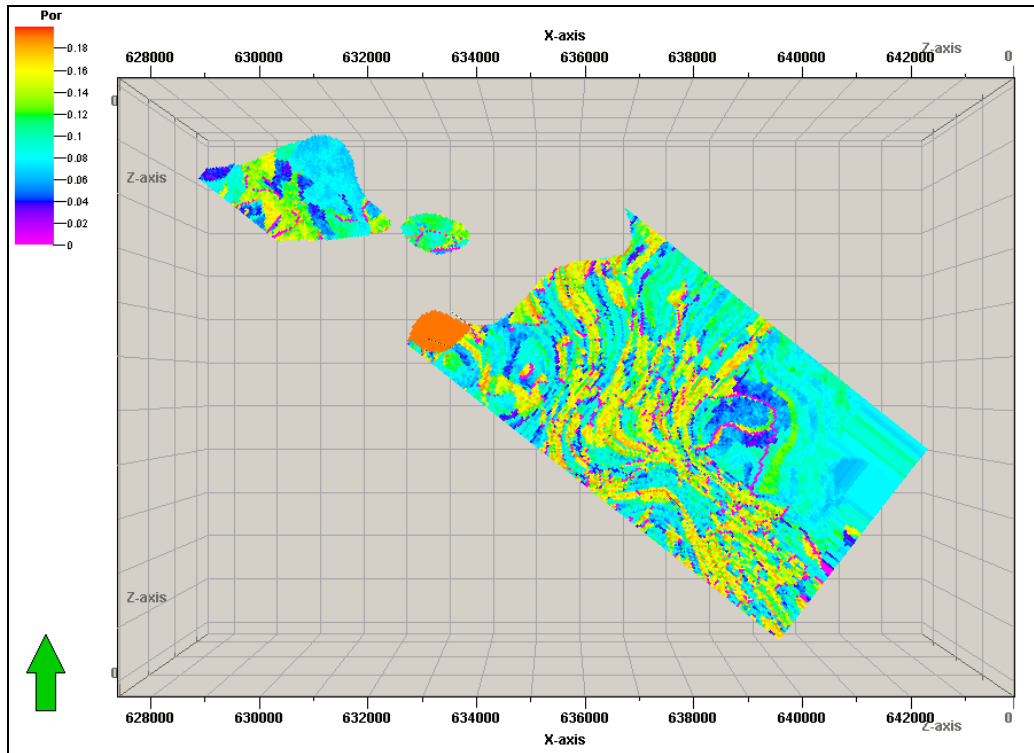


Figure 40: Porosity distribution within sequence 2 (units 4-5) of the BRM Group

We used the same principle for the Net to Gross ratio distribution than for the porosity distribution. All the Flumy facies have been defined as reservoir rock except the Overbank and Mud plug facies which have high shale content (**Figure 41 & Figure 42**).

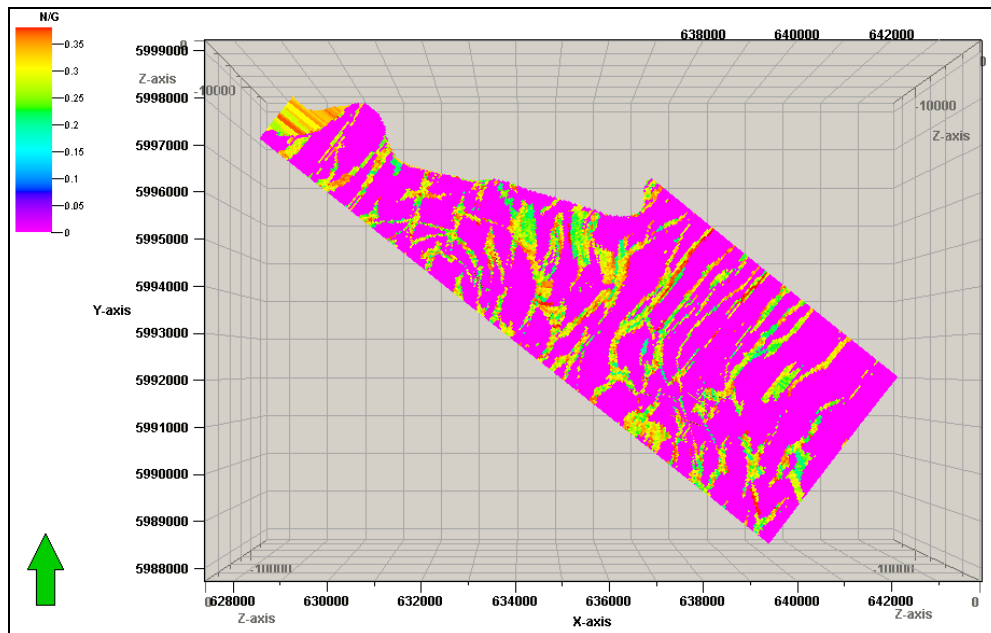


Figure 41: Net to Gross distribution within sequence 1 (units 1-2-3) of the BRM Group

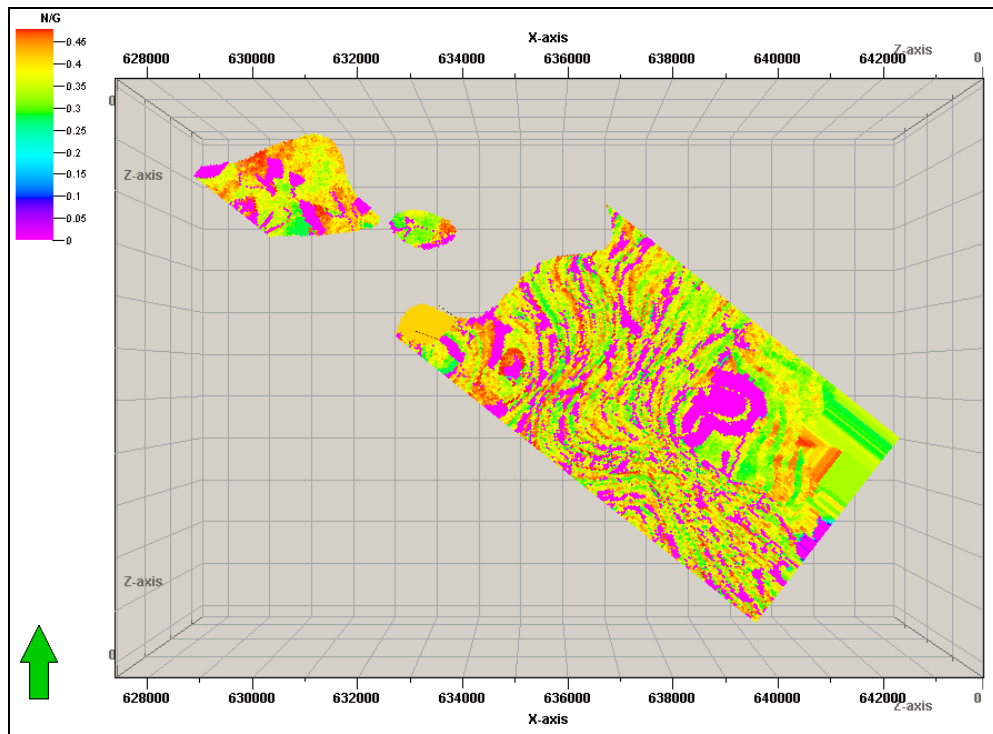


Figure 42: Net to Gross distribution within sequence 2 (units 4-5) of the BRM Group

B. Quantitative analysis

Reserves estimation is one of the most essential tasks in the petroleum industry. It is the process by which the economically recoverable hydrocarbons in a field, area, or region are evaluated quantitatively. Depending on the results of evaluation the future decision is made, whether field development is economically viable or not. In this project only volume calculations could have been computed, therefore the connectivity analysis and reserves estimation are missing.

1. Volumetric analysis

The volumetric analysis has been performed in Petrel. The bulk volume V_B , the net volume V_N and the pore volume V_ϕ have been computed (Table 6, Table 7, Table 8 & Table 9).

Formula:

V_B : volume of rocks above hydrocarbon-water contact

$$V_N = V_B \times N/G$$

$$V_\phi = V_N \times \phi$$

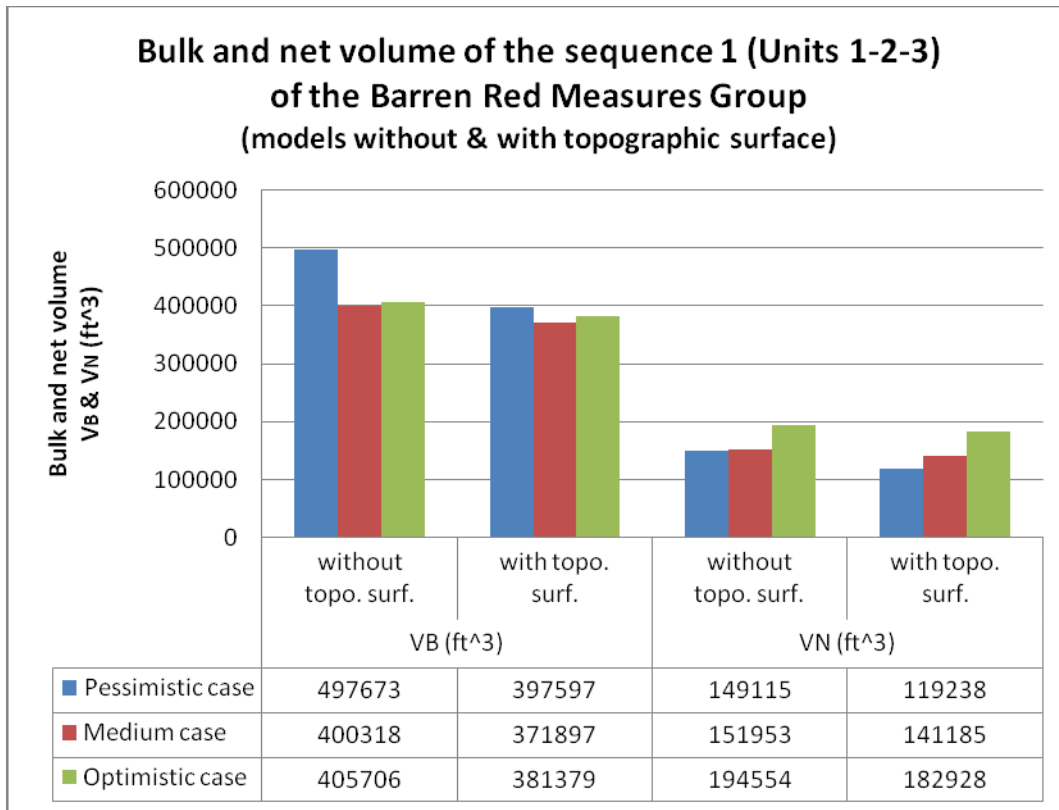


Table 6: Bulk and net volume of the units 1, 2 and 3 of the BRM Group (1ft³=0.02832m³).

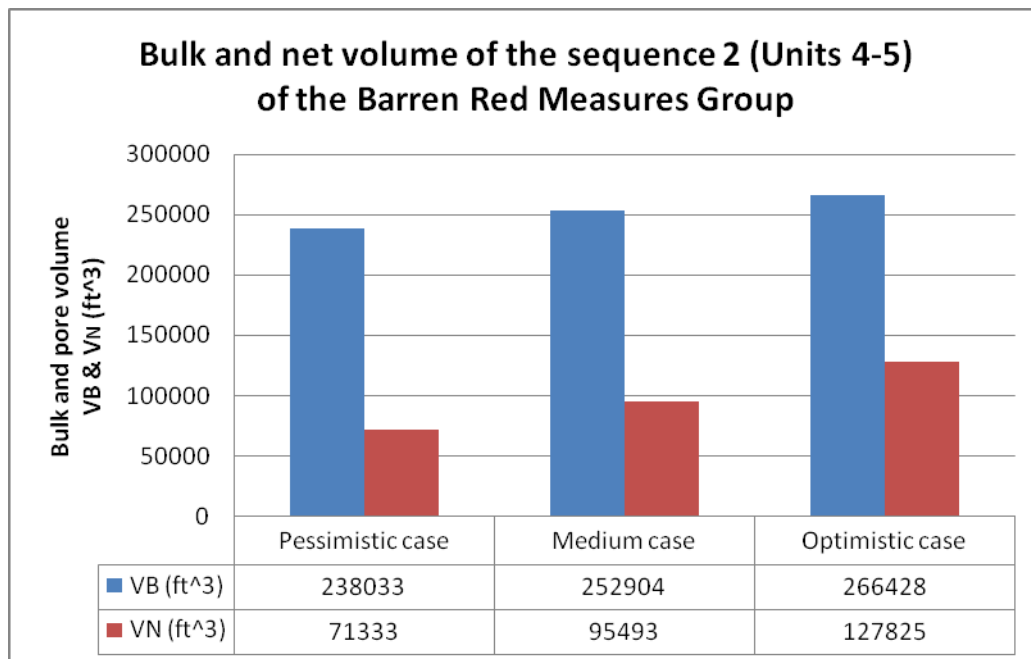


Table 7: Bulk and net volume of the units 4 and 5 of the BRM Group (1ft³=0.02832m³).

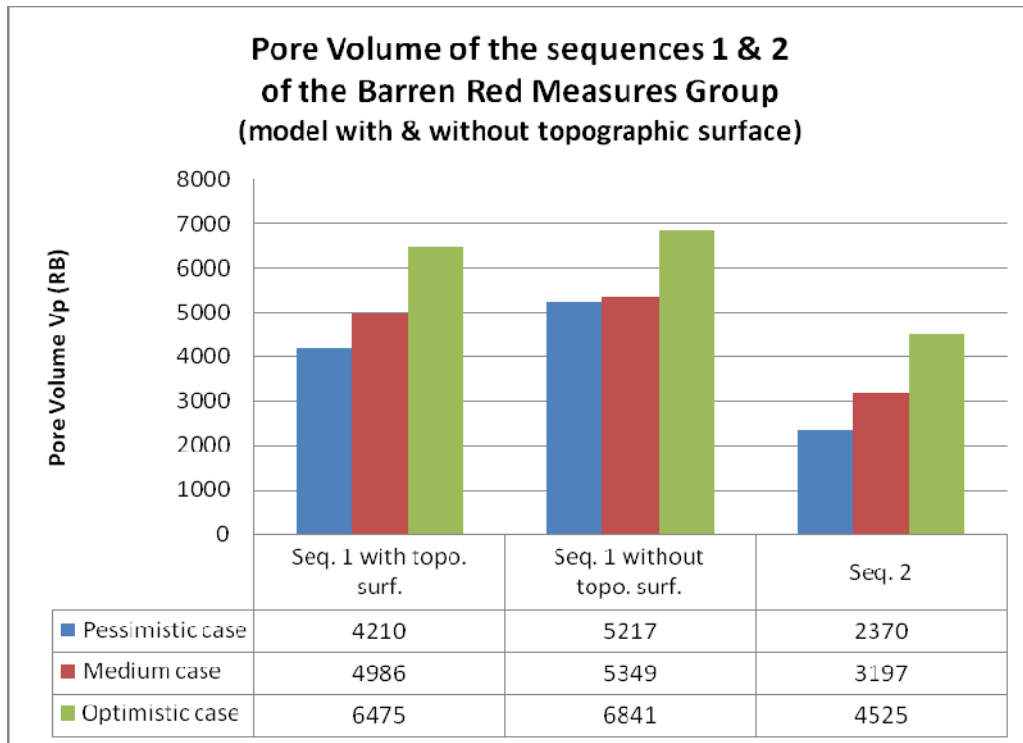


Table 8: Pore volume of the BRM Group (RB=reservoir barrel).

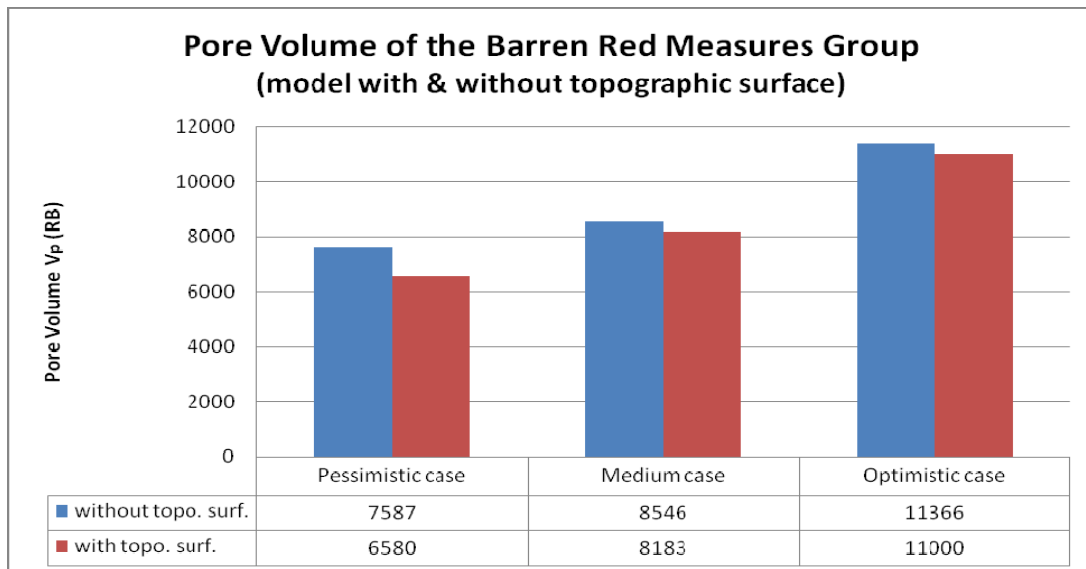


Table 9: Pore volume of the BRM Group for the pessimistic, medium and optimistic cases (RB=reservoir barrel).

Unfortunately the connectivity analysis hasn't been done due to numerical problems (Appendix B, p. 85). However the volume calculations have still been computed to compare the pessimistic, medium and optimistic cases.

2. Uncertainty analysis

In the oil industry, it is critical to perform proper volumes evaluation, which plays big role in the development of the field.

In this project the uncertainty is illustrated by the three models presented: pessimistic, medium and optimistic cases. They reflect the Net to Gross range according to the literature (Moscariello, 2003).

However it isn't the only parameter on which there is an uncertainty. The porosity values used have been extracted from the Gamma Ray logs, which is not completely reliable. Furthermore there are only eight well logs and few are even incomplete. According to the literature there are uncertainties concerning channels orientation and faults model. Unfortunately the well conditioning of the model hasn't been possible, thus the model isn't fitting even the few hard data obtained from well logs.

VII. Interpretation/Discussion

The histograms of the results show a difference in terms of net volume and pore volume between the pessimistic, medium and optimistic cases but also between the sequence 1 and 2. The sequences 1 and 2 have respectively an average of 35% and 29% of net to gross. Moreover the sequence 2 is 30% thinner than the sequence 1. We observed that the sequence 2 represents the equivalent of 63% for the net volume and 60% for the pore volume of the sequence 1. This difference is visible in the facies model too. Their geological features are well represented with isolated channels on one hand for the sequence 1 and with stacked channels on the other hand for the sequence 2. We can assume that the results of the sequence 2 are due to the presence of stacked channels. The channels connectivity within sequence 2 is better than within sequence 1.

The negative point is the variation of the bulk volume due probably to numerical problems during the modeling process. The facies model is built separately from the 3D model and it is difficult to estimate in Flumy the exact thickness of deposits modelled. This inconvenient could also explain the gap of bulk volume between the models built with and without a topographic surface.

The effective development of the Schooner field depends mainly on the proper understanding of the geological complexity of the low net to gross of the BRM fluvial reservoir. A first improvement has been done with a new sequence stratigraphy based on a chemostratigraphic correlation method. Now the major challenge is to improve the geological model and thus the recovery factor. Without seismic data it is difficult to decrease the uncertainty but new tools like Flumy can be used to obtain more realistic and reliable geological models with only few well logs.

The reservoir connectivity in fluvial reservoir is one of the key uncertainties due both to channel lateral discontinuity and fault compartmentalization. In that sense, Flumy can help to better model these complex geological processes.

Flumy is in principle a good modeling software to model the internal connectivity, stacking patterns and heterogeneities of fluvial reservoirs. Based on this study, unfortunately, Flumy is not a mature and deployable software as many bugs and fixes need to be done to make it fully workable. This work has highlighted a list of improvements which are reported in appendix. To understand and therefore use adequately this software good understanding of geology and fluvial sedimentology is required. Its correct use can be difficult for a beginner user and even more challenging for a non-geologist.

VIII. Conclusion & Recommendations

With the decline of the biggest hydrocarbons reserves, new technologies are developing and trying to improve the recovery factor. Many fields have a potential hydrocarbon volume, but with a low recovery factor. One of the challenges is to have a better understanding of their geological architecture.

Compared with the object-based or pixel-based method, the process-based stochastic approach allows to obtain more realistic and reliable geological models. It respects the complexity of sedimentary processes and thus represents with more accuracy the lateral and vertical heterogeneities of fluvial reservoirs.

The prototype software, Flumy, satisfies these expectations. However it is still under development and has limits and constraints which have been pointed during this project. The use of real field data allowed to test Flumy in real conditions with the aim to get better production forecasting.

Flumy is a tool which can be used to build a conceptual model for the geological interpretation. However a good geological interpretation and especially a good sequence stratigraphy analysis are still the most important. A modeling software will never replace the eye of the geologist.

In future work, it would be interesting to complete this project with a connectivity analysis and compare the results with the production data of the Schooner field. Therefore the compatibility problems noticed during this thesis between Flumy and Petrel should be solved. One solution is to use the Flumy plug-in for Petrel which is being developed by Shell.

Furthermore as soon as few numerical problems of Flumy will be solved, the well conditioning option should be fully tested as well as the other surface options like the import of an erosion surface.

Acknowledgements

I would like to thank Andrea Moscariello to allow me to get this interesting thesis and for his supervision while working and encountering different kind of problems.

I especially thank Isabelle Cojan, Jacques Rivoirard and Fabien Ors from the Ecole des Mines of Paris for helping me through the long process of facies modeling with Flumy.

I thank you Onno Houtzager from Shell for his precious advice and knowledge concerning Petrel and geological modeling.

Of course, I would like to thank Shell to allow me to work on this project by providing me the license.

I thank you Gert Jan Weltje for his valuable lectures on geostatistics.

At TU Delft, I thank you Adriaan Janszen for his help while encountering the problem of compatibility with Petrel.

Finally I would like to thank all my colleagues of the 2nd and 3rd floor of the Citg building and classmates for their support.

And I thank you my parents without whom nothing would have been possible.

“All models are wrong, but some are useful” [George Box]

References

ARMINES / ECOLE DES MINES DE PARIS 2009 - FLUMY Consortium version 1.606 of prototype software, User's guide – 42 pp.

ARMINES / ECOLE DES MINES DE PARIS 2009 – Tutorial FLUMY 1.4 — 32 pp.

BAILEY J.B., ARBIN P., DAFFINOTI O., GIBSON P. and RITCHIE J.S. 1993 – Permo-Carboniferous plays of the Silver Pit Basin - *In: Petroleum Geology of Northwest Europe: Proceedings of the 4th conference* – published by the Geological Society, volume 1 - edited by J.R. Parker – p.707-715

BRIDGE J.S. and TYE R.S. 2000 – Interpreting the Dimensions of Ancient Fluvial Channel Bars, Channels, Channel Belts from Wireline-Logs and Cores – AAPG Bulletin, V.84, No. 8 – p.1205-1228

CAERS J. 2005 – Petroleum Geostatistics – Society of Petroleum Engineers – 88 pp.

CAERS J. and ZHANG T. 2002 – Multiple-point geostatistics: a quantitative vehicle for integrating geologic analogs into multiple reservoir models – Stanford University, Stanford Center for Reservoir Forecasting – 24 pp.

CAMERON T.D.J., CROSBY A., BALSON P.S., JEFFERY D.H., LOTT G.K., BULAT J. and HARRISON D.J. 1992 – The geology of the southern North Sea – British Geological Survey, United Kingdom Offshore Regional Report – 152 pp.

Centre de Géosciences 2010 – MINES ParisTech - <http://www.geosciences.mines-paristech.fr>

COJAN I., FOUCHE O., LOPEZ S., RIVOIRARD J. 2004 – Process-based reservoir modeling in the example of meandering channel – Centre de Geostatistique, Ecole des Mines de Paris, Fontainebleau – *in: Geostatistics Banff* - Edited by Leuangthong O. and Deutsch C.V. – p.611-619

DAVIES P., WILLIAMS H., PATTISON S.A.J. and MOSCARIELLO A. 2009 – Optimizing 3-D Modeling Strategies of Shoreface Reservoirs Using Outcrop Data – 71st EAGE Conference & Exhibition, Amsterdam, The Netherlands, 8-11 June 2009, P292 - 5 pp.

DAVIES D.K., WILLIAMS B.P.J., VESSEL R.K. 1992 – Models for Meandering and Braided Fluvial Reservoirs With Examples From the Travis Peak Formation, East Texas – SPE 24692 – p.321-329

DOLIGEZ B., VERSLUYS V., LOPEZ S., TELES V., LERAT O., JOSEPH P., EUZEN T. 2007 – Quantification of Statistical Geological Parameters From Genetic Modeling of Channels – IPTC 11732 – 10 pp.

FALIVENE O., CABRERA L., MUNOZ J.A., ARBUES P., FERNANDEZ O. And SAEZ A. 2007 – Statistical grid-based facies reconstruction and modeling for sedimentary bodies. Alluvial-palustrine and turbiditic examples – *Geologica Acta*, Vol.5, n°3 - p.199-230

GLENNIE K.W. 1990 – Introduction to the Petroleum Geology of the North Sea – Blackwell Scientific Publications, third edition – 401 pp.

IKEDA S., PARKER G. and SAWAI K. 1981 – Bend theory of river meanders, part 1, Linear development – *Journal of Fluid Mechanics*, vol. 112 – p.363-377

LABOURDETTE R. 2007 – 3D Sedimentary Modeling Toward the Integration of Sedimentary Heterogeneities in Reservoir Models – PhD thesis, University of Montpellier – 681 pp.

LOPEZ S. 2003 – Modélisation de Réservoirs Chenalisés Méandriformes, Approche Génétique et Stochastique – Phd thesis of Ecole des Mines de Paris - 141 pp.

LOPEZ S., COJAN I. and GALLI A. 2002 – Accommodation Space in a Fluvial Meandering Process-based Stochastic Model – AAPG Annual Meeting, Houston, Texas - abstract

MIALL A. D. 1977 – Fluvial Sedimentology – Canadian Society of Petroleum Geologists, Calgary – 111 pp.

MIJNSSEN F.C.J. 1997 – Modeling of sandbody connectivity in the Schooner Field – *in: Petroleum Geology of the Southern North Sea: Future Potential* – Geological Society Special Publication No. 123 – Edited by K. Ziegler, P. Turner and S.R. Daines, – p.169-180

MOSCARIELLO A. 2003 – The Schooner Field, Blocks 44/26a, 43/30a, UK North Sea – *in: United Kingdom Oil and Gas Field, Commemorative Millennium Volume* – Geological Society Memoir No. 20 – Edited by J.G. Gluyas and H.M. Hichens – p.811-824

MOSCARIELLO A. 2009 - Unraveling Reservoir Architecture of Complex Low Net: Gross Red-Bed Fluvial Sequence Using Palaeosoils and Chemostratigraphy - Search and Discovery Article n°50173 – 38 slides

PYRCZ M.J. 2003 – Bank Retreat Meandering Fluvial Process-based Model – Department of Civil & Environmental Engineering, University of Alberta – 12 pp.

RHEE C. W. 2006 – Conceptual problems and recent progress in fluvial sequence stratigraphy – Geosciences Journal, Vol. 10, No. 4 - p.433-443

RIVOIRARD J., COJAN I., RENARD D. & GEFFROY F. 2008 – Advances in quantification of process-based models for meandering channelized reservoirs – GEOSTATS 2008, Santiago, Chile ; VIII International Geostatistics Congress – 10 pp.

ROBINSON J. W. & McCABE P. J. 1997 - Sandstone-Body and Shale-Body Dimensions in a Braided Fluvial System: Salt Wash Sandstone Member (Morrison Formation), Garfield County, Utah – AAPG Bulletin, V. 81, No. 8 – p.1267-1291

STONE G. & MOSCARIELLO A. 1999 – Integrated Modeling of the Southern North Sea Carboniferous Barren Red Measures Using Production Data, Geochemistry, and Pedofacies Cyclicality – Society of Petroleum Engineers, SPE 56898 – 8 pp.

SWANSON D. C. 1993 – The Importance of Fluvial Processes and Related Reservoir Deposits – SPE 23722, Swanson Consulting Services - p.368-377

Table of contents

I.	Introduction.....	6
II.	The challenge of 3D reservoir modeling	8
A.	Introduction.....	8
B.	Flumy model: a realistic process-based stochastic model	10
1.	Concepts.....	11
2.	Input parameters.....	12
III.	Characterisation of meandering and braided systems.....	14
A.	Fluvial environment.....	14
1.	Braided river system	16
2.	Meandering river system.....	16
B.	Fluvial sequence stratigraphy	18
IV.	Case study: The Schooner Field	20
A.	Regional geology	20
1.	Structure.....	20
2.	Stratigraphy.....	22
a)	Carboniferous.....	22
b)	From Permian to Quaternary	23
3.	Petroleum system.....	24
B.	The Schooner Field.....	24
1.	Structure.....	25
2.	Stratigraphy.....	26
a)	Barren Red Measures subdivision	26
b)	Sedimentary facies.....	31
(1)	Composite low-sinuosity channel fill	31
(2)	Single low-sinuosity channel fill	31
(3)	Proximal overbank deposits crevasse splay deposits.....	32
(4)	Floodplain deposits and paleosols	32
c)	Depositional setting	32
(1)	Units 1, 2 & 3.....	34
(2)	Units 4 & 5.....	34
V.	Data and workflow.....	35
A.	Workflow	35
B.	Data preparation.....	36
1.	Well data	36
2.	Topographic surface.....	37
3.	Sequence stratigraphy parameters.....	39
4.	Porosity analysis	43
5.	The Gas-Water contact	45
VI.	Results: Flumy & Petrel models	47
A.	Modeling.....	47
1.	Facies modeling (Flumy)	47
2.	3D static modeling (Petrel)	50
3.	The petrophysical model.....	53
B.	Quantitative analysis.....	56

1.	Volumetric analysis	56
2.	Uncertainty analysis.....	59
VII.	Interpretation/Discussion	60
VIII.	Conclusion & Recommendations	61

Table of figures

Figure 1: Three channel belts present in part of the Colville River flood plain, Alaska. Note the juxtaposition of the narrow channel belt of the Kogosukruk River (left) formed by a single, sinuous channel and the multiple, sinuous-to-braided channels in the much wider Colville River channel belt (center). Active and abandoned channels and bars are easily discernible. Photograph from July 1979 in the National Petroleum Reserve Alaska, approximately 40 km (25 mi) northeast of Umiat. (Bridge & Tye, 2000).	6
Figure 2: On the left: Three-dimensional facies simulation showing the architecture	9
Figure 3: (a) Training image of fluvial type reservoir. The indicator statistics were calculated from this image. Two categories were represented. White represents shale deposits, and black represents black deposits. (b) Indicator-based image created using multiple-point statistics (Caers & Zhang, 2002).	10
Figure 4: Top view of a channel meandering in time, depositing point bars (red to yellow) and mud plug (green) in abandoned loops obtained by using a stochastic process-based modeling method (Rivoirard <i>et al.</i> , 2008).	10
Figure 5: On the left: top view of a channel meandering (blue), its crevasse splay (orange to yellow), its levee (dark green) and its overbank deposits (light green);	13
Figure 6: the effect of rate of avulsion and rate of aggradation on the evolution of architectural elements. Top part: low rate of aggradation and avulsion allow for the development of extensive later accretion elements; Middle part: higher rate of aggradation with increased avulsion; Bottom part: high rate of aggradation results in isolated sand bodies (Pyrzcz, 2003).	15
Figure 7: Channel pattern classification recognising four classes of channels (Labourdet, 2007).	15
Figure 8: Schematic block model of A) meandering and B) braided channel systems illustrating lateral and vertical relationships among building blocks (no scale implied) (Davies <i>et al.</i> , 1992).	17
Figure 9: Comparison of channel sand bodies in high sinuosity (meandering) and low sinuosity (braided) systems (Davies <i>et al.</i> , 1992).	17
Figure 10: Vertical profiles illustrating the internal characteristics of Travis Peak meandering and braided channel deposits (Davies <i>et al.</i> , 1992).	18
Figure 11: evolution of the fluvial style in a relative sea-level cycle (Doligez <i>et al.</i> , 2007).	19
Figure 12: Schooner Field location in the North Sea (Stone & Moscariello, 1999).	20
Figure 13: Regional features map of the Southern North Sea with pointed in red the Schooner Field (Bailey <i>et al.</i> , 1993).	21
Figure 14: On right: Silver Pit Basin stratigraphic column highlighting reservoir, source and seal development (Bailey <i>et al.</i> , 1993); on left: details of the chronostratigraphic setting of the Westphalian Barren Red Measures and Coal Measures (Moscariello, 2003)	22
Figure 15: Structure map of the Top Carboniferous in the Schooner Area showing location of the discovery and appraisal wells (Mijnssen, 1997).	25
Figure 16: Lithostratigraphic correlation across Schooner Field (hung from Base of BRM) (Moscariello, 2009).	27

Figure 17: Chemostratigraphic correlation across Schooner Field (hung from base of BRM). Note that Units 4 and 5 are eroded towards the NW of the region (Moscariello, 2009).....	29
Figure 18: Chemostratigraphic correlation of the Schooner Field (Moscariello, 2009)...	30
Figure 19: Lithostratigraphic and Chemostratigraphic correlation – comparison between the old and new model (Moscariello, 2009).	31
Figure 20: Schematic block diagram showing the paleogeographical setting proposed for the deposition of Units 1-2-3 (bottom part) and Units 4-5 (top part) (Stone and Moscariello, 1999).	33
Figure 21: Workflow diagram of the project.	35
Figure 22: Wells location and structure map of the BRM Group.....	36
Figure 23: Wells correlation panel presenting the GR logs of the BRM Group and the units subdivision; few wells are incomplete: Units 1-2-3 are not logged at the SE part of the field and Units 4-5 are missing at the NW area of the field.	38
Figure 24: Topographic surface modelled in Petrel and then imported in Flumy.	39
Figure 25: Example of lateral correlation and pedofacies distribution for two wells in the Schooner Field (Upper Ketch Formation, Westphalian C/D). Occurrence and thickness of four types of pedofacies recognized in core are plotted against gamma ray log (Moscariello, 2003).....	40
Figure 26: Distribution of the N/G ratio in wells across the Silverpit Basin, shown by chemostratigraphic Unit (Stone & Moscariello, 1999).....	41
Figure 27: Thickness of the five units in the BRM Group at well logs.	41
Figure 28: Log/log cross plot of channel depth vs. channel belt width for various types of modern and ancient channel deposits (Robinson & McCabe, 1997).....	42
Figure 29: Example of porosity distribution used to do the new petrophysical model in Petrel.	44
Figure 30: Gas-Water contact of the BRM Group, 13 075 ft depth.	46
Figure 31: Sequence stratigraphy of the BRM Group versus the facies model built in Flumy.	47
Figure 32: Grid used in Flumy and in Petrel; there are 22 847 000 cells in total.	48
Figure 33: example of facies model of sequence 1 integrating a topographic surface.	49
Figure 34: Structural map and cross-section of the Schooner Field reservoir based on 1988 3D seismic survey. GWC: gas-water contact (Moscariello, 2003).....	50
Figure 35: Facies model of the sequence 1 (units 1-2-3) built with Flumy and imported in Petrel - medium case, top view and 3D view in Petrel	51
Figure 36: Facies model of the sequence 2 (units 4-5) built with Flumy and imported in Petrel - medium case, top view and 3D view in Petrel	52
Figure 37: Facies model of the BRM Group built with Flumy and imported in Petrel - medium case, 3D view in Petrel	53
Figure 38: Example of porosity distribution used to populate the new petrophysical model.	54
Figure 39: Porosity distribution within sequence 1 (units 1-2-3) of the BRM Group	54
Figure 40: Porosity distribution within sequence 2 (units 4-5) of the BRM Group	55
Figure 41: Net to Gross distribution within sequence 1 (units 1-2-3) of the BRM Group	55
Figure 42: Net to Gross distribution within sequence 2 (units 4-5) of the BRM Group ..	56

Tables list

Table 1: Reservoir property distribution for each BRM (Barren Red Measures) chemostratigraphic unit and CM (Coal Measures) (Moscariello, 2003).	40
Table 2: Table presenting the guidelines for the Flumy key parameters (Flumy userguide, 2009)	43
Table 3: Reservoir property distribution for each BRM (Barren Red Measures) chemostratigraphic unit and CM (Coal Measures) (Moscariello, 2003)	45
Table 4: Table presenting the main parameters used during the facies modeling in Flumy.	48
Table 5: Table presenting the N/G ratio values used for the three models built in Flumy.	49
Table 6: Bulk and net volume of the units 1, 2 and 3 of the BRM Group ($1\text{ft}^3=0.02832\text{m}^3$).	57
Table 7: Bulk and net volume of the units 4 and 5 of the BRM Group ($1\text{ft}^3=0.02832\text{m}^3$).	57
Table 8: Pore volume of the BRM Group (RB=reservoir barrel).	58
Table 9: Pore volume of the BRM Group for the pessimistic, medium and optimistic cases (RB=reservoir barrel).	58

Appendix A

Input parameters used in Flumy

Unit 1 – Medium Case

Initialization		Channel mean depth (m)				Sandbodies extension / channel depth				Net to gross (%)			
		default	small	medium	large	default	small	medium	large	default	small	medium	large
		3,75				50				38			
domain		Lag		Grid size		Number of nodes		Grid origin		Rotation		Slope along flow direction	
		DX (m)	DY (m)	Length (m)	Width (m)	NX	NY	OX (m)	OY (m)	*working OX = flow direction	231,5	0,002	Initial elevation at origin
		50	50	5450	16700	110	335					0	
Erodibility		Emap		erodibility coefficient		longitudinal margin (multiple of channel width)		10?		10?			
		constant	loaded from file										
channel		Width (m)	Mean depth (m)	Import centerline of channel									
		145m	3,75										
Avulsions		Regional		lateral margin (multiple of channel width)		levee breaches		Crevasse plays					
		never	always	periodic	Poisson	never	always	periodic	Poisson	probability for transition from CSI to CSII	probability for adding a new CS channel		
Aggradation		Changes		Variation (m)		Thickness (m)		Wetland proportion		Draping facies			
		elevation (m)	never	always	periodic	Poisson	constant	uniform	normal	lognormal	Overbank	Draping	
		1000											
Overbank Flood/Drain Profile		Occurrence		Thicknes (m)		Draping facies		Draping					
		never	always	periodic	Poisson	constant	uniform	normal	lognormal	undefined	Draping		
Exp. Decrease Thickness/Grainsize (m)		Levee width		Levee width		Levee width		Levee width					
		never	always	periodic	Poisson	constant	uniform	normal	lognormal	undefined	Draping		

Unit 2 – Medium case

initialization	non-exp	Channel mean depth (m)				Sandbodies extension / channel depth				Net to gross (%)			
		default	small	medium	large	default	small	medium	large	default	small	medium	large
		3,75				50				33			
domain	Lag	Grid size		Number of nodes		Grid origin		Rotation		Slope		Initial	
		DX (m)	DY (m)	Length (m)	Width (m)	NX	NY	OX (m)	OY (m)	*working Ox= flow direction	along flow direction	elevation n at origin	
		50	50	5450	16700	110	335			231,5	0,002	0	

Erodibility	erodibility	Emap		erodibility coefficient	
			built from actual up to		3,00E-08
		loaded from file	imported topograph y		longitudin al margin (multiple of channel width)
channel	Width (m)	Mean depth (m)		Import centerline	
		145m	3,75	10?	

Avulsions	Avulsion	Regional		lateral margin (multiple of channel width)		levee breaches		Crevasse splays				
		never	always	periodic	Poisson			during aggradati on	never	always	periodic \\ (200)	probability for transition adding a new CS channel

Aggradation	Equilibr um Flood/ Drain profile	elevation (m)		Changes		Variation (m)		Overbank		Draping		
		1000	never	always	periodic	Poisson	constant	uniform	normal	lognormal		\\
						\\ (10)	\\ (0.5)					
	Overba nk	Occurrence		Thickness (m)		Wetland proportion		Draping facies				
		never	always	periodic	Poisson	constant	uniform	normal	lognormal	undefined	Draping	
						\\ (0.2)						\\
	Exp. Decrease Thickness	Levee Grainsiz width										

Unit 3 – Medium case

Initialization	Channel mean depth (m)			Sandbodies extension / channel depth			Net to gross (%)		
	default	small	medium	large	default	small	medium	large	large
	3,75				50		35		
domain	Lag		Grid size		Number of nodes		Rotation		Slope along flow direction initial elevation at origin
	DX (m)	DY (m)	Length (m)	Width (m)	NX	NY	Ox (m)	OY (m)	
	50	50	5450	18700	110	335	231.5	0.002	
Erodibility	Emap		erodibility coefficient		erodibility coefficient		erodibility coefficient		erodibility coefficient
	constant	loaded from file	built from actual up to imported topography	erodibility coefficient	erodibility coefficient	erodibility coefficient	erodibility coefficient	erodibility coefficient	
				3.40E-08	3.40E-08	3.40E-08	3.40E-08	3.40E-08	
channel	Mean depth (m)		Importal centerline (multiple of channel)		Longitudinal margin (multiple of channel)		Longitudinal margin (multiple of channel)		Longitudinal margin (multiple of channel)
	Width (m)	Mean depth (m)	Importal centerline (multiple of channel)	Longitudinal margin (multiple of channel)	Longitudinal margin (multiple of channel)	Longitudinal margin (multiple of channel)	Longitudinal margin (multiple of channel)	Longitudinal margin (multiple of channel)	
	145m	3,75							
Avulsions	Regional		lateral margin (multiple of channel width)		levee breaches		Crevasse plays		probability for adding a new CS channel
	never	always	periodic	Poisson	never	always	periodic	Poisson	
Aggradation	Changes		Variation (m)		Thickness (m)		Wetland proportion		Wetland proportion
	elevation (m)	never	always	periodic	constant	uniform	lognormal	lognormal	
	1000								
Overbank Flood/Drainage profile	Occurrence		Levee width		Levee width		Levee width		Levee width
	never	always	periodic	Poisson	constant	uniform	lognormal	lognormal	
Exp. Decrease Thickness/Grainsize	Levee width		Levee width		Levee width		Levee width		Levee width
	never	always	periodic	Poisson	constant	uniform	lognormal	lognormal	

Unit 4 – Medium case

Initialization	non-exp	Channel mean depth (m)				Sandbodies extension / channel depth				Net to gross (%)											
		default	small	medium	large	default	small	medium	large	default	small	medium	large								
		2				50				28											
Erodibility	domain	Lag		Grid size		Number of nodes		Grid origin		Rotation		Slope along flow direction		Initial elevation at origin							
		DX (m)	DY (m)	Length (m)	Width (m)	NX	NY	OX (m)	OY (m)	%working	Ox = flow direction										
		50	50	5450	16700	110	335					231.5	0.002								
Erodibility	erodibility	Emap		built from actual up to imported topography		erodibility coefficient		7.00E-08		longitudinal margin (multiple of channel width)		10?									
		constant	loaded from file																		
		Width (m)	Mean depth (m)	Import centerline																	
		58m	2																		
Avulsions	Avulsion	Regional		lateral margin (multiple of channel width)		10?		levee breaches		during aggradation		never		always		periodic		\ (100)		Crevasse plays probability for transition from CSI to CSL	
		never	always	periodic	Poisson																
Aggradation	Overbank Flood/Drainage	elevation (m)		Changes		Poisson		Variation (m)		constant		uniform		normal		lognormal		Overbank		Draping	
		185	never	always	periodic <td>\ (10)</td> <td></td> <td></td> <td></td> <td></td> <td></td> <td></td> <td></td> <td></td> <td></td> <td></td> <td></td> <td></td> <td></td> <td></td>	\ (10)															
		Occurrence	never	always	periodic	Poisson	constant	uniform	normal	lognormal	Wetland proportion	Draining facies	Draining facies	Draining facies	Draining facies	Draining facies	Draining facies	Draining facies	Draining facies	Draining facies	
		Thickness	Grainsize	Levee width	\ (17)																

Unit 5 – Medium case

Initialization	non-exp	Channel mean depth (m)				Sandbodies extension / channel depth				Net to gross (%)						
		default		small	medium	large	default		small	medium	large	default		small	medium	large
		2					50					30				
domain		Lag		Grid size		Number of nodes		Grid origin		Rotation		Slope along flow direction at origin				
		DX (m)	DY (m)	Length (m)	Width (m)	NX	NY	OX (m)	OY (m)	*working Ox = flow direction	Initial elevation at origin					
		50	50	5450	16700	110	335			231.5	0.002					

Erodibility	erodibility	Emap				erodibility coefficient									
		built from actual up to imported topography		7.00E-08		longitudinal margin (multiple of channel width)		10?							
		constant	loaded from file			Mean depth (m)	Import centerline width (m)								
	channel	Width (m)	2												
		58m													

Avulsions	Avulsion	Regional		lateral margin (multiple of channel width)		levee breaches		Crevasse plays		
		never	always	periodic	Poisson	during aggradation	never	always	periodic	probability for transition from CSI to CSII
				\ (50000)	10?			\ (100)		

Aggradation	Overbank Equilibrium profile	elevation (m)		Changes		Variation (m)		Overbank		Draping		
		185	never	always	periodic	Poisson	constant	uniform	normal	lognormal	Overbank	Draping
		never	always	periodic (4)	Poisson	constant	uniform	normal	lognormal	Wetland proportion	Undefined	Draping
		Exp. Decrease		Levee width		Levee width		Levee width		Levee width		
		Thinnest		Grainsize		Grainsize		Grainsize		Grainsize		

For pessimistic and optimistic cases, only few parameters are changing:

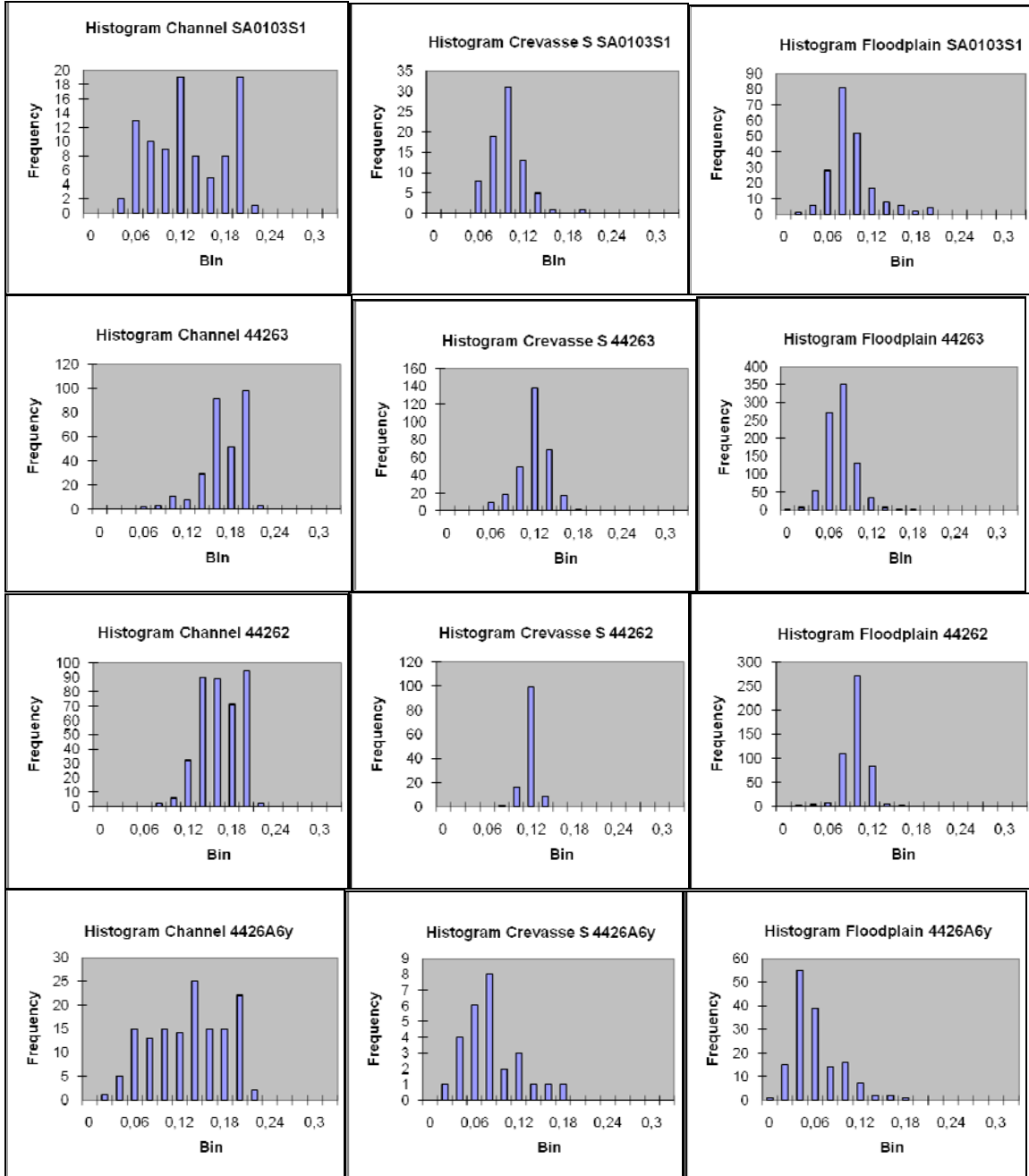
Pessimistic case:

- U1: Erodibility coeff.: 2,00E-08
- U2: Erodibility coeff.: 1,00E-08
- U3: Erodibility coeff.: 1,40E-08
- U4: Erodibility coeff.: 5,00E-08 ; overbank flood freq.: 8
- U5: Erodibility coeff.: 7,00E-08 ; overbank flood freq.: 8

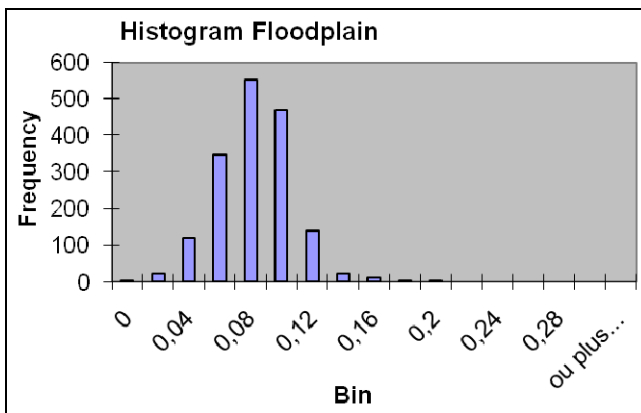
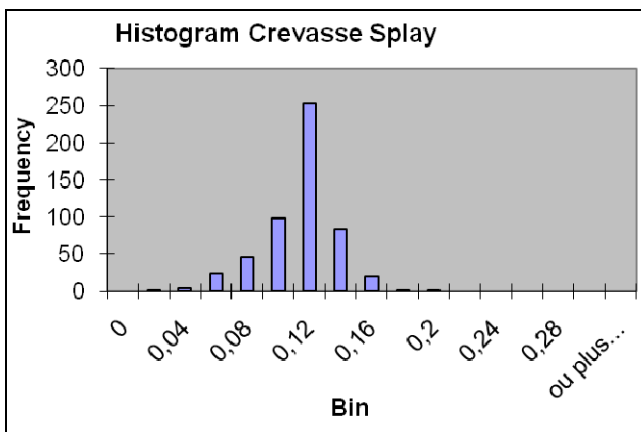
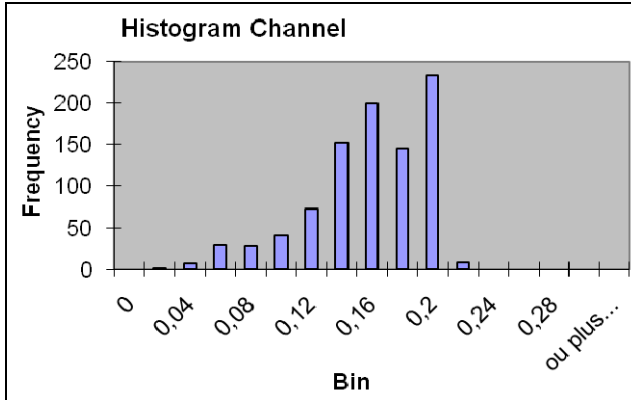
Optimistic case:

- U1: Erodibility coeff.: 5,80E-08
- U2: Erodibility coeff.: 4,60E-08
- U3: Erodibility coeff.: 5,00E-08
- U4: Erodibility coeff.: 6,50E-08 ; overbank flood freq.: 21
- U5: Erodibility coeff.: 8,50E-08 ; overbank flood freq.: 22

Porosity analysis of 4 well logs:



Porosity analysis of the 4 well logs together:



Porosity & Net to Gross distribution used for the petrophysical model in Petrel

Legend:

cc composite channel fills

sc single channel fills

cs crevasse splay

fp floodplain

		Porosity distribution			
	facies code	mean	std	min	max
U1	cc & sc	0,16	0,02	0,10	0,19
	cs	0,09	0,02	0,07	0,12
	fp	0,07	0,02	0,03	0,16
U2	cc & sc	0,15	0,03	0,09	0,20
	cs	0,10	0,02	0,09	0,13
	fp	0,08	0,02	0,04	0,12
U3	cc & sc	0,15	0,04	0,07	0,20
	cs	0,10	0,02	0,07	0,13
	fp	0,07	0,02	0,03	0,10
U4	cc & sc	0,15	0,03	0,08	0,20
	cs	0,10	0,01	0,08	0,11
	fp	0,06	0,02	0,02	0,09
U5	cc & sc	0,16	0,03	0,08	0,19
	cs	0,09	0,02	0,06	0,13
	fp	0,06	0,02	0,02	0,12

		Net to Gross distribution			
	facies code	mean	std	min	max
Medium case	cc & sc	0,30	0,106	0,20	0,38
	cs	0,30	0,106	0,20	0,38
	fp	assign values - cst: 0			
Pessimistic case	cc & sc	0,20	0,106	0,10	0,30
	cs	0,20	0,106	0,10	0,30
	fp	assign values - cst: 0			
Optimistic case	cc & sc	0,38	0,106	0,28	0,48
	cs	0,38	0,106	0,28	0,48
	fp	assign values - cst: 0			

At each Flumy facies code has been assigned a Petrel facies code for the porosity and net to gross distribution:

code	facies	Petrel facies code
1	Channel lag	0: composite channel fills ; 1: single channel fills
2	Sand plug	
3	Point bar	
4	Crevasse splay I	2: crevasse splay
5	Splay II channels	
6	Crevasse splay II	
8	Levee	
7	Mud plug	
10	Overbank	3: floodplain

Appendix B

The following points are presenting the different problems encountered in Flumy or linked to Flumy.

1\ Flow direction

The channels in Flumy are modelled with a flow direction from left to right side of the grid. It isn't possible to change it, for example to model them diagonally to the grid. However there is a “flow direction” option which allows to change the overall orientation of the grid. In other words, once the grid has been exported from Flumy to import it in Petrel, the grid is oriented.

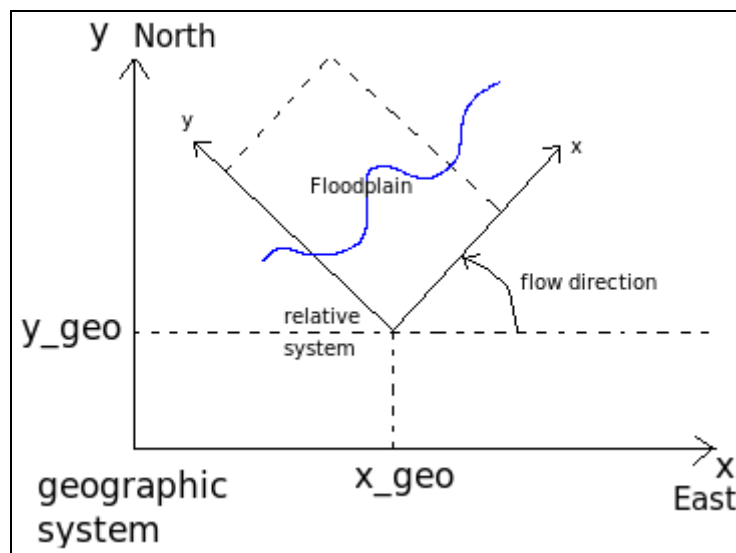
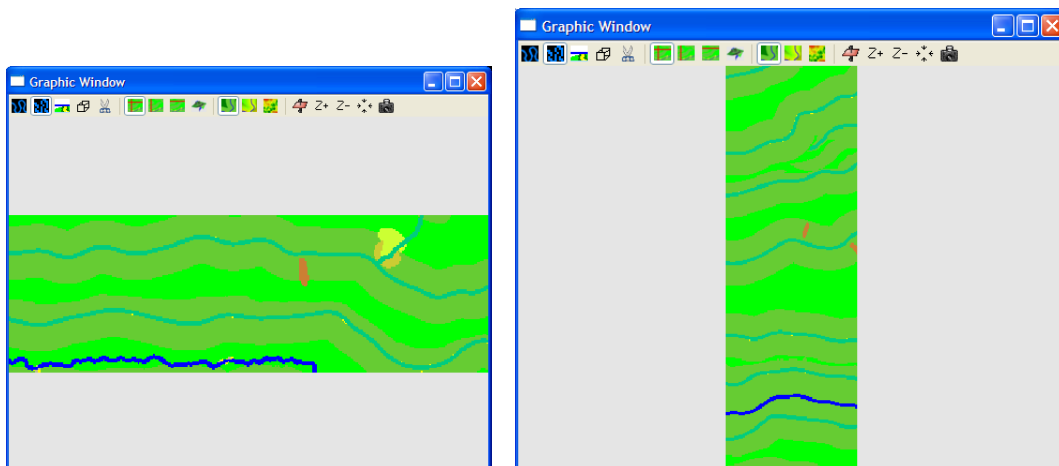


Figure representing the use of the flow direction option in Flumy (Flumy userguide, 2009)

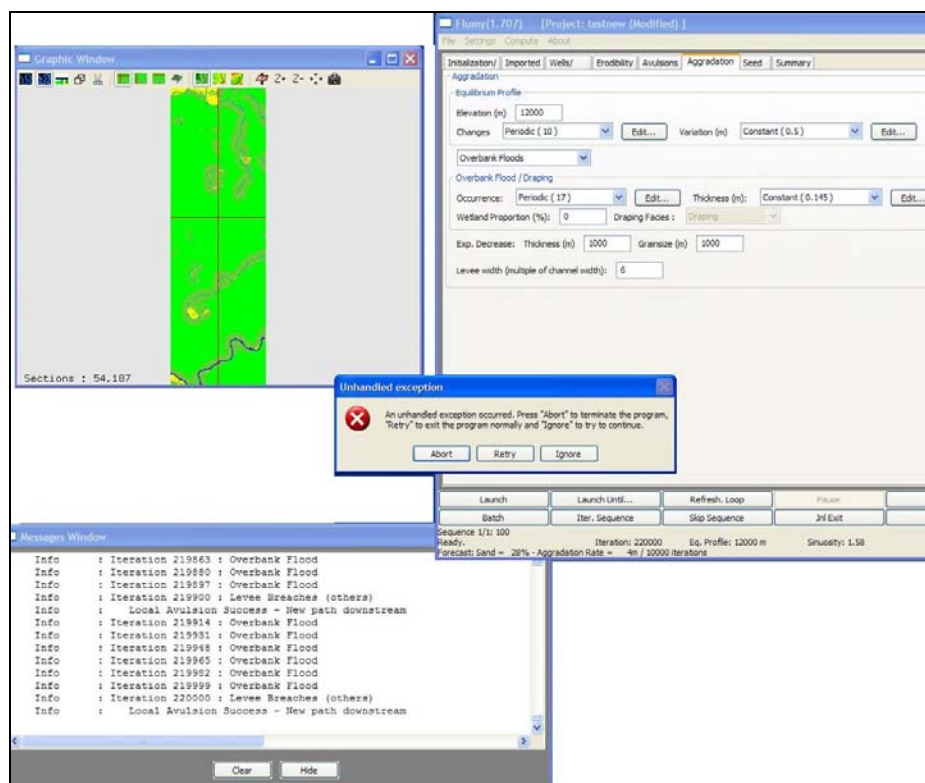


Screenshots of top view models in Flumy: the flow direction is from the left to the right (channels are in blue).

The problem is that the user doesn't really have the choice of the flow direction, only the grid orientation. Furthermore there are few compatibility problems in Flumy itself and with Petrel because of this orientation problem (see following error points). Finally all the data imported in Flumy (well logs coordinates, topographic surface orientation etc) have to respect this specific flow direction and have to be modified if necessary.

2\ Flumy crashes

In Flumy, it is possible to model different sequences together. The input parameters can be changed while modeling, except the grid size and other main parameters. However when the model starts to be heavy, after ~ 400 000 iterations or 250m of deposits, the software crashes and the model is lost.



Screenshot of Flumy while crashing.

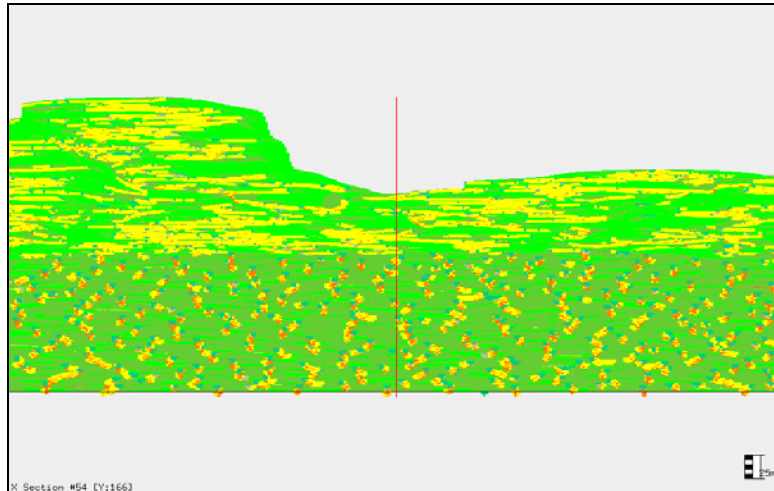
For the project, the sequences 1 and 2 have been modelled separately to avoid this problem. Unfortunately the consequence is that the two sequences are not linked in Petrel to calculate the reservoir rock connectivity.

3\ Difficulty to model a sequence with a low regional avulsion

The sequence 2 of the BRM Group has a low regional avulsion and because of this aspect, it was difficult to model it.

Firstly the sequence 2 was very long to model because of a low aggradation rate. Secondly when the sequence 2 was associated with the sequence 1, few unusual features were appearing:

- on the edges of the model, after ~ 200 000 iterations (sequence 1 included) the deposits were incised dramatically (same type of incisions presented in the error point 4)
- on the edges of the model, the deposits were accumulating without filling the accommodation space in the middle of the model



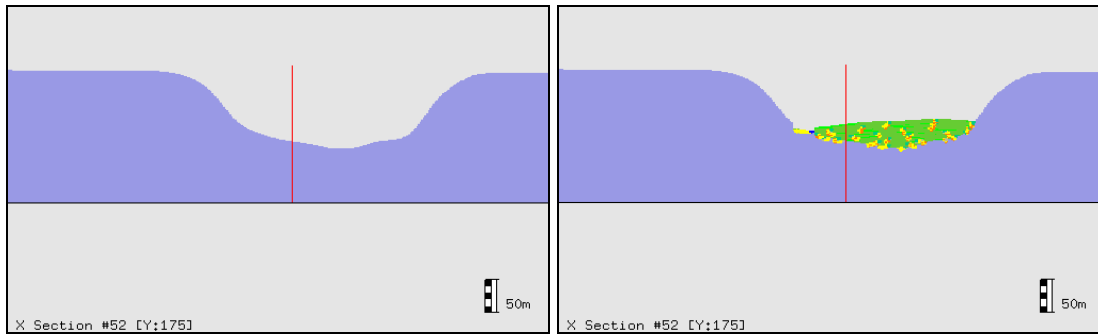
Screenshot of a cross-section model in Flumy after 380 000 iterations: the sequence 1 is the lower part and the sequence 2 is the upper part (channels fills in yellow).

The sequence 2 has been modelled separately to avoid this problem. Moreover we observed that lower is the regional avulsion, more difficult it is to model this sequence. The modeling of the sequence 2 of the optimistic case (high Net to Gross, so low aggradation rate) was very difficult and even the sequence couldn't reach the proper thickness of deposits (~110m) without Flumy crashes.

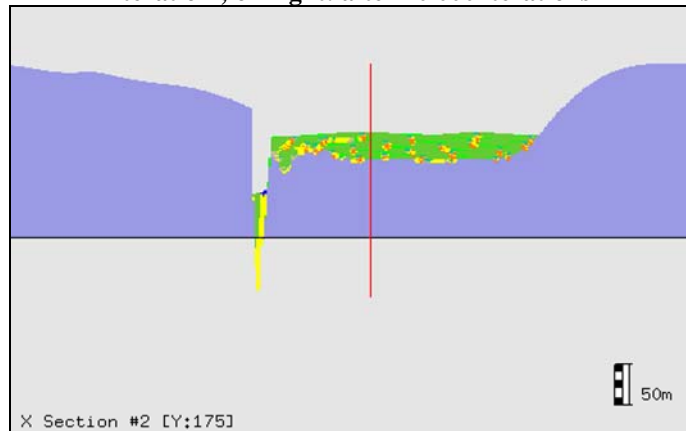
4\ Topographic surface

A topographic surface has been extracted from the 3D model of Petrel and then imported in Flumy to get a more realistic model. In the project, the topographic surface presents a small paleovalley up to 50-60 m depth only. However different topographic surfaces have been tested. It appeared that there aren't problems to model with a topographic surface with a low relief, while incision features are developing with a higher relief (~100m depth).

It seems that it is the same kind of problem than presented in the error point 3.



Screenshot of a cross-section model in Flumy including a topographic surface in blue – on left: after 1 iteration ; on right: after 10 000 iterations



Screenshot of a cross-section model in Flumy including a topographic surface in blue – after 20 000 iterations (channels fills in yellow)

Another problem is the impossibility to add a topographic surface and to define a flow direction together. In that case, Flumy doesn't simulate.



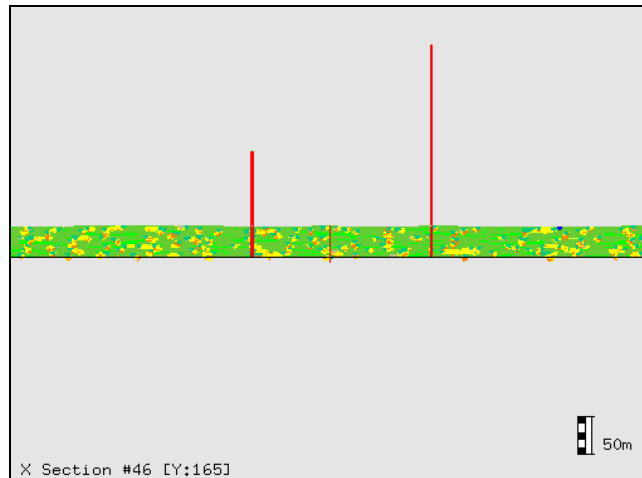
Error message if topographic surface and flow direction options are active.

5\ Well conditioning

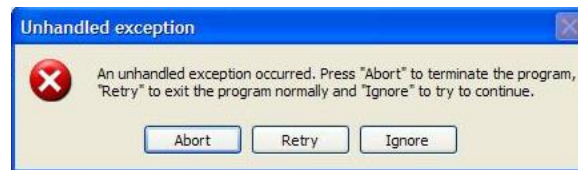
When the Flumy model is conditioned by wells, the simulation time is doubled:

- without well conditioning 100m of deposits (sequence 1) are modelled within 60 000 iterations
- with well conditioning less than 50m of deposits (sequence 1) are modelled within 60 000 iterations

Furthermore Flumy crashes while modeling the sequence 1 (~50-100m of deposits) when the well conditioning option is active. Usually Flumy crashes while modeling the sequence 2, so after 200m of deposits.



Screenshot of a cross-section model in Flumy including well conditioning (wells are in red).



Screenshot of Flumy while crashing

It seems that the well conditioning is a heavy process which cannot handle the modeling of a “thick” reservoir.

Moreover the well conditioning option cannot be combined with the definition of a flow direction (same error than seen in the error point 4).



Error message if well conditioning and flow direction options are active.

6\ Flumy project not saved

During the project, four versions of Flumy have been tested: 1.606, 1.707, 1.708 and 1.709.

The version 1.708 is the best one for now: Flumy crashes less easily and the sequence 2 can be more or less well modelled. Unfortunately there is a problem when saving the project. When we want to open a saved project the following error message appears:



Error message when we want to open a saved project

Finally it is impossible to open a saved project. The best is to export the Flumy block systematically at the end of the modeling.

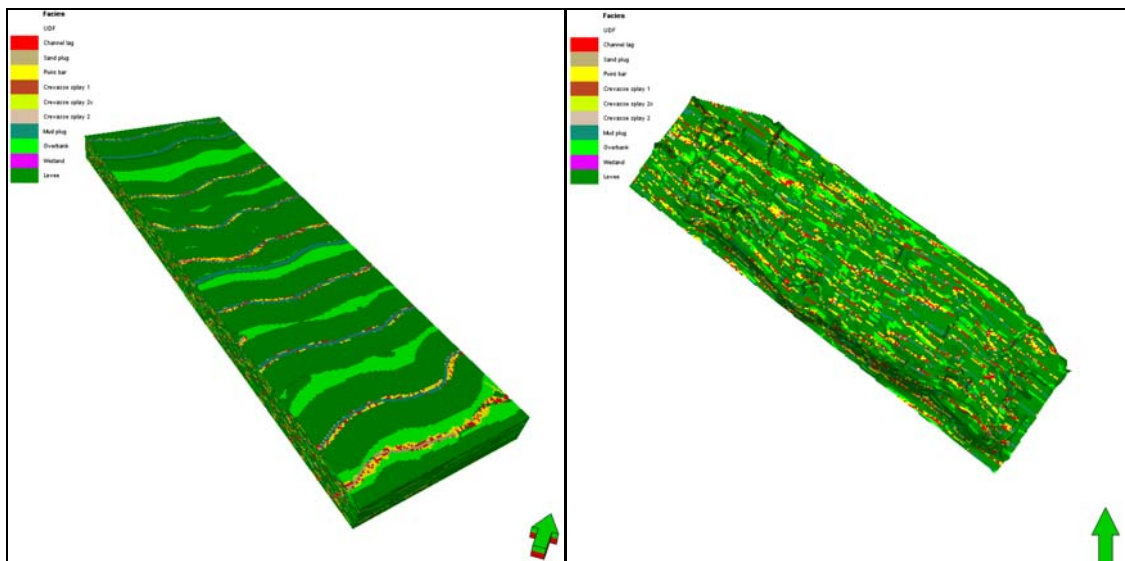
7\ Compatibility with Petrel

The biggest problem encountered during the project was the compatibility of the Flumy model with the Petrel model.

The facies model built by Flumy is exported under a GSLIB format. The grid has 110 cells in the x direction and 335 cells in the y direction.

In Petrel, the initial model including well logs and structural model has 335 cells in the x direction and 110 cells in the y direction.

Therefore the GSLIB file isn't read properly when imported directly in the initial Petrel model. X axis is read as y axis and vice versa. Then the channels are "deformed" and follow the wrong axis.



3D view in Petrel of the GSLIB after import – on left: when using a VIP file at first (NX 110 x NY 335) ; on right: when importing directly the GSLIB file in the initial Petrel model (NX 335 x NY 110)

We succeed to avoid this problem by importing at first a VIP file with 110 cells in the x direction and 335 cells in the y direction into Petrel. Then we import the GSLIB file into this new 3D grid. The negative point is the impossibility to add well logs and fault model to this new grid.

8\ VIP file / GSLIB file

At first we tried to export the Flumy block under the VIP format. The VIP format is heavy, so only a discretisation of 4 or even 6m applied in Flumy could allow to import the file into Petrel. Otherwise Petrel was crashing while importing the VIP file. The discretisation was then too coarse: ~40 or 27 cells only in the z direction representing ~160m of deposits.

So we decided to try the GSLIB format. Then the discretisation in Flumy changed for 0.5m, ~320 cells in the z direction. It is the format under which we could work. The only difference with the VIP format is that the 3D grid has to be created in Petrel at first, before to import the GSLIB file. With the VIP file a 3D grid was automatically created in Petrel.

Appendix C

Extra information to be added to the Flumy userguide.

Well data

To import well data in Flumy, the well logs files from Petrel have to be modified.

1\ Export well logs interpreted in Petrel:

- Input table: right click on a well with log data (including depofacies interpretation)
- Select “export”, format: Well logs (ASCII)
 - o Specified MD
 - o Depofacies
- Click ok

2\ Change the log files with Excel:

- Delete the header of the file
- In Excel: file → open → select the log file → fixed width → advanced (decimal separator “.” ; thousands separator “”) → finish
- First column: depth (ft)
Second column: facies code (each 1ft)
0: composite channel fills
1: single channel fills
2: crevasse splay
3: floodplain
- Delete the useless data → keep the top level of each layer
- Replace the Petrel facies code by the Flumy facies code (use the “replace” option in Excel)
Facies code 3 (floodplain) replaced by code 8 (overbank)
Facies code 2 (crevasse splay) replaced by code 4 (crevasse splay I)
Facies code 1 (single channel) replaced by code 3 (point bar)
Facies code 0 (composite channel) replaced by code 3 (point bar)
- Change the units, calculation of layer thickness initially in [ft] by in [m]
Layer depth calculates from top to bottom in [m] (select only the reservoir segment)
- Save the file under txt format with the following configuration:

#

=====

Well extracted from MCRC simulation (ix=14,iy=99)

Coordinates, depth and thickness are expressed in meters

#

#

=====

Well Location

X_WELL=1260

Y_WELL=9760

#

Bottom elevation

Z_BOTTOM=0

Top elevation

Z_TOP=93.57

#

Deposits From top to bottom

Facies_id Facies Depth Thickness Time

Warning : Depth from top of deposit basis

FACIES_COLUMN=1

DEPTH_COLUMN=3

~Ascii

3	PB	3.66	3.66
---	----	------	------

4	CSI	3.96	0.30
---	-----	------	------

3	PB	4.27	0.30
---	----	------	------

4	CSI	5.18	0.91
---	-----	------	------

3	PB	7.92	2.74
---	----	------	------

4	CSI	9.14	1.22
---	-----	------	------

8	OB	9.45	0.30
---	----	------	------

3	PB	12.50	3.05
---	----	-------	------

8	OB	14.32	1.83
---	----	-------	------

.	.	.	.
---	---	---	---

.	.	.	.
---	---	---	---

.	.	.	.
---	---	---	---

- Define the well location, X and Y coordinates (take into account the Flumy grid: x and y origin coordinates of the grid and the flow direction)
- Add one empty line at the end of the file
- Import the file into Flumy

From Flumy to Petrel

To import the facies model from Flumy to Petrel.

1\ In Flumy:

- Build a grid with the proper number of cells in the X and Y direction (the filling doesn't matter, the purpose is to get a grid with the required size)
Example: NX 110 ; NY 335 ; DX and DY 50
Choose a flow direction if the field is oriented, in our example: 231.5°
- Export the file under the VIP format

2\ In Petrel:

- In the Models tab: right click on the model, select “import (on selection)”
- Select the VIP file exported from Flumy (not tick the “negate Z-value when mostly positive” box ; undefined value: 0)
- Do the “make horizons”, “make zones” and “layering” processes as usually done in Petrel to build a 3D model

3\ In Flumy:

- Build the facies model required, the grid size has to be exactly the same than the one used to create the VIP file
Example: NX 110 ; NY 335 ; DX and DY 50
Only NZ will be different
- Export the file under the GSLIB format
- Choose 0.5m for the vertical discretisation

4\ In Petrel:

- Adjust the layering of the 3D grid: NZ in Petrel has to be the same than the one written in the GSLIB file
- Right click on the property folder of the 3D grid
- Select the GSLIB file exported from Flumy
(undefined value: 255 ➔ ok)

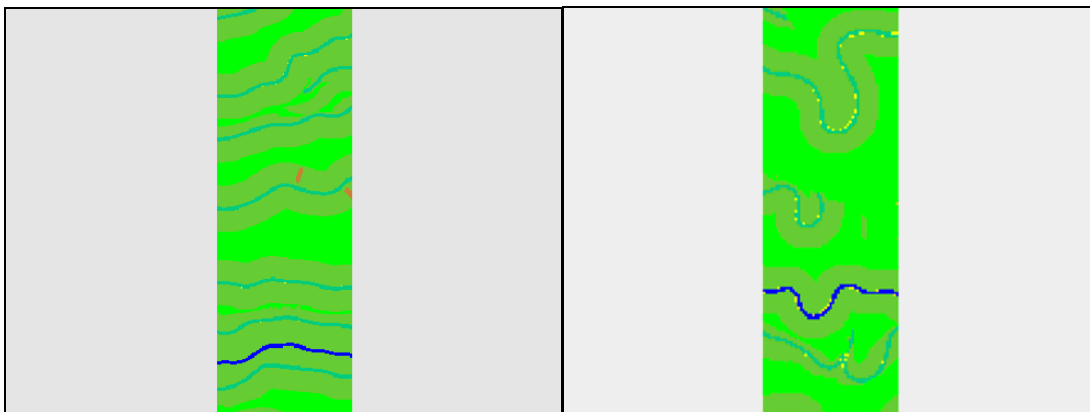
Appendix D

Comments about Flumy to improve it (excluding remarks of the annexe B).

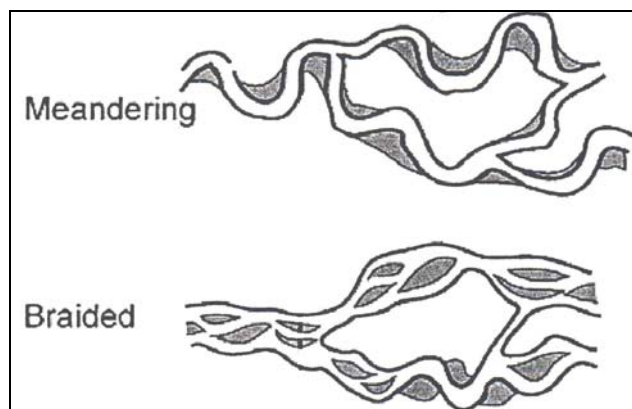
Meandering/braided systems

As specified, Flumy models meandering rivers. However it would be better to add a braided river option. For the project we managed to build a model (sequence 1) which looks like more or less a braided system.

However few braided features are missing: impossibility to model channels belt or even composite channels. Flumy models only single channels. For example, a sinuosity option could define the river system.



Screenshot of a top view model in Flumy – on left: Sequence 1 (braided system) ; on right: sequence 2 (meandering system)

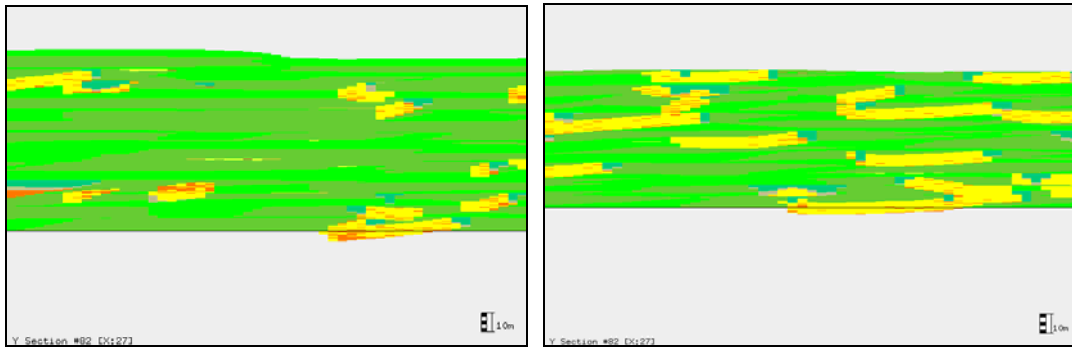


Top view of a meandering and a braided systems with channels belt and composite channels

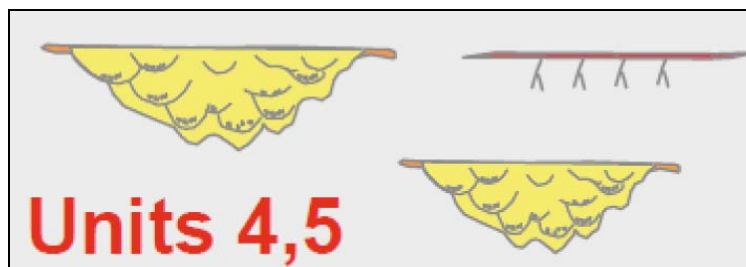
Stacking pattern

When we want to model a sequence with stacked channels, we decrease the frequency of the regional avulsion and then the aggradation rate is lower. The problem is that Flumy doesn't model properly the stacking pattern. The channels “derived” towards one

direction on top of each other with a small gap, instead of migrate and move from one side to another side in a restricted area.



Screenshots of a cross-section model in Flumy – low regional avulsion, low aggradation rate



Cross-section view of stacked channels

Pedofacies development

With a low regional avulsion, it should be associated the development of pedofacies/peat deposits. It will model stable area and increases the realism of the geological model.

More options

Few more options could be added to improve Flumy:

- sea level change data
- an index of rock compaction
- Vertical Proportion Curve (VPC) definition: to define the channels distribution over the field
- The choice of the units (meters, feet...)
- The geometrical shape of the field (not only rectangular or square)
- The flow direction (not only the grid orientation)
- Possibility to define the maximum thickness of deposits to model

Userguide

More information could be added to the Flumy userguide: well data preparation, compatibility with Petrel etc... And few examples of input parameters set could be presented to help the beginner user to familiarize with Flumy and to understand the influence of the input parameters on the model.

